Spring 1987

The Stratigraphy of Late Quaternary Deposits in the Payan Mining District, Narino, Colombia, South America

Richard Alan Barringer
Old Dominion University

THE STRATIGRAPHY OF LATE QUATERNARY DEPOSITS IN THE PAYAN MINING DISTRICT, NARINO, COLOMBIA, SOUTH AMERICA

by

Richard Alan Barringer
B.S. August 1982, Old Dominion University

A Thesis Submitted to the Faculty of
Old Dominion University in Partial Fulfillment of the
Requirements for the Degree of

MASTER OF SCIENCE
GEOLOGICAL SCIENCES

OLD DOMINION UNIVERSITY
MAY, 1987

Approved By:

Dr. Dennis A. Darby

Dr. G. Richard Whittecar

Dr. Joseph H. Rule

Dr. Ramesh Venkatakrishnan

ABSTRACT

THE STRATIGRAPHY OF LATE QUATERNARY DEPOSITS IN THE PAYAN MINING DISTRICT, NARINO, COLOMBIA, SOUTH AMERICA

Richard Alan Barringer

Old Dominion University, 1987

Director: Dr. Dennis A. Darby

Late Quaternary gold placer terrace deposits along the Rio Magui in the Payan Mining District consist of thick layers of auriferous cobbly gravels with thin interbeds of discontinuous organic-rich auriferous sands. Thick volcanic ash caps most terraces. Based upon detailed plane table and alidade surveying, section descriptions, observed field relationships of strata, and physical and chemical analyses of sampled horizons, an informal stratigraphic framework for a small part of the Colombian Pacific Coastal Plain is proposed.

Terrace deposits appear to unconformably overlie a well cemented volcanic tuff (Ananias Formation). The overlying terrace deposits are composed primarily of thick

cobble to gravel units. These gravels are subdivided into two formations (Antigua Formation and Panambi Formation) on the basis of comparisons of cobble lithology, cobble size, depth of weathering, geomorphic relationships, and heavy mineral assemblages. Carbon-14 dates from wood debris found in the discontinuous sand lenses within these gravel units suggest that the higher elevation Antigua Formation is older (greater than 40,000 YBP) than the Panambi Formation (less than 25,000 YBP) which is restricted to lower terraces within the modern river valleys.

Two separate ash units were identified based on differences in mineralogy and magnetite element composition. These ashes buried active depositional surfaces of the paleo-fan and allow for paleoslope and depositional sequence interpretation of the fan deposits. The San Juan Ash paraconformably overlies the Antigua cobble gravels and the Magui Ash paraconformably overlies the Panambi gravels. The present-day Rio Magui channel and overbank deposits (Payan Formation) form another gravel with abundant sand and mud interbeds similar to the Panambi Formation, but finer textured and more mineralogically mature than the Antigua gravel unit.

DEDICATION

To Mom and Pop for their patience. understanding, support, and faith, during all the years of my life.

ACKNOWLEDGEMENTS

This work is the culmination of nearly five years of graduate study at Old Dominion University. The completion of this thesis would not have been possible without the guidance and assistance of several individuals. I would first like to thank Dr. Dennis A. Darby and Dr. G. Richard Whittecar for allowing me the opportunity to participate in this international geological research. Jim Garrett and Mike Babuin were also involved in this research and should share the credit for the vast amount of work accomplished during our three month field experience.

I want to express my personal thanks to the Cal-Colombian Mining Company for sponsoring this geological research, especially Jack Winn, Danny Janelli, Fernando Padilla, and Carlos Cadavid for their cooperation and assistance in making strangers in a strange land feel welcome and somewhat at ease. Special thanks to the mine laborers who directly assisted our field research, namely; Harmington, Bermudez, Luis, Efrien, and in particular Wilfredo and Hermogene.

I would like to thank Dr. and Mrs. Hal Ellis of the Ellis Industrial and Mining Development Corporation (EIMDEC) and Annabelle Napierkowski for their invaluable translations from the Spanish language. I would also like to thank Marian Anderson of the Mercedes Benz Corporation for her translations from the German language.

The completion of this research was aided by the cooperation of several Old Dominion University graduate students in the Geological Sciences Department. T. Britt McMillan and Richard D. Lutz assisted in the various computer analyses. Edward A. "Chip" Council assisted in the atomic absorption spectrophotometric procedure and analysis. Mary K. Goeke and Janet S. Emry assisted in the preparation of the thesis manuscript. Many other students also assisted in the completion of this thesis.

In addition, I wish to express my deepest and most sincere gratitude to the members of my thesis committee: Drs. Dennis A. Darby, G. Richard Whittecar, Joseph H. Rule, and Ramesh Venkatakrishnan. Their patience and encouragement, as well as that of other faculty members of the Old Dominion University Geological Science Department is hereby formally acknowledged and sincerely appreciated.

"Somewhere, in another lifetime, I once read that the jungle either accepts you or rejects you. Did it accept me? or did I accept it? Does it matter? I walked on thinking only that I was on my way, to something."

Tobias Schneebaum
Keep the River on Your Right
Grove Press Inc., New York
1969.

TABLE OF CONTENTS

TABLE OF CONTENTS - continued

LIST OF FIGURES

LIST OF FIGURES - continued

LIST OF TABLES

CHAPTER 1: INTRODUCTION

1.1 General Introduction

Gold occurs both in primary lode deposits in the Andes Mountains and in secondary placer deposits within thick fluvial deposits adjacent to the Andes Mountains. In southwestern Colombia, the Pacific Lowland is an alluvial plain built by streams draining the western slope of the Western Andes. Spaniards conquered this area in 1600, and quickly reported that much gold was found in this province. Alluvial mining has continued from that time (Restrepo, 1886). Practically every stream in the Colombian Pacific Lowlands has been worked by European miners during the past 300 years, yet to the scientific community, this tropical rain-forest remains one of the least known regions in Latin America (West, 1952).

1.2 Purpose

It is the purpose of this study to examine the geology in an area of active placer gold mining in the Colombian coastal plain to determine the sedimentologic character and stratigraphic correlation of the sediments. This work improves our understanding of the processes responsible for the deposition of the sediments in a humid tropical

fan and provides guidance for gold exploration in the area.

1.3 Location and Setting

The study area lies in the central portion of the Department of Narino in southwestern Colombia (Figure 1.1). The Compania Minera de Colombia Y Texas, S.A. Inc. (CMCT) originally was granted the gold mining concessions (numbers 8704, 8705, and 8706) surrounding the village of Payan about 60 kilometers east of the Pacific port of Tumaco. The concessions are less than 40 kilometers from the foothills of the Western Andes.

Placer mining is the main industry of the local population, most of whom are the descendants of African slaves brought to this area by the Spaniards in the 17th century. Colonial placering techniques, many of which have Indian origins, are still used by the native miners today. This type of mining involves the cutting back of a side of a terrace with crude pointed bars and washing the sediments in a ground sluice to extract the placer gold particles from the sediments (Bullman, 1892; Johnson, 1912; Ward, 1913; and West, 1952a, 1952b, 1957). This mining technique leaves near vertical outcrops of up to 10 meters in an area which otherwise would not afford any natural exposures except along rivers.

The annual precipitation in the Payan region typically exceeds 1000 centimeters. The mean daily temperature

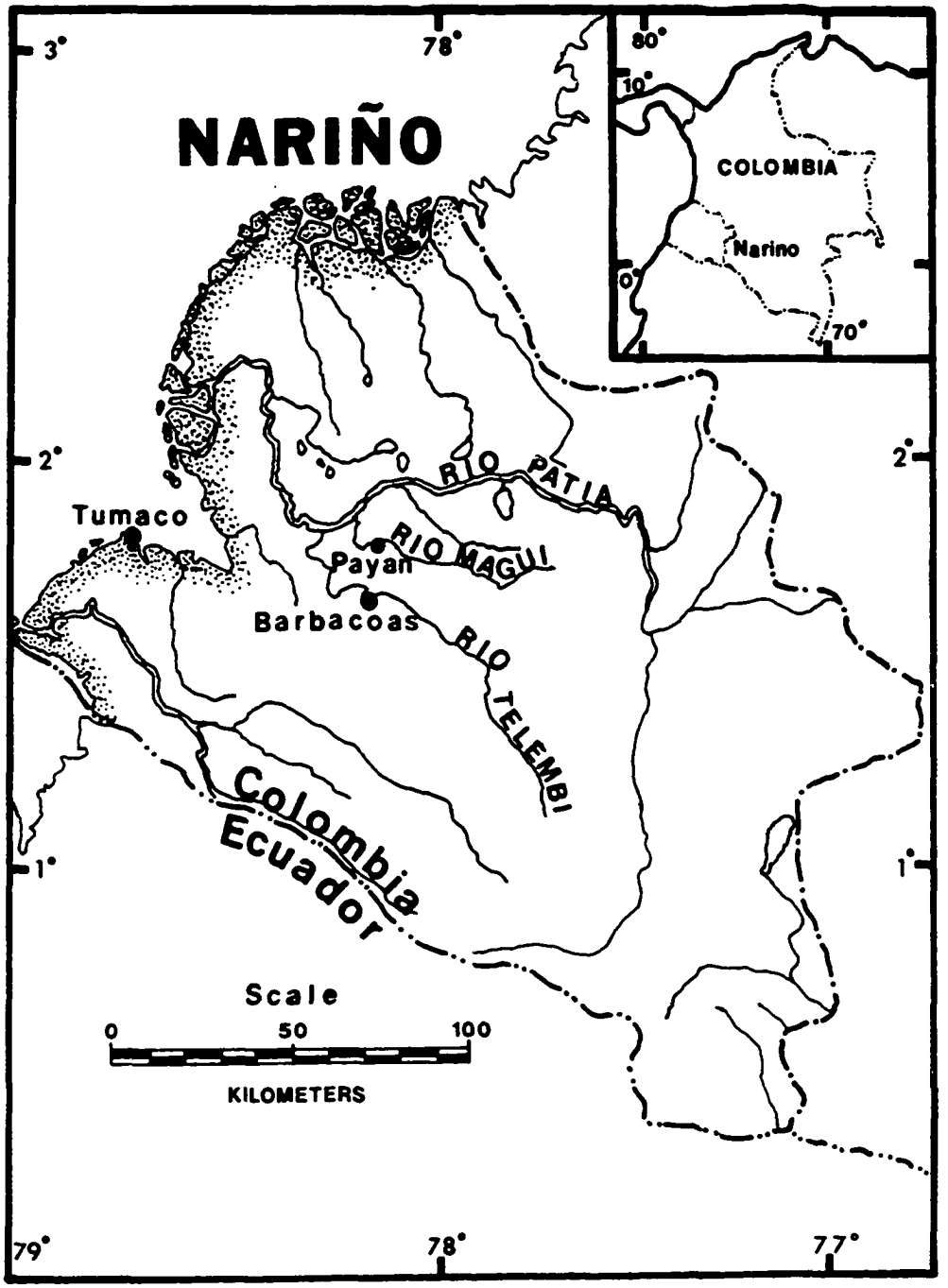

Figure 1.1 Location map of the Department of Narino, Colombia showing the principal rivers and coastal plain population centers. The study area is located in the area around the village of Payan.

(26° C) shows little variation throughout the year. This hot and very wet environment supports a dense tropical rain forest (West, 1957).

The terrain consists of multiple gravel and ash terraces, which have been thoroughly dissected by the many minor streams tributary to the Rio Patia. The Rio Magui, flowing past Payan, is one of these tributaries and like the other streams in the area has a moderate gradient and a large range of flow velocities due to the torrential nature of the rainfall (Babuin, 1985). The local relief in the Payan Mining District is approximately 80 meters, maximum elevations estimated at less than 130 meters.

The terraces are made up of nearly horizontal layers of fluvial gravels and sands amd volcanic ash. Thick volcanic ash also caps these terraces. Fine-grained gold occurs in nearly all non-volcanic deposits and ranges from widely desseminated grains to concentrations as high as 0.1 ounce per cubic yard (Garrett, 1985).

Thick stratigraphic sequences in alluvial fans, such as seen near Payan, are relatively rare. Nilsen (1982) states that a vertical sequence analysis of alluvial fan deposits is limited because (1) little vertical section is seen in modern fans, (2) coring of fan sequences has generally been difficult because of abundant conglomeratic intervals, (3) fans have not been widespread exploration targets, and (4) many ancient conglomeratic sequences recognized as fan deposits have not appeared to contain

systematic vertical changes, so vertical sequence analysis has not been extensively applied to facies analysis of fan deposits. In addition, Schumm (1977) states that the lack of extensive exposure prevents sampling of modern humid alluvial fans except at the surface and in gullies; Nilsen (1982) also adds that because of vegetation cover, soil formation, and human development, suprisingly little significant work has been done on fans in non-arid regions, particularly humid ones. The Payan area, although heavily vegetated, provides a rare opportunity to view vertical sequences of humid alluvial fan deposition, due to the labors of the many family operated placer mines in the area.

CHAPTER 2: REGIONAL GEOLOGIC SETTING

2.1 Introduction

The geology of the Payan Mining District is closely tied to the history of the Andes Mountains. In Colombia, the Andes form a "knot" (the Nudo de Pasto) in the Department of Narino (Ramirez and Aldrich, 1977), and spread out to the north and northeast to form three distinct subparallel ranges - the Central, Eastern, and Western Cordillera. Although each range is geologically distinct and different in age, all contain primary gold deposits associated with distributions of igneous and metamorphic rocks.

Several major rivers drain these primary gold districts and have formed some of the richest placer deposits in the New World (Utter, 1984). The largest of these rivers are the Magdalena, which drains the valley between the Eastern and Central Cordillera; the Cauca, which drains the valley between the Central and Western Cordillera; the Atrato and the San Juan, which drain the Western slope of the Western Cordillera; and the Patia, which drains the southern Cauca valley, crosses the Western Cordillera, and empties into the Pacific Ocean (Figure 2.1).

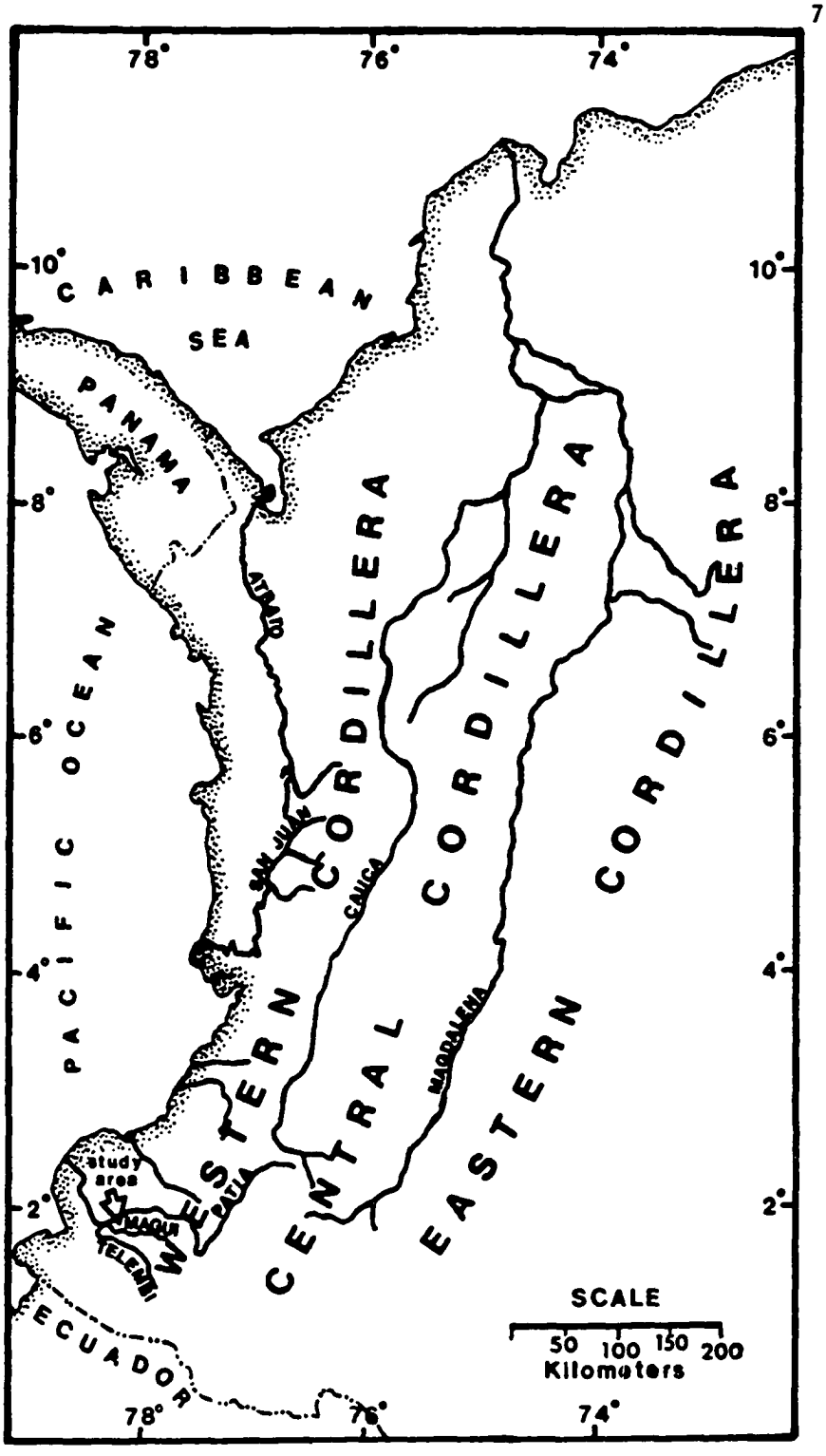

Figure 2.1 Map of Western Colombia showing the three major ranges of the Andes and the principal rivers which drain them.

2.2 Western Cordillera

The Western Cordillera is composed of eugeosynclinal rocks deposited during the Mesozoic and deformed in the Late Cretaceous (Ramirez and Aldrich, 1977). The rocks of this cordillera are characterized by thick tholeiitic volcanics dating from the Late Mesozoic which are associated with equally thick and slightly metamorphosed pelitic sediments. These Mesozoic volcanics and sediments are divided into the Diabase Group and the Dagua Group. The Diabase Group includes gabbro, serpentinite, greenstone, diabase, pillow basalt, and some interstratified cherts. The Dagua Group contains the fine-grained and slightly metamorphosed sediments typical of a eugeosynclinal series (Figure 2.2). Various authors have interpreted this belt of basic igneous rocks and metasedimentary rocks as a Late Mesozoic island arc or as an oceanic element that became welded to the overall orogen during the Tertiary (Zeil, 1979). This interpretation appears to agree well with that of Mooney (1980) who proposed a westward-stepping subduction zone as the mechanism for the emplacement of mafic/ultramafic oceanic crust along the continental crust of the Central and Eastern Cordillera.

Of particular significance to this research is a 50 kilometer-long gold lode belt in southeastern Narino, associated with Tertiary quartz-diorite plutons that were first described by Pereira-Gamba (1909) and later by

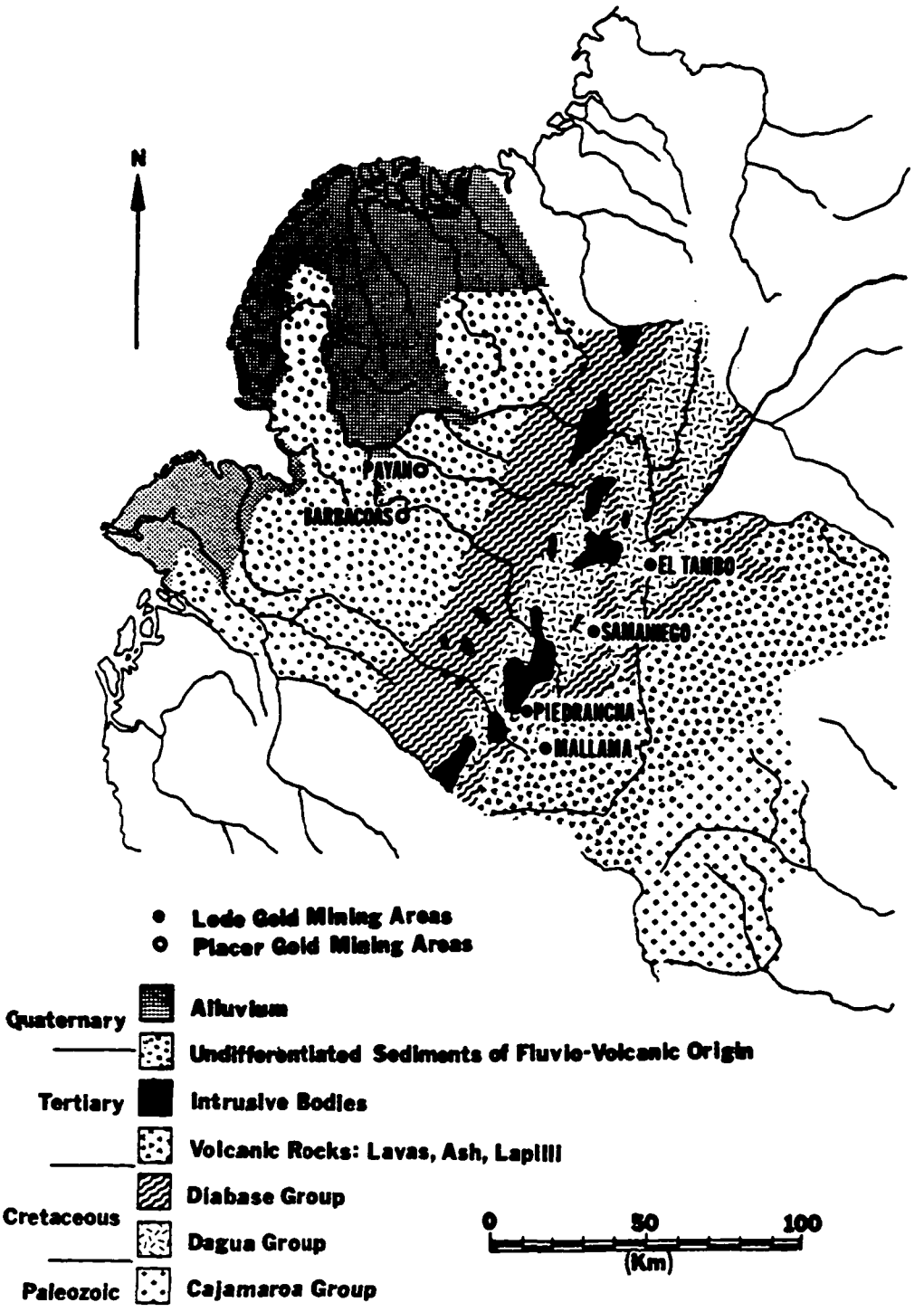

Figure 2.2 Generalized geologic map of Narino showing the Tertiary quartz-diorite auriferous bodies intruded into the Dagua and Diabase Group rocks (modified from Arango and Ponce, 1982).

Miller and Singewald (1919). The location of this mineralized belt appears to correspond to the mapped contact between several quartz-diorite intrusive stocks and the surrounding metamorphosed Diabase and Dagua Group rocks of Arango and Ponce (1982), (Figure 2.2)and are discussed in detail by Radelli (1965).

2.3 Pacific Coastal Basin Geology

To the west of the Western Cordillera lies the Pacific Coastal Basin. This narrow basin parallels the trend of the Western Cordillera and has an approximate area of 56,000 square kilometers (Bueno S. and Govea R., 1976). Recent studies indicate that the Nazca oceanic plate is subducting beneath the South American plate (Campbell, 1974a, 1974b; Barazangi and Isacks, 1976; Lonsdale and Klitgord, 1978; Hall and Wood, 1985), (Figure 2.3). Case et al. (1971) indicate that the complex and active interplay of the American, Caribbean, and Nazca crustal plates produced sporadic uplifts of the Colombian Cordilleras. This complex plate interaction has not only resulted in sporadic Cordilleran orogenies, but in volcanic outbursts as well. Despite the fact that the volcanoes of the Colombian Andes are confined primarily to the Central Cordillera, their influence upon the stratigraphy of the surrounding basins has been quite profound. Although evidence of Paleozoic volcanism has been reported in the literature by numerous authors

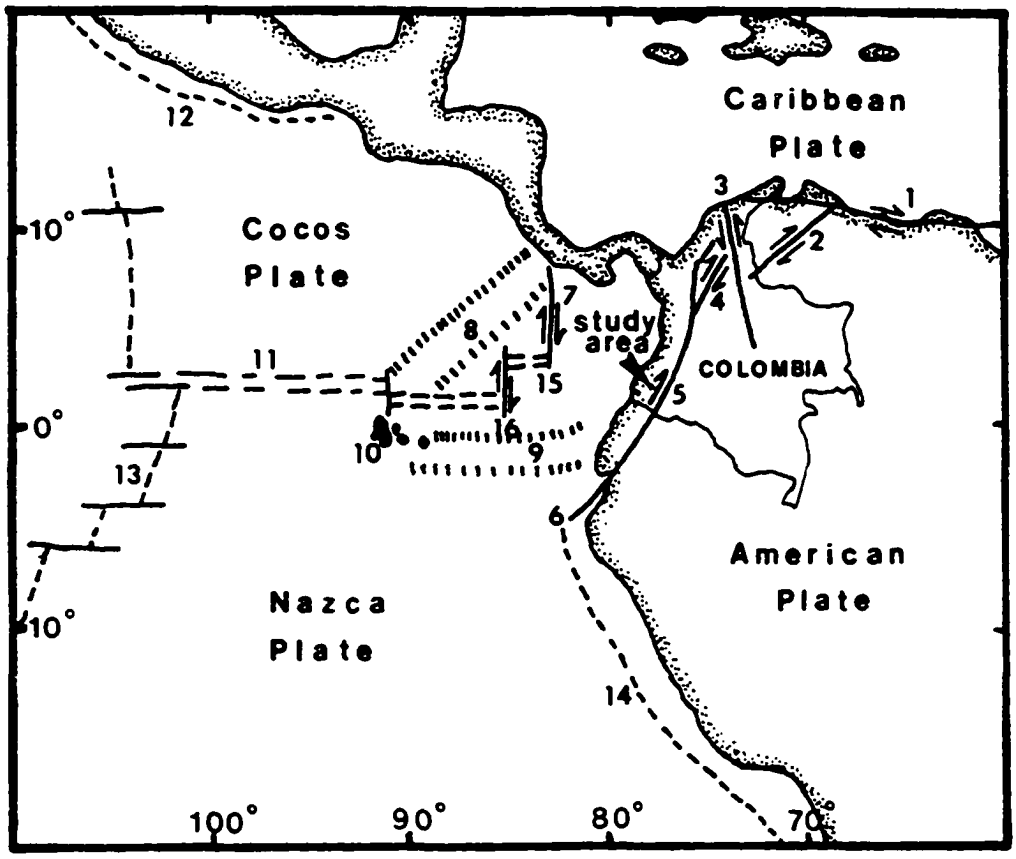

Figure 2.3 Regional tectonic map showing the complex interplay of several tectonic features in western South America and southern Central America.

Tectonic Features

1. Oca-El Pilar Fault
2. Bocono Fault
3. Santa Marta Fault
4. Palestina Fault
5. Dolores-Guayaquil Megashear
6. Huancabamba Deflection
7. Panama Fracture Zone
8. Cocos Ridge
9. Carnegie Ridge
10. Galapagos Islands
11. Galapagos Fracture Zone
12. Middle America Trench
13. East Pacific Rise
14. Peru-Chile Trench
15. "Costa Rica" Rift Zone
16. "Ecuador" Rift Zone

(Irving, 1975), the majority of volcanic activity in Colombia appears to be synchronous with a post-Andean orogenic event, occurring in the Miocene and Pliocene (Van Houten and Travis, 1968). During this late episode of Cenozoic orogeny, regional uplift resulted in major streams eroding successive, broad gravel-capped terraces. Farther downstream, alluvial fans spread across the eroded lowlands and continuing acidic volcanic outbursts in the Central Cordillera produced local mudflows and fans along basin borders which spread ash and pumice that choked some valleys (Van Houten and Travis, 1968). Several volcanic peaks occur within 150 kilometers of the study area and include Chiles, Cumbal, Azufro, Galeras, Bordoncillo, and Dona Juana. Apparently these volcanoes, together with other more distant volcanoes in Colombia and northern Ecuador were responsible for the sequences of ash deposits that are observed both capping and interbedded within the thick alluvial gravels of the Pacific Coastal Basin.

2.4 Pacific Coastal Basin Structural Geology

Structurally, the Pacific Coastal Basin can be divided into three sub-basins (Figure 2.4). The Payan Mining District occurs within the Tumaco sub-basin, which is structurally less complicated than the coastal sub-basins to the north and has regional structures trending along a northerly strike (Bueno S. and Govea R., 1976). The Tumaco sub-basin extends south from Gorgona Island to the

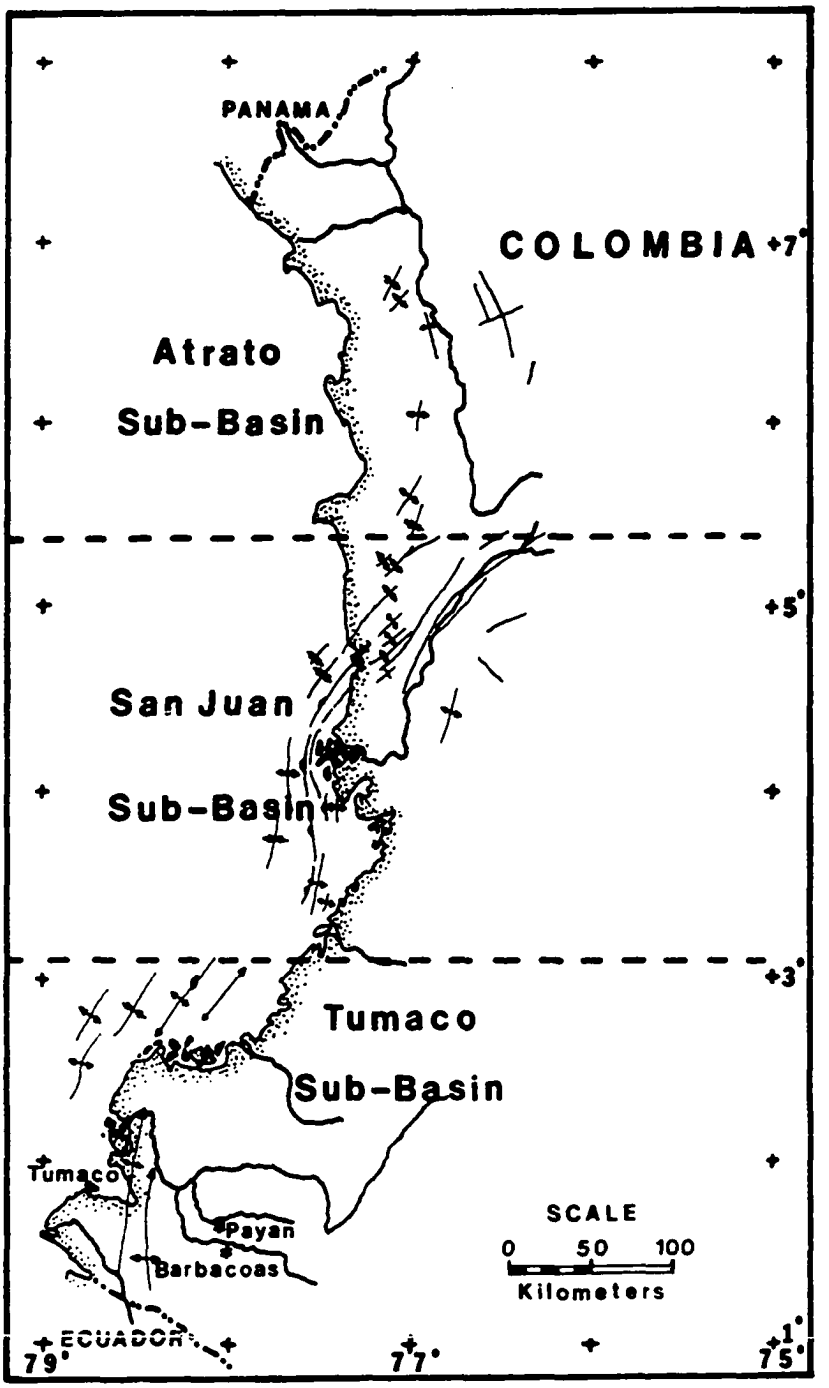

Figure 2.4 Structural geologic map of the Colombian Pacific coastal and shelf basins (after Bueno S. and Govea R., 1976).

Colombia-Ecuador border. Slightly folded structures, trending approximately north-south occur in many parts of the coastal plain in the Tumaco sub-basin and appear to control the trellis stream pattern that characterizes the middle and upper sections of the main rivers in this area (West, 1957). These folds are often expressed as hills of Tertiary age sediments and volcanics which protrude through the cover of Quaternary to Recent fluvial sediments and volcanics. Arango and Ponce (1982) mapped several north-trending anticlines and synclines, however, only two major anticlines are noted by Bueno S. and Govea R. (1976). The Remolino Grande Anticline lies north-northeast of Tumaco and plunges north into the lowermost Patia river valley. The Chagui Anticline, east of Tumaco Bay, also plunges to the north. It is one of the largest surface features in the basin, nearly 45 kilometers long and 15 kilometers wide (Bueno S. and Govea R., 1976), and forms a prominent radial drainage anomaly.

Mobil Exploration drilled the Chagui anticline approximately midway between Tumaco and Payan for oil in 1955 and although drilling went as deep as 3,995 meters, Eocene age strata was never reached (Bueno S. and Govea R., 1976). Oppenheim (1949) also observed similar very thick sequences of conglomerates, bluish-gray claystones, and siltstones, with recent deposits of tuffs and agglomerates. Additional offshore drilling locations

confirm that the Tertiary strata slope and thicken oceanward as a simple homocline (Irving, 1975).

2.5 Tumaco Sub-Basin Geomorphology

Like the rest of the Pacific coastal basin to the north, the Tumaco sub-basin can be divided into two distinct physiographic provinces: (1) the hill lands, and the Recent coastal alluvium (West, 1957). The hill lands comprise the greater part of the basin, especially south of Buenaventura, as a twenty to forty mile wide belt of low hills between the Western Cordillera and the Recent coastal alluvium. A product of recent stream dissection of Tertiary and Pleistocene sediments, the hill lands present a variety of land forms distinct from those of the alluvial plains. Although steep slopes prevail in most sections, along some streams narrow alluvial Pleistocene terraces occur with rolling to flattish topography. In their upper courses the streams have incised themselves deeply into the Tertiary sediments, in places creating shear rock cliffs that rise 15 to 35 meters above the water°s edge (West, 1957). Away from the main rivers, a maze of steep jungle covered slopes prevails, with local relief between 35 and 70 meters. The entire Tumaco - lower Patia area appears to be one of recent uplift, evidenced by former sea cliffs now stranded one to two miles inland from the sea and by steep-walled canyons incised by the Patia and Mira rivers in their lower,

middle, and upper courses. Moreover, numerous flat-topped hills in the lower Patia area and an extensive elevated plain (possibly the Chagui Anticline) north of the Mira suggest old erosional surfaces (West, 1957).

The landforms of the recent alluvial plain are formed chiefly by stream deposition and include present-day levees, levee remnants, and backswamp area. In places, such as near Buenaventura and Tumaco, Tertiary materials interrupt the continuity of the alluvium, and outcrop in low cliffs along the oceanfront. A great number of streams, large and small have deposited this coastal alluvium. Among the larger rivers are the Baudo, San Juan, Patia, and Mira, the latter two draining basins east of the Western Cordillera. Along its entire length, the coastal alluvial fringe appears to have been formed by coalescing of deltas and the lower alluvial fans of these rivers (West, 1957). Low natural levees and backswamps are common forms throughout, while mangrove, backed by freshwater swamp, predominate along the actual coastline.

In the northern half of the Tumaco sub-basin, the coastal plain rarely exceeds 25 kilometers in width, and is crossed by short rapid streams, such as the Micay, Naya, and Timbiqui (West, 1952a). In the southern half, the wide alluvial plain immediately north of the lower Patia measures 45 kilometers in width and is also crossed by the shorter Tapaje, Sanguianga, and Santini rivers to the north. This large deltaic/alluvial complex appears

anomalous, and may be chiefly the result of former deposition and subsequent abandonment by the Patia river system (Figure 2.5).

The upper and middle courses of the streams in the Tumaco sub-basin, like those along the rest of the western coast of Colombia are gold-bearing. Ancient gravels which form the hilly interfluves of the modern streams also contain gold. A belt of almost continuous upland gravels, five to ten miles wide, stretches along the base of the Western Cordillera from the upper Atrato area to the Colombia-Ecuador border. Most of these gravels appear to have been deposited in the late Pliocene or Pleistocene time by streams that had eroded into the gold-bearing massif that underlies the Western Cordillera (West, 1952a). Owing to recent tectonic forces, the modern streams have incised themselves into old alluvial surfaces, exposing in places the gold placers which occur within paleochannels. The modern river sands and gravels that form low terraces, bars, floodplain scrolls, and stream bottoms probably derive the bulk of their gold content from the old gravels which they have cut rather than from the lodes at their headwaters (West, 1952a; Garrett, 1985).

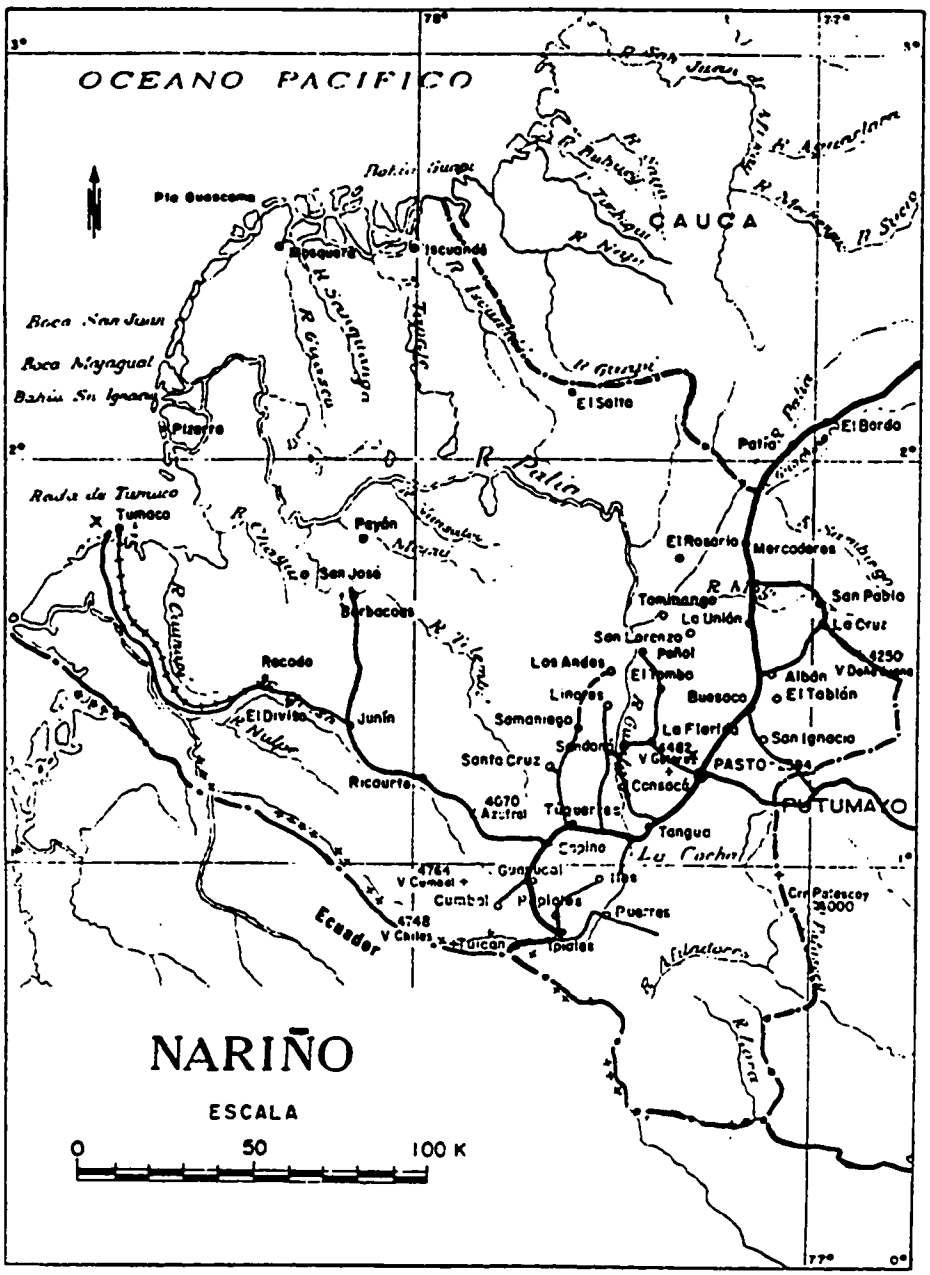

Figure 2.5 Generalized drainage map of the Tumaco sub-basin illustrating the short, high gradient streams to the north and the larger rivers like the Patia and Telembi to the south (after Rodriguez Guerrero, 1961).

CHAPTER 3: PREVIOUS WORK IN PAYAN MINING DISTRICT

3.1 Introduction

The Payan Mining District is defined here as a 12 square kilometer area surrounding the village of Payan and occurs within the drainage basin of the Rio Magui (basin area approximately 328 square kilometers, Figure 3.1). The village of Payan, on the banks of the Rio Magui, is the major population center along this river. To the south, along the Rio Telembi, lies the Barbacoas Mining District (Figure 1.1). Like the Payan Mining District to the north, the Barbacoas Mining District also contains rich placer gold deposits. The town of Barbacoas, which serves as the seat of government for this remote jungle region, is also the center of much of the present day gold transactions in both the Payan and Barbacoas Mining Districts. The village of Payan served as the field headquarters of CMCT which owned and operated the mining concessions immediately adjacent to Payan until 1986.

3.2 Early Reports (Pre-1980)

Although the Magui River basin area has been mined for placer gold since before the time of Pizzaro, little work has ever been published concerning the geology of the area

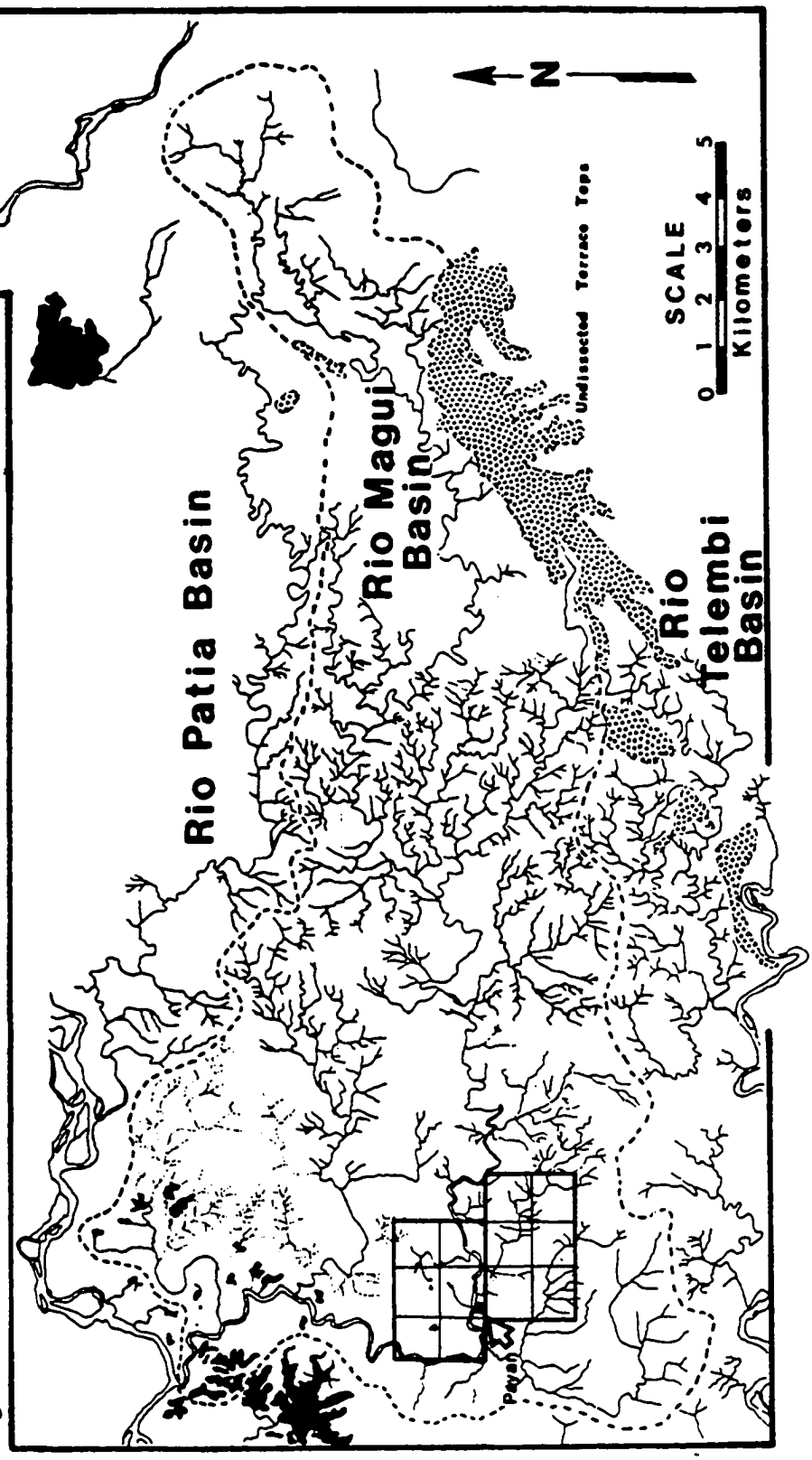

Figure 3.1
Map of the Rio Magui drainage basin (area inside the dashed lines) showing sections of the Rio Patia to the north and the Rio Telembi to the south. The grid pattern (around Payan) represents the study area (Plates 1 and 2). Note the high level terraces, dammed tributary lakes, and non-flowing streams (swamps and lagoons).

or the gold deposits. In 1937, Compania Minera de Narino drilled 317 holes into the Rio Magui floodplain near Payan, but gold values were below what was considered commercially feasible for mining at that time and no further work was done. The drilling was confined to the alluvial plains as their main concern was reserves for river dredge operations (Isenor, 1941). The Colombia Ministry of Mines undertook a drilling program of the Rio Magui alluvial plains and several unspecified terrace gravels in the Payan Mining District during the mid-1960's. Marginal gold values were encountered, but these were based on fire assays of the samples, which are often very erractic and not valid for evaluative purposes (Lusney, 1981).

Some Payan terrace gravels were sampled in 1975 in order to estimate the approximate gold content of the reserves (Darby, 1976). These preliminary results were very encouraging, but somewhat speculative due to the low density sampling scheme, an average of one sampling site per 0.2 square kilometers. Figure 3.2 depicts Darby's numbered sampled locations and the names and locations of other area mines. Some of Darby's tentative conclusions were as follows:

1) Pay zones of the Piccinini and La Junta Mines were considered the same horizon due to the similarity in stratigraphic sequence, gravel size occurrence of wood debris within sand units, similar elevations, and the proximity of the sites.

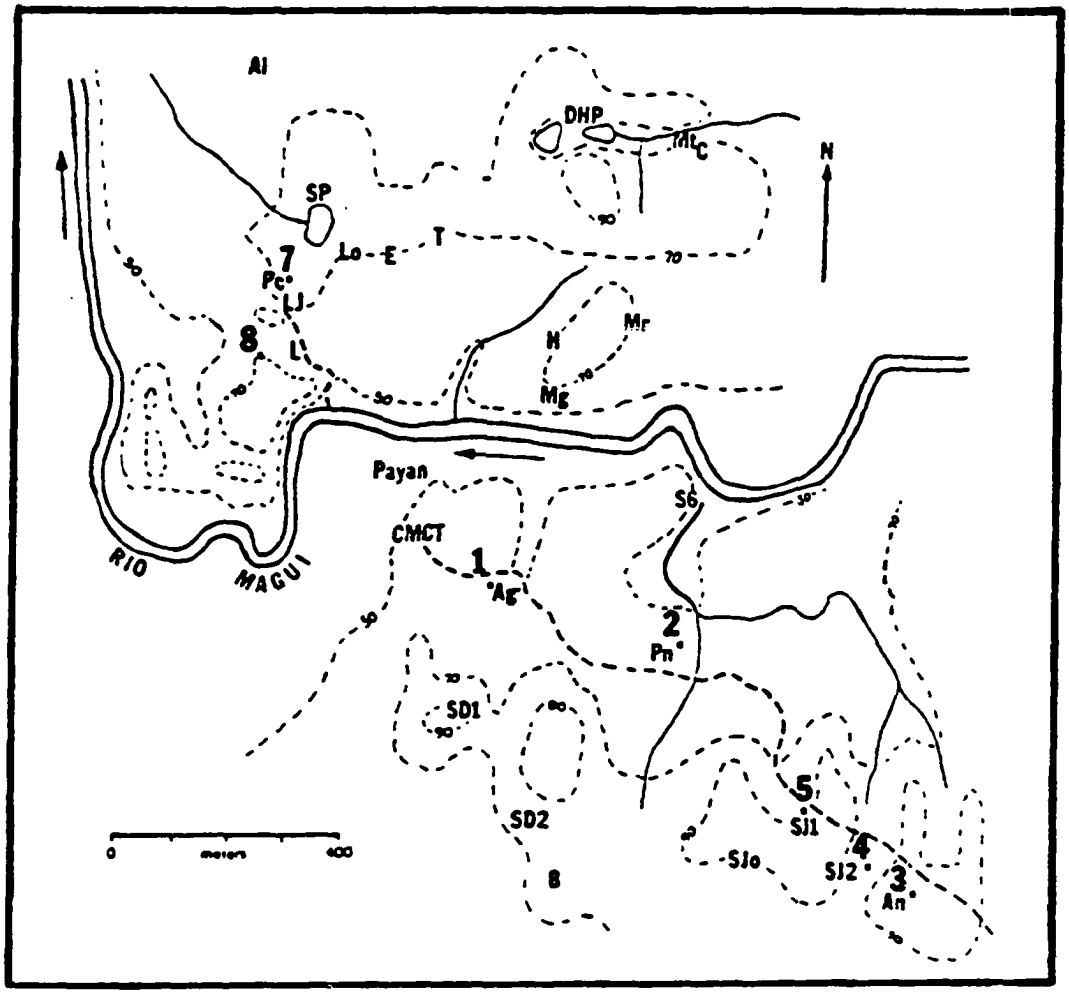

Figure 3.2 Generalized topographic map of Payan study area showing mine locations and sampled localities within the mining concession. The numbered locations (1 through 8) refer to the sampled locations of Darby (1976). The lettered locations are those features noted in Darby and Whittecar (1984) and this research (after Whittecar and Darby, 1984).

Mine Sites

Al = Alcose	Mr = Mariana
An = Ananias	Mt = Marta
Ag = Anguino	Pn = Panambisito
B = Blandito	Pc = Piccinini
C = Clarissa	SD1 = Santo Domingo I
E = Eepimenio	SD2 = Santo Domingo II
H = Hipolito	SJ1 = San Juan I
LJ = La Junta	SJ2 = San Juan II
Lo = Louisa	SJo = San Joaquin
L = Luis	S6 = Site 6
Mg = Magdalena	T = Travesia

2) Although the heavy minerals of the Anguino and San Joaquin Mines appeared to correlate with the heavy minerals of the Piccinini and La Junta Mines, they were not considered the same due to differences in gravel size, gravel types, weathering conditions, and stratigraphic sequence.

3) The San Joaquin Mine was tentatively correlated with the San Juan and Ananias Mines based on the similarity of heavy minerals, stratigraphic sequences, and the close proximity of the San Juan and Ananias Mines.

4) The gravels of the Piccinini and La Junta Mines contain pumice fragments similar to those occurring above the gravels at sites 2, 3, 4, and 5. This information, together with dip and imbrication data appears to support a paleoflow direction from the southeast to the northwest and implies that the Piccinini and La Junta Mines are stratigraphically higher (thus younger).

5) The gravels at the Anguino and Site 6 Mines are considered to be equivalent due to the similarities in heavy minerals, predominance of chert gravel, similarity of gravel texture and matrix color, and stratigraphic elevations.

3.3 CMCT Associated Studies

In 1981, CMCT contracted a professional engineer, J.E. Lusney, to visit the mining concessions and give recommendations on an exploration and exploitation program for the properties. His report emphasized the need for further geologic study, along with an extensive program for surveying the company land (Lusney, 1981).

To fulfill the needs pointed out by Lusney, CMCT hired a field geologist, H. Ortiz, to construct the necessary geologic maps and supervise the sampling and drilling

program. Ortiz (1982a) provided the first detailed lithologic descriptions for the Payan Mining District, and an informal stratigraphic framework. The mining concessions were divided into two parts, the north area was named the Piccinini Area, and the area south of the Rio Magui was named the San Juan Area. The following unit descriptions are those of Ortiz (1982a), (Table 3.1).

Within the Piccinini Area, (north of the Rio Magui), four lithologic units are identified:

1) Lowermost and oldest in the sequence is the Magdalena Formation. This lithified, blue-colored mudstone appears intercalated with layers of fine blue-colored sandstone, and is generally covered by recent sediments. The Magdalena Formation is the "bedrock" for the overlying gold-bearing "conglomerate" named the Piccinini Formation.

2) The Piccinini Formation is a cobble gravel with an intercalation of blue-gray auriferous "sandstone" (sand), often rich in wood debris. This formation is tentatively divided into three members: a lower "conglomerate" (cobble gravel) member, a middle "sandstone" (sand) member, and an upper "conglomerate" (cobble gravel) member. At least 18 meters of this formation are visible in the shaft and exposures in the Piccinini Mine.

3) Overlying the Piccinini Formation is the volcanic cover of the San Juan Formation - cineritic tuffs, agglomerates, and lapilli tuffs of dacitic composition. It is moderately to well cemented, fairly impervious, and generally little weathered. On the surface and towards the top, intense weathering has transformed the volcanic ash cover to sticky clay. This formation has thicknesses that vary between 5 and 30 meters.

4) The fourth unit of the Piccinini Area is the Recent Alluvium, (referred to as the Payan Formation in later reports by Ortiz), and is

Table 3.1 The stratigraphy of the Payan Mining District as proposed by Ortiz (1982a).

The Piccinini Area (north)		The San Juan Area (south)	
Alluvium (recent flood plain)			
Cineritic tuff, lapilli tuff, and agglomerates	San Juan Formation	Cineritic tuff, lapilli tuff, and agglomerates	San Juan Formation
------Paraconformity-------		------Paraconformity------	
Gold-bearing Upper Conglomerate Member	Piccinini Formation	Gold-bearing Conglomerate	San Joaquin Formation
Bluish-gray Middle Sandstone Member (containing wood pieces)			
Gold-bearing Lower Conglomerate Member			
////Angular Unconformity////		////Angular Unconformity////	
Blue mudstone and sandstone (Bedrock)	Magdalena Formation	Blue and white sand size tuff, with volcanic ash intercalations showing lapilli of dacitic composition	Ananias Formation

composed of the present floodplain sediments and gravels on the river benches of the Rio Magui system. This unit unconformably overlays the Magdalena Formation and the lower member of the Piccinini Formation.

In the San Juan Area (south of the Rio Magui), three lithologic units are identified:

1) Lowermost and oldest in this sequence is the Ananias Formation, a blue to white volcanic arenite, with intercalations of cineritic, lithic tuff and lapilli of dacitic composition. Only the top of the formation is observed, with thicknesses ranging between 1 to 5 meters. The Ananias Formation is also the "bedrock" of the auriferous San Joaquin Formation that unconformably overlies it.

2) The San Joaquin Formation "conglomerate" (cobble gravel) contains lenses of yellow "mudstone" (mud) and gray "sandstone" (sand) with wood fragments. The thickness of this unit ranges from 10 to 20 meters and is unconformably overlain by the volcanic cover of the San Juan Formation.

3) The San Juan Formation of this southern area is composed of cineritic tuff of dacitic composition, agglomerate, and by an underlying bed of cinerite, partially altered to kaolinite and montmorillonite. Observed thicknesses were typically between 7 and 20 meters.

Ortiz (1982a) established no general correlation between the strata exposed and described in these two areas. However, a speculative correlation was made between the strata at the Mariana Mine (north of the Rio Magui) and strata at the Anguino Mine (south of the Rio Magui); both were classified by Ortiz as comprising the three members of the Piccinini Formation.

Additional reports by Ortiz (1982b; 1983) discussed details of gold values based upon data from mine exposures, trenches, and shafts. The additional details did not change the overall stratigraphic framework previously established. Although Ortiz (1983) provided a geologic cross-section from Payan to the San Juan Mine, the field relationships between the Ananias Formation and Magdalena Formation and the Piccinini and San Joaquin Formations were not clearly defined.

Based on Ortiz's work, additional samples were collected, primarily from the "middle sandstone member" of the Piccinini Formation as defined by Ortiz (1982a), to further characterize the units, as well as propose possible depositional processes for their origin. Sieve, pipette, X-ray diffraction, and heavy mineral analyses of these samples enabled Darby (1983a) to make the following conclusions:

1) Principal component analysis did not confirm the expected correlation of the sand units in the Piccinini and Santa Ana Mines with the sands of the Hipolito and Mariana Mines, possibly due to the low number of samples from each sand outcrop.

2) Step-wise discriminant analysis unexpectedly grouped sand samples from the Piccinini Mine with sand samples in the San Joaquin Formation, relative to gray sands in the Mariana and Hipolito Mines.

3) Due to the low number of samples, relative to the larger number of variables; and due to the fact that several samples were panned in the field, caution should be exercised when any conclusions or interpretations are made concerning this heavy mineral data.

4) This approach confirms the correlation of the gray sands within closely spaced outcrops, but long distance correlations would require more detailed sampling.

5) Rounded and euhedral heavy mineral grains (i.e. monazite, sphene, and zircon) suggest a dual source area system, with both a distal source area and a more proximal source area.

Darby also stated that although there was insufficient evidence to separate sands of the Piccinini and San Joaquin Formations, their apparent differences in elevation and stratigraphic section (Ortiz, 1982a) warranted their tentative separation. Although a generalized cross-section of the strata in the area was presented, particular relationships such as that between the Magdalena and Ananias Formations were unknown. Based upon the shape, width/depth ratio, abundance of wood debris, and general lack of bedding structures, Darby (1983a) concluded that the sand layers were probably the result of braided streams eroding gold-bearing debris flows or "conglomerates" (gravels) upslope, and depositing medium to coarse sand in shallow channels along the valley floor. Darby's recommendations were primarily concerned with the need for a more detailed approach to sampling and mapping in the area, with special emphasis on the mapping and stratigraphy of the terraces (Darby, 1983a).

As an extention of the earlier work of Darby (1976, 1982a, 1982b, 1983) and Ortiz (1982a, 1982b, 1983), D.A. Darby and G.R. Whittecar proposed a research study to CMCT

to determine the geologic, geomorphic, and hydrologic characteristics of the Payan Mining District. The project involved three months of field research in the study area, during the summer of 1983, conducted primarily by Jim Garrett, and Michael Babuin and myself. The principal tasks of this field research were to:

1) prepare a topographic and geologic map of the study area based on elevations and locations established by surveying;

2) analyze the stratigraphic relationships between the gold-bearing units and adjacent deposits;

3) develop a history of geologic processes in the study area that may aid mining or future ex loration;

4) determine the gold content of the auriferous units at accessible sites (usually active or abandoned mine sites) throughout the concession areas; and

5) to assess the impact of the proposed mining upon the volume of flow, navigability, and water quality of the Rio Magui.

In their report, Darby and Whittecar (1984) revised the Payan Mining District stratigraphy of Ortiz (1982a) based upon field observations and preliminary laboratory evaluations. A comparative table of the various stratigraphic nomenclature and correlation of the surficial deposits in the Payan Mining District is presented in Table 3.2. The revised stratigraphy of Darby and Whittecar (1984) is as follows:

The Ananias Formation

Lowermost in the stratigraphic sequence is a lithified and compact ash with volcanic fragments (glassy to aphanitic andesite), subangular

	ARANGO AND PONCE (1982)	ORTIZ (1982)	DARBY & WHITTECAR (1984)
QUATERNARY	UNNAMED FORMATION "terraces and fans of fluvio-volcanic origin...."	PAYAN FORMATION	PAYAN FORMATION
			MAGUI FORMATION (included in the San Juan Fm. of Ortiz)
			PANAMBI FORMATION (included in the Piccinini Fm. of Ortiz)
		SAN JUAN FORMATION	SAN JUAN FORMATION
		PICCININI FORMATION SAN JOAQUIN FORMATION	ANTIGUA FORMATION
TERTIARY(?)		MAGDALENA FORMATION ANANIAS FORMATION	ANANIAS FORMATION

Table 3.2 A comparative table of the various stratigraphic nomenclature used for the Payan Mining District (after Darby and Whittecar, 1984).

quartz, and minor amounts of mica, basalt fragments, and magnetite (plus other opaques). Thin agglomerate layers (less than 20 centimeters thick) are interbedded with ash and reworked ash which show slump features and occasional convolute bedding. This ash, only observed in mine sluiceways, was informally named the Ananias Formation by Ortiz (1982a) and is named for the type section exposure in the Ananias Mine. The total thickness of this formation is unknown, but observations in mine sluices in the southeastern portion of the Payan Mining District substantiate thicknesses of at least 10 meters.

The Antigua Formation

Unconformably overlying the volcanic ash of the Ananias Formation is a basaltic cobble gravel unit of unknown thickness. Field observations from the Piccinini Mine show thick sequences of cobble gravel containing several lenticular bodies of sand. The deepest extent of this cobble gravel is observed only through drill hole and mine shaft excavations. According to Ortiz (1982a), this cobble gravel extends to a depth of at least 40 meters beneath the terrace surface. This cobble gravel was originally divided into two formations (the Piccinini Formation and the San Joaquin Formation) by Ortiz (1982a) on the basis of elevation and location differences. Based upon field exposures and laboratory analyses, these two formations are combined and informally renamed the Antigua Formation. It is believed to underlie most of the Payan Mining District and has placer gold accumulations within both the matrix of the cobble gravel and the discontinuous sand lenses that occur within the unit.

The San Juan Formation

Stratigraphically above the Antigua cobble gravel lies another ash deposit, informally named the San Juan Formation (Ortiz, 1982a). This ash appears as a white, blocky bedded ash with individual beds up to 2 meters, but normally less than 0.5 meter thick. Although this unit is exposed in all mines except for Anguino, Panambisito, Site 6, and Clarissa, the top of the San Juan Ash was not identified due to erosion or jungle cover. This ash is believed to have covered an active depositional surface of an alluvial fan. An examination of the numerous upper contacts of the Antigua Formation by the

San Juan Formation confirm that the calculated paleoslope closely approximated that of other humid alluvial fans.

The Panambi Formation

Following deposition of the San Juan Formation ash, streams incised deep valleys into the ash and Antigua gravels. A second cobble gravel unit, the Panambi Formation formed as a valley fill within the Magui River system. The Panambi Formation is named for the type section in the Panambisito Mine on the Panambi River. Typically observed within terraces with broad tops approximately 20 meters above the present day river system, this gravel unit contains smaller clasts than the older Antigua Formation cobble gravel and is composed primarily of chert and quartz-rich gravel clasts. It is postulated that the Panambi Formation was an extensively reworked gravel derived from weathered Antigua cobble gravels. The Panambi Formation also contains isolated lenses of volcanic muds and sands and is unconformably juxtaposed against both the Antigua Formation and the San Juan Formation.

The Magui Formation

Following the deposition of the Panambi Formation gravel valley fill, a very large volcanic event affected the area. Thick sequences of ash, observed in thicknesses as much as 10 meters, covered the Rio Magui basin. The Magui Ash occurs as the uppermost stratum on all terraces, except where removed by erosion. Informally named here as the Magui ash, this deposit is often extremely weathered to a clayey red mud.

The Payan Formation

Much of the mud derived from the San Juan Ash and the Magui Ash is observed today in the present-day alluvial plains of the Rio Magui. The sequences of sands, muds, and fine gravels found in the levees and flood plains of the Rio Magui are informally named the Payan Formation (Ortiz, 1983). The Payan Formation is documented extensively by Babuin (1985).

The data used for the preliminary results of Darby and Whittecar (1984, 1985) and Whittecar et al. (1984, 1985) also served as the basis for a trilogy of theses by Babuin (1985), Garrett (1985), and myself.

CHAPTER 4: FIELD AND LABORATORY PROCEDURES

4.1 Introduction

A four-phase plan was developed to determine the sedimentologic character and the stratigraphic correlation of the terrace sediments in the Payan Mining District. The preliminary results of this research appeared in Darby and Whittecar (1984). Since this publication, additional data has provided a fuller understanding and a greater certainty of the terrace deposits of the Payan Mining District.

4.2 Field Mapping

The first phase of the research involved mapping of the field area. Although recent maps of the mining concessions were available (Ortiz, 1982a), these maps were constructed using the pace and compass method which can be prone to error, especially in moderate relief and in heavily vegetated areas such as the Payan region. Use of a plane table surveying technique produced more accurate results. Initial base maps (1:2500 scale) were made by copying aerial photographs (approximately 1:60,000 scale) taken in 1960 onto slide film, projecting the slide at the proper scale, and tracing the location of rivers, ponds, cleared fields, buildings, and landmarks onto acetate field sheets.

The Bogota Grid System of longitude and latitude was incorporated onto these field maps based upon the maps of Ortiz (1982a, 1982b). All surveyed points were tied to the location and elevation of a brass benchmark in the Payan town square (47.42 meters above mean sea level: Ortiz, personal communication).

A plane table, alidade, and stadia rod were used to plot the location and elevation of each surveyed point on the base maps. Where possible, existing footpaths and trails were used to survey from the benchmark to outcrop locations. Often the extremely thick foliage had to be cleared by machete to permit surveying. Great pains were taken to survey to all known geologic exposures within the mining concessions so that later regional correlations could be made. With very few exceptions, nearly all exposures occurred within active or recently abandoned placer mine sites. The survey traverses were designed to intersect other traverses for closure accuracy. Between different surveys, the locations of the same mapped point varied by less than 12 meters (0.5 centimeter map scale). Elevations for the same point on separate traverses differed by no more than 0.8 meter, usually less than 0.3 meter.

Detailed survey data from the Santa Ana-Mirabel terrace was obtained from an unpublished report by Geoterra Y Asociados LTDA. Their surveying along five traverses was systematically checked and observed to be

consistently 12.5 meters lower than the currently surveyed data points. The Geoterra elevations were corrected by 12.5 meters to correspond to the present survey and the mapped locations incorporated into the survey maps. Contouring of the mapped survey points was done in conjunction with examination of stereographic aerial photographs of the field area. Although absolute surface elevations could not be determined from the photos, reliable approximations of the surface topography were derived on the basis of relative tree top heights. The new maps not only provided precise locations of these mine sites, but allowed contouring of the terrace configurations, and more importantly, allowed accurate elevation data to be applied to the geologic contacts exposed in the sediments. These data are very important for the stratigraphic correlation and depositional model studies.

4.3 Geologic Sampling

The second phase of the research involved the logging of the exposed sections within the mine sites and sampling of the observed units. This research was undertaken concurrently with the mapping phase. The logging and sampling of the exposures were conducted in relation to the elevation data so that precise elevations of the sedimentologic contacts and sample locations were available. The stratigraphic analysis included a primary

field description of the observed units followed by laboratory examinations of the collected samples. The sediment descriptions included sediment color, sediment texture, orientation of clasts, bedding structures (especially those which might serve as indicators of flow direction and flow regime), bed thicknesses, the amount of organic material (wood debris), and the nature of the contacts between observed units.

A total of 146 representative samples (each weighing approximately 450 grams) were collected in a vertical sequence at regular intervals or where visible sedimentological differences were present. A 10 gram split from 113 of the samples was wet seived at 2 phi size intervals from -1 to 4 phi, with all fractions examined under a binocular microscope for the following: overall mean grain size, maximum grain size, and type and relative abundance of grain lithologies. Samples included lithified volcanic lapilli of the lowermost ash unit; pebbles, sand and gravel, and wood fragments from the cobble gravel units; and ashes from the ash units which overlie them. In addition, heavy mineral fractions were field panned from 1.0, 0.5, or 0.25 cubic meter sand and gravel samples in order to obtain estimates of gold yield (Darby and Whittecar, 1984; Garrett, 1985). The estimated gold yields (in troy ounces/cubic yard) for the various sampled horizons in each mine are also listed in the stratigraphic sections in Appendix A.

4.4 Field and Laboratory Analyses

The third phase of research determined the mineralogic and sedimentologic character of the sediment samples in an attempt to correlate the stratigraphic levels that were sampled. After qualitative and quantitative methods described below identified discrete units within the sediments, an appropriate stratigraphic scheme was developed. This was no simple task, because stratigraphic studies in Colombia are hampered by a lack of a uniform code of stratigraphic nomenclature. Not only is the Pacific Coastal Basin poorly covered in the published literature, but the problem is further complicated by the complex tectonic and sedimentary history of the area, where abrupt vertical and horizontal facies changes are the rule rather than the exception (Bueno S. and Govea R., 1976).

4.4.1 Cobble Lithology Analysis

Within the exposed cobble gravel units, samples of 100 representative cobble clasts were identified as to lithology. The cobbles typically ranged in size from 10 centimeters to 35 centimeters, although occasional boulders were encountered which measured up to 2 meters in diameter. The condition of the cobbles varied from extremely weathered "mudballs" to relatively unweathered. Initially, it was thought that the degree of weathering and the thicknesses of the cobble weathering rinds would

aid in determining relative ages of the deposits. However, examination of the deposits in the field indicated that the cobble weathering was often influenced by the thickness of the ash overburden, the thicker overburdens tending to inhibit cobble weathering.

I used a type of cluster analysis to attempt to recognize the relationship between the cobble units and the various observed lithologies. The unweighted pair-group method was selected because all samples are given equal weight in the computation of the sample correlation. In principal, each sample in a cluster group has equal influence on the similarity measures of the whole cluster. The essential feature of theis particular method are as follows:

1) The correlation coefficient is used as a similarity measure.

2) Highest similarities are clustered or linked first.

3) Two samples can be connected only if they have the mutually highest corrleation with each other.

4) After two samples are clustered, their correlations with all other samples are averaged.

The computer program takes the information concerning the sample correlations and plots a dendrogram which graphically represents the correlation of the samples and clusters (or groupings of highly similar samples) with one another.

4.4.2 Cobble Orientation Analysis

The dip and direction of plunge of the longest axis of the same 100 elongated cobbles used for cobble lithogies was also recorded. This analysis involved removing matrix material from around the cobble and determining the longest axis of the cobble. A Brunton compass was used to measure the azimuth and dip of the long axis in the hopes of determining a preferential cobble orientation caused by the depositional processes often observed in fluvial/alluvial fan environments (Nilsen, 1982). These data were plotted on rose diagrams to evaluate cobble imbrication and paleoflow conditions (see also Appendix B).

In order to interpret if statistically significant preferred orientations existed in the collected cobble orientation data, I used the Tukey X^2 test to calculate the central tendency of the orientation distributions, as well as to test the significance of the determined trend (High and Picard, 1971).

4.4.3 Cobble Gravel Matrix Analysis

The cobble gravel units and the sand units that appear within them are the placer gold-bearing units in the area. It is for this reason that many of the earlier correlative studies (Ortiz, 1982a and 1983; Darby, 1983a) attempted to stratigraphically relate these units between terraces across the study area. Heavy mineral analysis of

28 cobble matrix samples were done for the 2 to 4 phi fraction (Darby and Whittecar, 1984).

Principal component analysis (PCA) was selected to examine this heavy mineral data because it requires no *a priori* classification of the samples and is conducted in an R-mode fashion, thus removing the problems of a closed array (the heavy mineral data summing to a constant value). Because PCA is a mathematical manipulation, rather than a statistical procedure, there is no test level of significance or measure of probability (Kim, 1975). It is simply one way to view this multidimensional problem in a reduced fashion, so that observations concerning samples and heavy mineral interrelationships can be made.

4.4.4 Volcanic Ash Analysis

Volcanic ashes, agglomerates, and lapilli tuffs in the field area occur above, below, and occasionally within the gold-bearing sands and conglomerates. Volcanic deposits are often useful stratigraphic markers. By correlating distinct ash horizons, not only is it be possible to correlate synchronous deposits, but it permits an estimation of the paleotopography because ashes often bury active erosional and depositional surfaces.

Due to the nature of the tropical climate of this area, extensive weathering of much of the ash material has occurred. Because this weathering has altered the texture

and composition of these ashes, a "whole rock" type of analysis would be useless. Magnetite grains within the ash samples were selected for analysis because of their easy separation, their resistance to weathering relative to volcanic glass, and their use in previous tephrochronology studies.

A 100 gram aliquot of each ash sample was placed separately into a blender and homogenized with a 1% sodium hexametaphosphate dispersant solution to aid in clay removal. The resulting solution was wet seived at 2 phi intervals between 0 and 4 phi. The 0 to 2 phi and 2 to 4 phi fractions were oven dried and further disaggregated with a rubber stopper. The 2 to 4 phi fraction was then sprinkled onto a paper sheet. A strong hand magnet behind a sheet of plexiglass was used to separate the magnetic grains from the non-magnetic grains. Two passes of the magnet suffuciently removed the majority of the magnetic grains. The magnetic separates were sonified in deionized water. The water was changed at 15 minute intervals and continued to be changed and sonified until the solution remained colorless. This procedure removed any remaining clay or alteration coatings. In an effort to remove any remaining non-magnetite grains from the sonified samples, heavy liquid separations were conducted using tetrabromoethane). A centrifuge procedure was selected using the methodology presented by Steen-McIntyre (1977). Acetone was used to wash the tetrabromoethane from the

magnetite grains. The resulting samples (22 including replicates) were then examined under a binocular microscope and any remaining non-magnetite grains were hand-picked and removed with a fine camel hair brush.

A small portion of each cleaned magnetite sample (approximately 0.01 g) was ground in an agate mortar to a fine powder and pipetted onto a glass slide for X-ray diffraction analysis. This procedure was used to determine the purity of the separations and would indicate if the sample were sufficiently clean for chemical analysis. If non-magnetite intensity peaks were encountered, then the sample was recleaned. Once sufficiently pure, the magnetite separations were fused and dissolved for trace element analysis with an atomic absorption spectrophotometer (AAS). Potassium pyrosulfate ($K_2S_2O_7$) was used as the fluxing agent in the fusion process (Reeves and Brooks, 1978; Bock, 1979; Jeffery and Hutchinson, 1981; and Tsang, 1985). The main usefulness of the pyrosulfate fusion technique is the conversion of insoluble oxides (e.g. magnetite) into more soluble sulphates. The mode of action of these melts is similar to that of sulphuric acid, but much higher temperatures can be reached.

Potassium pyrosulfate was produced by heating potassium hydrogen sulfate ($KHSO_4$) to 280° C which drove off water vapor and yielded $K_2S_2O_7$. The cleaned magnetite separations (approximately 0.1 g) were

mixed with potassium pyrosulfate in a 1:10 ratio. The mixture was then placed in a quartz crucible and fused in a muffle furnace at 350° C and slowly heated to 725° C. Samples were swirled at 425° C and 525° C during the fusion process to insure complete sample fusing. The potassium pyrosulfate begins to decompose at 300° C, is strongly oxidizing, and converts almost all metals to their sulfate form (Bock, 1979). Although sulfate gas is quickly produced between 500° C and 600° C, the fused melt was heated to 725° C to insure a complete reaction.

Samples were removed from the furnace and allowed to cool 5 to 7 minutes. Ten milliliters of 50% HNO_3 (redistilled nitric acid) was added directly to the crucible and allowed to dissolve the fused crystallized samples. The resulting solution was gravity filtered through prerinsed #2 Whatman Paper into a 50 milliliter volumetric flask and brought to volume with deionized water to a final concentration of 10% HNO_3. The filtrate was then analyzed for trace elements according to standard operating procedures with a Perkin-Elmer atomic absorption spectrophotometer (AAS). The AAS analysis of the volcanic ash magnetites provided elemental data for the following constituents: aluminium, calcium, magnesium, copper, iron, manganese, nickel, zinc, vanadium, titanium, and chromium. Standard addition analysis was incorporated into the procedures to evaluate the potential of matrix

chemical interferences. The results showed only negligible signs of any matrix interferences.

Discriminant function analysis was selected to statistically analyze the magnetite composition of each ash sample. This discriminating technique follows an initial computation of a linear combination of the variables which produces maximum separation of sample groups. This procedure requires that the initial data matrix have an *a priori* grouping of the samples. Except for the sample locations, the elevation of the sample was the only other parameter available for any type of an *a priori* classification scheme. Three ash groupings were selected which corresponded to the low elevation ash samples (less than 60 meters), middle elevation ash samples (70-90 meters), and high elevation ash samples (greater than 100 meters).

4.5 Stratigraphic Model Development

The fourth phase of this research was primarily concerned with determining the sequences of depositional events responsible for the emplacement of the observed sequences of sediments. Once the stratigraphy was established, a logical sequential pattern of development could be recognized. These results provide an improved model of humid tropical fan and terrace development as well as guidelines for future placer exploration in the area. Stratigraphic correlation of the terrace strata is

essential to permit accurate assessment of the auriferous deposits. An understanding of the processes responsible for the deposition of the sediments is also necessary for successful exploration.

CHAPTER 5: RESULTS

5.1 Introduction

This chapter relates the results of the field and laboratory procedures described earlier. For the purposes of objective discussion in this report, an informal stratigraphic scheme is used in this chapter. Fluvial units are labelled I, II, and III (oldest to youngest); and volcanic units are A, B, C, and D. After describing and discussing these informally named units, this stratigraphy will be compared to the formations proposed by previous workers.

5.2 Map of Payan Field Area

The newly surveyed map of the mining concessions in the vicinity of the village of Payan is presented in two parts. The Payan North Quadrangle (Plate 1) shows the location of Payan, the Rio Magui, and those surveyed areas to the north of Payan and the Rio Magui. This map represents an ara of approximately 6 square kilometers and contains 14 identified mine locations. General topography of this area is also indicated (contour interval is 10 meters).

The Payan South Quandrangle (Plate 2) shows the area immediately to the south and east of Plate 1. This map also represents an area of 6 square kilometers, but has only 9 indentified mine locations. Tributaries of the Rio Panambi (a minor tributary of the Rio Magui) drain much of this southern area, although some swampy areas are observed in an inter-terrace area 1 kilometer due south of Payan. As in Plate 1, the general topography is indicated along with a few cultural features. As can be seen from the maps, the area has a total relief of approximately 80 meters. Generally, the terraces appear to increase with elevation away from the Rio Magui; the highest terraces surveyed are greater than 120 meters elevation and occur more than 2 kilometers from the river.

5.3 Lithologic Unit Descriptions

Although each mine site had its own particular individual characteristics, most mines showed similar layers of near horizontal volcanic ash and cobble gravel strata. For detailed descriptions of mine sections see Appendix A. Darby and Whittecar (1984) developed a stratigraphy for the area based upon available field information and limited laboratory data. Based upon my detailed examination of the mine sections, observations of field relationships, and additional analyses of samples, I will present the sequence of informal stratigraphic units for the Payan Mining District (Figure 5.1). The

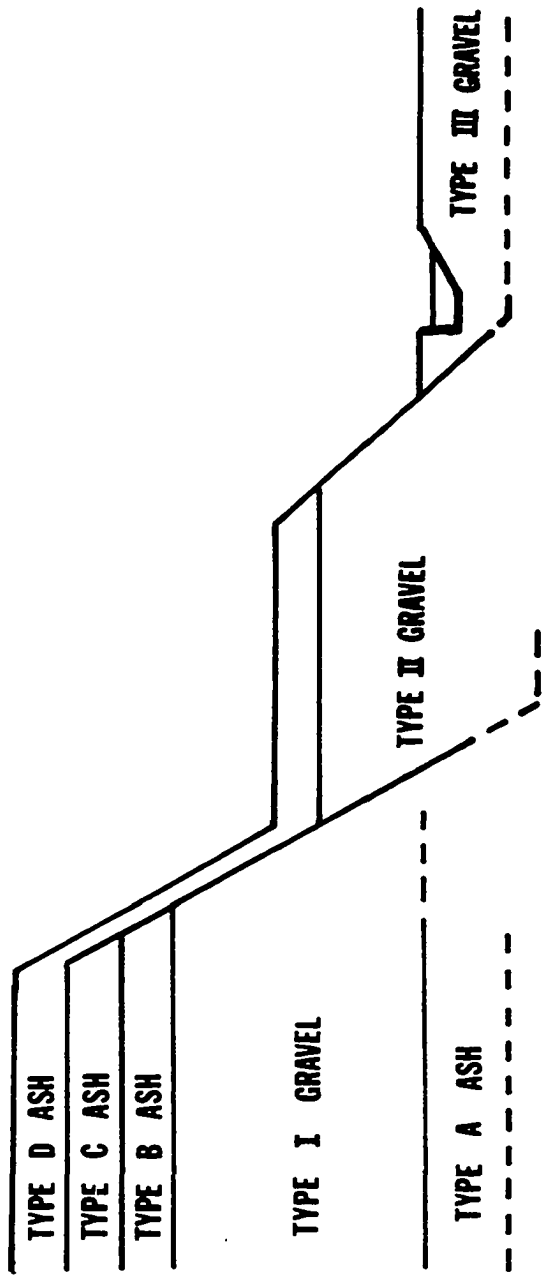

Figure 5.1 Generalized stratigraphic section of the Payan Mining District.

discussion chapter will determine if this stratigraphy is geologically accurate or if further revision is necessary to stratigraphically correlate the deposits in the Payan Mining District.

5.3.1 Type A Ash

The lowest stratigraphic unit observed in the Payan Mining District is a well indurated, reworked andesitic ash and agglomerate (Type A ash). The cemented and well indurated ash and agglomerate of the Type A ash forms the only true lithified rock unit in the Payan Mining District. The Type A ash is observed only in mine sluiceways. As much as 10 meters of this formation are observed in a deep sluiceway near the Ananias Mine. It is also identified in the San Juan Mine, with similar indurated ash mudstones in the sluiceways of the Hipolito, Magdalena, Mariana, and Santo Domingo I Mines. It is thought that the Type A ash may underlie the entire basin.

5.3.2 Type I Cobble Gravel

Unconformably overlying the Type A ash are the Type I cobble gravels. The unit is best observed in the exposure at the Piccinini Mine where the terrace had been cleared by CMCT during exploration. In addition, mine shaft and drill hole data extended the vertical extent of outcrop to over 30 meters. The Type I cobble gravel comprised over 20 meters of this exposure which included two weathered

sand lenses in the upper 10 meters. The cobbles were well rounded, primarily in contact with one another, and appeared to be somewhat imbricated. Average cobble size ranged between 15-20 centimeters, however several large (greater than 40 centimeters) boulders were observed. Matrix material is a coarse sandy gravel that has been generally weathered to clay. Overall there appears to be no observable bedding structures in the cobble gravel sequences, however this massive nature may be due in part to the extensive weathering of these exposures which might tend to remove or obscure the more subtle stratification features. The only apparent bedding is observed within the sand lenses of this formation.

The lower sand lens seen in outcrop at the Piccinini Mine is approximately 1 meter thick and is continuous across the outcrop (Appendix A). Although the sand is medium to coarse in original texture, it has weathered to sticky clay. Occasionally trough and ripple cross-bedding has been preserved in the sand lenses, with abundant wood fragments typically dispersed throughout the sand. The upper sand lens measured 40 centimeters at its thickest point and wedged out at both ends of the outcrop. Wood debris is absent from this lens as well as the depositional structures observed in the lower lens. Weathering has also altered this medium sand to clay.

5.3.3 Type B and C Ashes

The Piccinini Mine also afforded one of the few exposures of the surficial volcanic ash deposits. The Type I cobble gravel is paraconformably overlain by the Type C ash, a red to gray volcanic ash unit that measures nearly 10 meters in thickness. The Type B and Type C ashes are observed in outcrop in the San Juan Mine, and appear as possibly separate members of a volcanic ash. The Type B ash is lowermost, and is a white, blocky unit that has been altered to kaolinitic clay and is observed only in the San Joaquin and Ananias Mines. Paraconformably overlying the Type B ash within these two mines is the red clayey ash-agglomerate here referred to as the Type C ash. The Type C unit is observed in very thick sequences in the Santo Domingo I Mine, and comprises the ash which paraconformably overlies the Type I gravels in the other mines in the area.

5.3.4 Type II Cobble Gravel

The Type II cobble gravel is best observed in a section that occurs along the Rio Panambi (Plate 2) within the Panambisito Mine. The Type II cobble gravel is very different from the Type I cobble gravel by the fact that Type II displayed extremely variable bedding pattern and contained interbedded muds, silts, sands, and fine gravels, within small clast-size (average size 10 centimeters) cobble gravels. At the Panambisito Mine,

logs and tree stumps (not in life position) of up to 50 centimeters in length were also recorded. The exposures of the Type II Unit exhibit channel-like stratification of the cobble gravel units, which is not the case in the Type I cobble gravels.

Within the sequence in the Piccinini Mine, the stratigraphic relationship between the Type C ash, the Type II cobble gravels, and the Type D ash is observed. Overlying the Type C ash, is a red-brown cobble gravel that is approximately 1 meter in thickness. This cobble gravel is quite different from the underlying Type I cobble gravels in clast size and composition. This uppermost cobble gravel unit fits the description of the Type II cobble gravel and is most likely part of this unit. Above this cobble gravel is another red to white ash layer (the Type D ash) which grades into the surficial soil. The uppermost ash is observed blanketing all mine exposures except where removed by erosion.

5.3.5 Type D Ash

The Type D ash paraconformably overlies the Type II cobble gravel. This ash unit is observed in only a few mine sites as it forms the surface of the terraces and is altered by soil development or covered with dense jungle vegetation. In several mine sites, as in the Panambisito Mine, clear examination was possible. The Type D ash has weathered to a sticky red clay. The ash typically reaches

thicknesses of greater than 5 meters, but a total thickness is not known. Stratigraphic structures such as distinct layering observed in the Type C ash are not present. Any initial bedding features have been weathered out completely and the Type D ash appears as a massive ash unit.

5.3.6 Type III Gravel

The youngest unit in the Payan Mining District consists of floodplain silts and muds and channel sands and gravels of the present-day Rio Magui. Hand augering of the floodplain deposits during the summer of 1983, and the earlier report of Isenor (1941) have established thicknesses of several meters of these fluvial sands and gravels. The surficial floodplain deposits along the Rio Magui are typically silty, fine-grained sands 1-2 meters thick with occasional clay lenses. Below these surficial sand layers lies a coarse sand and gravel unit which comprises the bed of the Rio Magui for most of the surveyed length of the river (Babuin, 1985). The sands and gravels within the present-day channel exhibit a variety of sedimentary features such as ripples (straight crested, undulatory, and lingoid), sand waves, lunate megaripples, winnowed heavy mineral concentrations, and cross-bedding (planar, trough, and ripple) (Babuin, 1985).The Type III gravels are small, well rounded, almost entirely chert and quartz lithologies, and contain some

cobble sized clasts typically on the upstream portions of mid-channel, side, and point bars. Also of some significance are the organic deposits of leaf mats and wood debris observed in the bar sequences. The wood debris included reeds, bamboo stems, logs, tree trunks, and in certain instances entire trees, which appears to be similar to that observed in the Type II cobble gravel.

5.4 Cobble Lithology Analysis

Most of the cobble gravel units exposed in the mine sites appeared to be dominated by basalt and basalt porphyry cobble lithologies (Table 5.1). The most noticeable feature of the cluster analysis based on the cobble lithologies is that the strongest groupings occur among adjacent or nearby mine locations within the same terraces (Figure 5.2). The Piccinini and La Junta Mines, which occur on opposite sides of the same terrace, show the highest similarity coefficient (0.9953). This high correlation might be expected given the close proximity of these mine sites.

Another factor that might influence the clusterings of these samples could be the stratigraphic position or elevation of the sample. A change of source area lithology would result in a change in cobble lithologies derived from that source rock. In outcrop, a stratigraphically lower (older) cobble gravel would reflect the lithology supplied to the basin or reworked at

Table 5.1 Clast lithologies from cobble gravel units based upon counts of 100 clasts at each mine site. Upper and lower designations refer to the position of the sample relative to a bedded sand layer.

COBBLE LITHOLOGY / MINE SITE	ALCOSE	ANANIAS	ANGUINO	BLANDITO	HIPOLITO	MAGDALENA	MARIANA (Upper Gravel)	MARIANA (Lower Gravel)	MARTA	PICCININI (Upper Gravel)	PICCININI (Lower Gravel)	LA JUNTA	PANAMBISITO	SANTO DOMINGO I	SANTO DOMINGO II	SAN LUIS (Upper Gravel)	SAN LUIS (Lower Gravel)	SAN JOAQUIN	SAN JUAN	TRAVESIA
BASALT	20	13	--	10	45	7	4	14	46	23	35	27	2	22	11	22	26	46	30	7
WEATHERED BASALT	26	4	--	21	--	13	3	--	2	39	17	37	6	18	24	46	46	3	22	12
BASALT PORPHYRY	11	50	--	--	--	39	1	38	--	8	17	10	--	--	26	3	2	25	1	25
WTHD. BASALT PORPHYRY	26	3	3	24	10	11	1	25	12	18	19	20	24	23	10	10	17	4	7	27
CHERT	6	2	55	5	--	--	3	1	--	4	2	2	88	7	--	10	5	--	2	--
QUARTZ	4	--	20	13	1	2	7	4	7	3	--	--	--	14	--	2	1	11	--	1
GRANODIORITE	6	--	--	--	--	--	--	1	--	--	--	--	--	--	--	--	--	4	--	--
DIORITE	--	--	--	--	--	--	--	3	--	1	--	1	--	16	15	--	--	--	--	1
WEATHERED DIORITE	--	20	--	--	--	--	1	7	--	6	--	--	--	--	--	--	--	--	4	--
DACITE TUFF	--	5	--	--	--	--	5	--	--	--	--	--	--	--	--	--	--	--	6	--
WEATHERED DACITE TUFF	--	--	--	--	--	8	--	--	--	--	--	--	--	--	--	--	--	--	--	--
SCHIST	--	--	--	--	--	2	1	--	--	--	--	--	--	--	--	--	--	--	--	--
WEATHERED SCHIST	--	--	--	--	--	1	1	--	--	--	--	--	--	--	--	--	--	--	--	--
GNEISS	--	--	--	--	--	--	19	--	--	--	--	--	--	--	--	--	--	--	--	--
WEATHERED GNEISS	--	--	--	--	--	--	24	1	--	--	--	--	--	--	--	--	--	--	--	--
RHYOLITE	--	--	--	--	--	--	--	--	--	2	2	3	--	--	--	2	3	--	--	--
RHYOLITE PORPHYRY	--	3	--	--	--	--	--	1	--	--	--	--	--	--	--	4	--	--	--	--
"MUDBALL"	--	--	22	27	44	--	17	4	33	3	3	1	--	--	8	--	1	2	27	8
OTHER	3	--	--	--	--	16	15	1	--	--	--	--	--	--	6	--	--	6	--	--
TOTAL COUNT	102	100	100	103	100	94	106	104	98	102	104	102	102	100	105	98	102	102	99	101

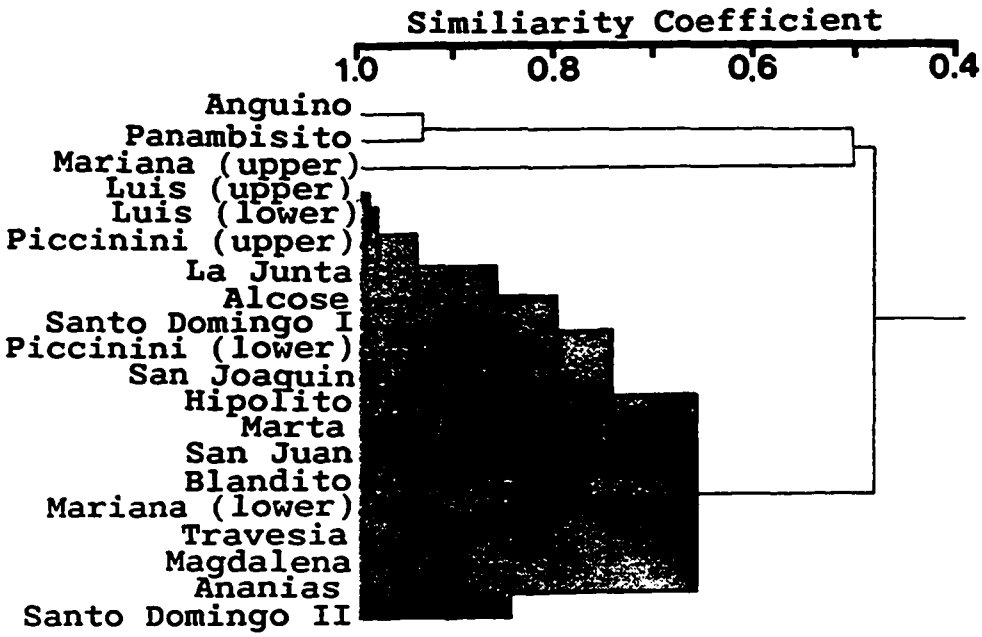

Figure 5.1 Cluster analysis dendrogram of the cobble lithology data. Upper and lower designations refer to the position of the sample relative to bedded sand layers. Shaded samples were primarily basalt, while the white samples were predominately quartz and chert.

that time. A stratigraphically higher cobble gravel, even derived from similar source areas reflects the source materials available at that time. Thus, the cobble lithologies have a temporal relationship and could be expected to subtly change with time. It would seem sensible that cobble samples taken from adjacent mine locations and at similar elevations should tend to be similar if indeed they are the same cobble unit and deposited at the same time.

Nearly all the cobble samples display a high similarity and correlate above the 0.75 similarity coefficient. This relatively high correlation is probably due to the fact that most mine site cobble gravels are dominated by basaltic cobble lithologies. Notable exeptions to this general observation are the cobble units exposed in the Anguino Mine, the Panambisito Mine, and the upper cobble gravel unit exposed in the Mariana Mine. An examination of the cobble lithologies shows that these exposures are relatively deficient in basalt. The Anguino and Panambisito Mines are rich in chert and quartz-rich rocks, while the upper cobble gravel unit in the Mariana Mine is predominantly metamorposed basalt cobbles. The upper Mariana Mine sample was basaltic in nature, however, they appeared to have a slight metamorphic character, as well as possessing a high degree of quartz veining. It is for this reason that the upper Marina Mine was classified as sheared basalts and cluster separately on the cluster

dendrogram (Figure 5.2). The Anguino and Panambisito Mines are nearly devoid of the basaltic cobbles that are so prevalent in practically all sampled locations. These two mine locations are also in the lower elevation terraces which are closer to the Rio Magui than terraces containing basaltic cobbles. In addition, these two sites also have smaller overall cobble sizes than the other mine sites. Several mines had cobble units with boulders as large as 1.5 meters, but the average cobble size was about 25 centimeters. In the Anguino and Panambisito Mines, cobbles were typically less than 15 centimeters (long axis).

5.5 Cobble Orientation Analysis

Individually, the rose diagram plots of the cobble orientatin appear to show various paleoflow directions (Figure 5.3). When significant central tendencies are plotted on a map, the relations become more easily visible (Figure 5.4). Most of the cobble units exhibit a rose diagram which indicates flow from the east and southeast. This trend follows the modern drainage to the west. The general pattern of the Tertiary and Quaternary alluvial formations appear to indicate a paleodrainage from the southeast to the northwest. Most of these paleoflow orientations were significant based on the Chi-square tests (Appendix B). Random orientations were observed only in the Marta, Luis, and Travesia Mines.

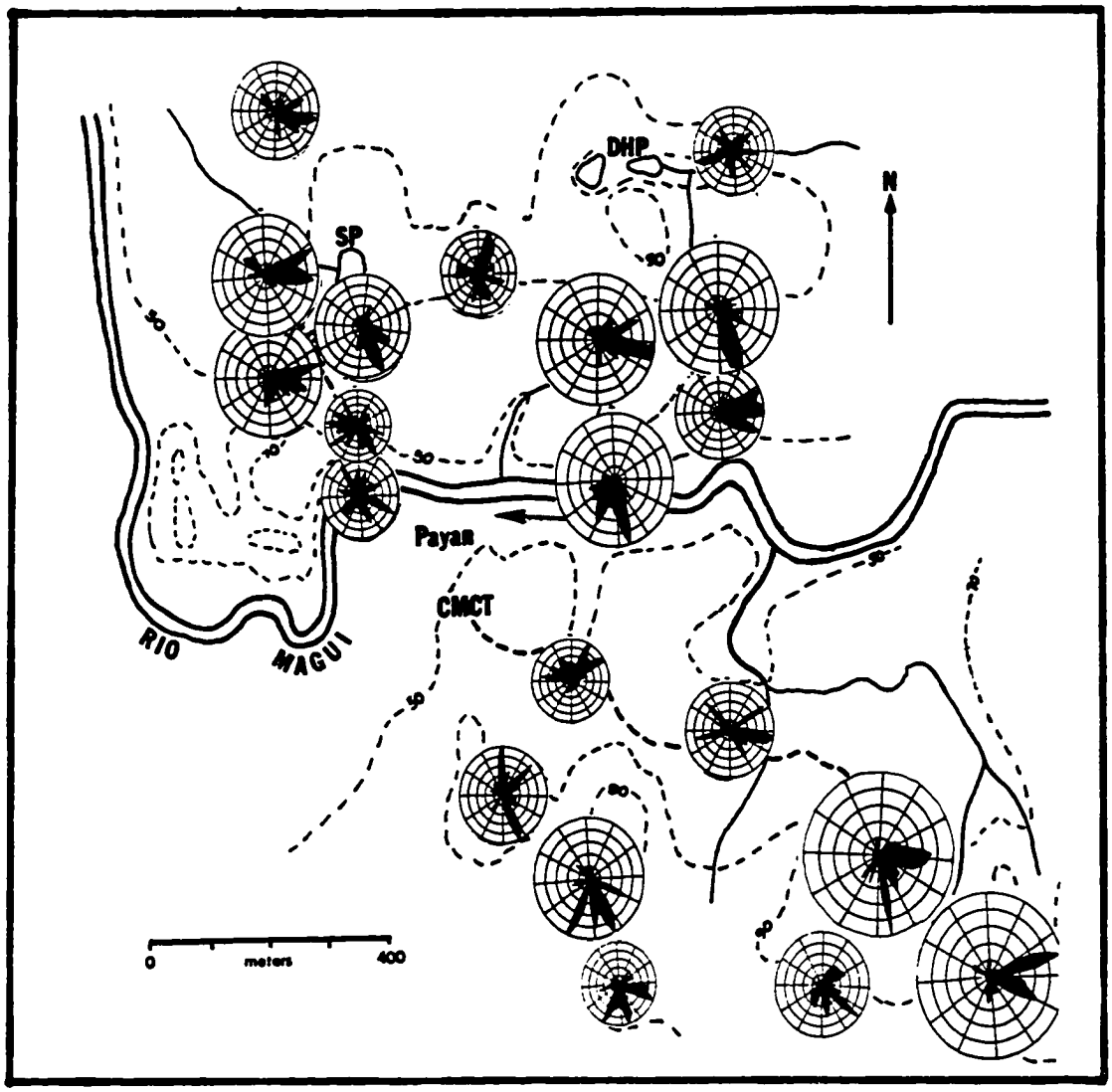

Figure 5.3 Map of the study area with rose diagrams of the cobble imbrication orientations for the various mine sites. Peak frequencies and tests of significance are located in Appendix B.

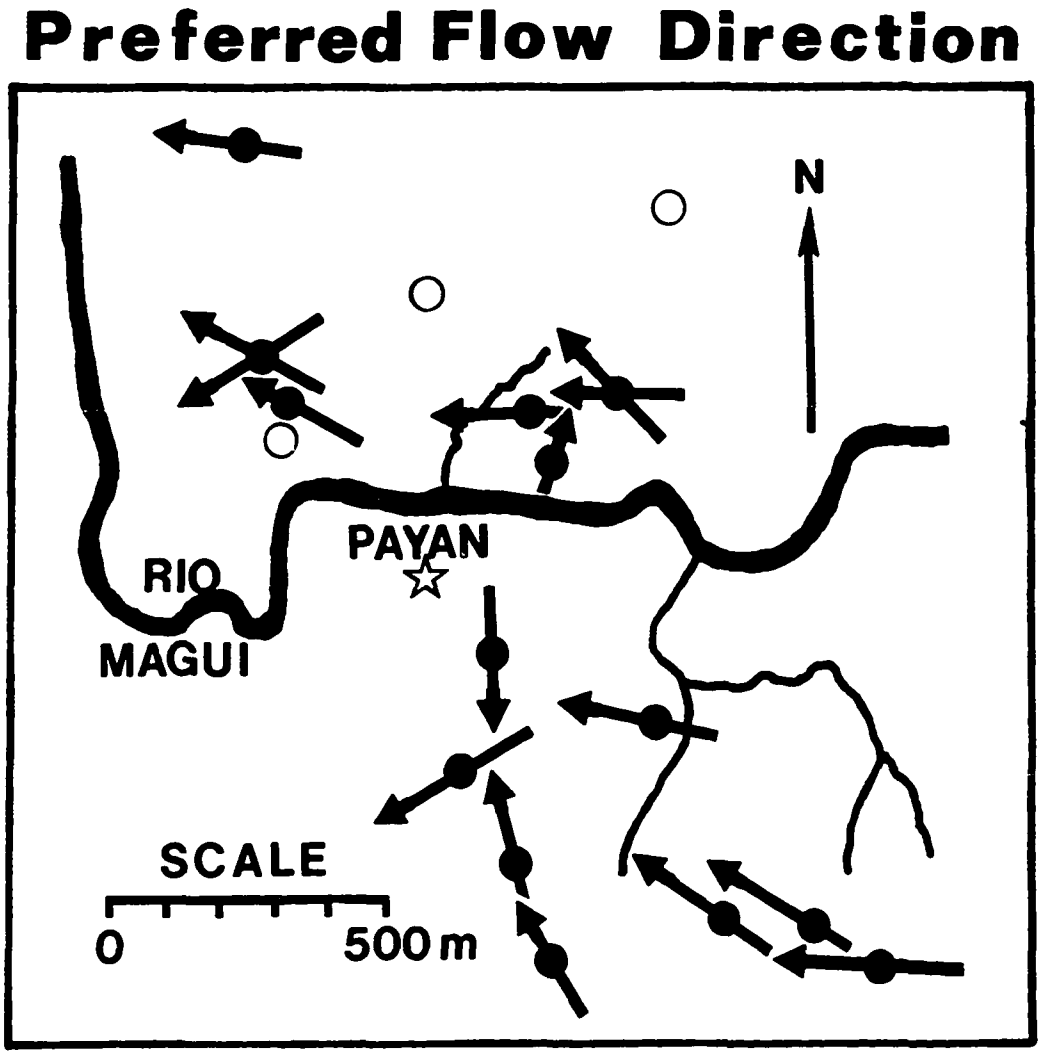

Figure 5.4 Generalized study area mine location map showing the preferred flow directions for the imbricated cobble gravels in each mine site. Open circles indicate those locations which displayed no significant trend. Arrows show paleoflow direction (downstream).

5.6 Cobble Gravel Matrix Analysis

Both rounded and euhedral mineral grains, suggesting a dual source involving proximal and distal sources were found in nearly all heavy mineral samples from the Antigua Formation. The percentage of rounded hornblende and zircon, sphene and monazite ranged between 60% and 95% for all but four samples. These four samples had 10% to 40% rounded grains and may reflect a greater influence from the proximal source area (Table 5.2).

Examination of the computer results (Appendix C) indicates that nearly 90% of the total variance can be accounted for in the three eigenvectors; 95%, if the first four eigenvectors are considered. These results suggest that plots of the first to third principle components show a fairly accurate rendition of 17 dimensional space reduced to two dimensions and illustrate the maximum variance between groups of samples.

The first three eigenvectors accounted for 90% of the variance (Appendix C). Factor 1 represents nearly 55% of the variance and hornblende is the most important variable, having a 0.991 loading on the primary eigenvector. Zircon and sphene also rank high in importance, -0.706 and -0.626 respectively, however the loadings are negative, meaning that these variables are inversely related to the first principle component. Factor 2 represents an additional 23% of the total variance and has high positive loadings from both

Figure 5.2 Heavy mineral (specific gravity greater than 2.89) percentages for cobble gravel matrix (0.06 - 0.25 millimeter) exposed at Payan mine sites. See Appendix A for sample locations.

	SAMPLE NUMBER													
MINERALS	ALC-3	HIP-6	MAR-8	ANG-3	HIP-9	HIP-3	SJO-4	TRA-3	MAG-5	ANA-1	EPI-1	SJU3/4	Site 6-1	SJO 5
HORNBLENDE (ROUNDED)	14 (40)	13 (90)	6 (85)	5 (70)	7 (70)	4 (80)	12 (80)	39 (30)	43 (85)	40 (15)	32 (65)	22 (85)	18 (35)	25 (85)
ZIRCON	12	14	22	16	19	32	15	11	4	Tr	3	13	8	0
SPHENE	12	20	8	18	15	0	15	3	8	8	5	0	10	0
MONAZITE (Z,S,M, ROUNDED)	16 (35)	13 (90)	18 (90)	10 (75)	11 (70)	5 (85)	0 (85)	0 (25)	2 (95)	8 (15)	15 (60)	0 (90)	3 (30)	15 (75)
EPIDOTE	0	0	0	Tr	0	0	0	0	1	0	0	3	0	0
ANDALUSITE	36	36	40	45	43	48	44	37	33	35	31	45	46	37
ALUNITE	0	0	0	0	0	0	5	0	0	0	0	8	0	0
WOLLASTONITE	0	2	4	0	0	0	0	0	0	2	0	0	0	16
HEMATITE	0	0	0	0	0	0	0	0	0	0	5	0	0	0
APATITE	0	2	0	0	0	0	0	2	0	0	0	0	1	0
BIOTITE	2	0	3	5	1	4	4	0	2	0	2	7	5	3
OLIVINE	0	0	0	0	0	0	0	0	0	0	0	0	0	0
RUTILE	0	0	0	0	0	0	0	0	0	0	0	0	0	0
GARNET	1	0	0	0	2	0	0	4	4	0	0	0	0	0
CASSERITE	0	0	0	0	0	0	3	1	0	2	0	0	5	0
TOPAZ	7	0	0	0	1	2	2	0	0	5	7	2	0	0
TOURMALINE	0	0	0	0	0	4	0	3	4	0	0	0	3	5

Table 5.2 Concluded.

MINERALS	SAMPLE NUMBER													
	SDI-3	MAR-4	SDI-2	SJO-3	SDII-9	SDII-7	MAG-2	MAR-3	MAG-7	MIP-4	PAN-3	ANT-1	ANG-2	PAN-2
HORNBLENDE (ROUNDED)	46 (20)	50 (10)	62 (10)	57 (85)	53 (35)	31 (15)	36 (75)	40 (50)	23 (85)	16 (55)	4 (85)	7 (90)	4 (80)	6 (15)
ZIRCON	7	9	3	7	2	9	27	13	7	19	39	20	13	46
SPHENE	7	10	0	0	2	20	0	15	13	28	20	19	34	22
MONAZITE (Z,S,M, ROUNDED)	8 (10)	2 (5)	8 (15)	3 (90)	1 (35)	13 (15)	13 (70)	11 (55)	15 (90)	5 (60)	10 (90)	26 (85)	32 (75)	0 (10)
EPIDOTE	0	0	0	0	11	1	0	0	0	1	0	0	0	0
ANDALUSITE	23	21	11	20	25	24	20	20	27	25	13	12	15	8
ALUNITE	0	0	0	0	2	0	0	0	0	0	0	0	0	4
WOLLASTONITE	0	0	0	0	0	0	0	1	0	0	12	8	0	0
HEMATITE	0	0	0	0	0	2	0	0	0	0	0	0	0	0
APATITE	0	2	Tr	0	Tr	0	2	0	4	0	0	0	0	0
BIOTITE	0	1	1	3	1	0	4	0	0	0	0	1	0	0
OLIVINE	2	0	0	1	0	0	0	0	4	1	0	0	0	0
RUTILE	0	1	5	0	0	0	0	0	0	0	0	0	2	1
GARNET	0	0	0	0	0	0	0	0	3	0	0	0	1	11
CASSERITE	0	0	0	0	0	0	0	0	0	0	0	0	0	0
TOPAZ	Tr	0	0	0	3	0	0	0	0	0	2	0	0	0
TOURMALINE	7	5	9	9	0	0	0	0	4	6	0	7	0	2

No counts made on sample numbers: Site 6-2, MAG-1, BLA-4, BLA-3, CLA-1, and CLA-2 as all were nearly 100% opaques.

andalusite (0.975) and biotite (0.629). Hence, these two minerals have the most significant contribution to the second principle component. Factor 3 accounts for nearly 12% of the total variance. Monazite has a positive loading of 0.736, while zircon has a negative loading of -0.602. Thus it can be observed that the first three eigenvectors have a total of six variables (hornblende, zircon, sphene, andalusite, biotite, and monazite) which are the most influential from the total of 17 variables.

In the plot of the first two principle components (Figure 5.5), a noticeable separation of sample groupings occurs. The low elevation samples (Pan-3, Pan-2, Ang-2, and Ant-1) from the Panambi Formation of Darby and Whittecar (1984) clearly separates from the other samples. Oddly enough, samples Ang-3 and Site 6-1, which are located in low elevation terraces near the river and also believed to be from the Panambi Formation, group with other higher elevation mine samples instead (Figure 5.5). Both of these samples have 5% biotite and contain about three times the amount of andalusite (45%) as that of other Panambi Formation samples (0% to 1% biotite and 8% to 15% andalusite) (Table 5.2). In general most Panambi samples tend to exhibit a heavy mineral assemblage impoverished in hornblende and biotite and enriched in zircon and sphene.

Figure 5.5 Plot of the two principal components of the heavy mineral types in the cobble gravel matrix samples. Note the relative separation of the Type I samples (squares) from the Type II samples (circles).

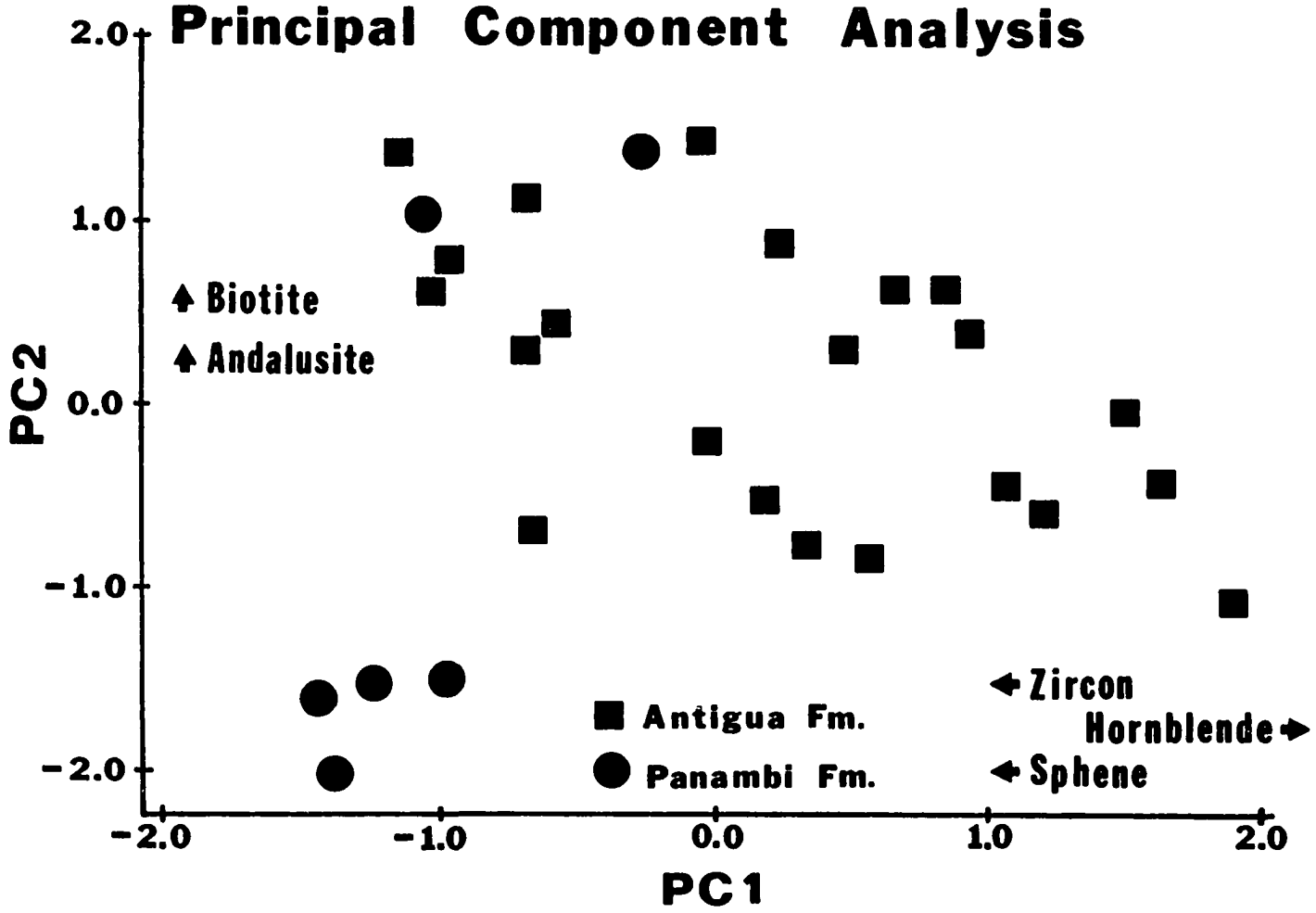

5.7 Volcanic Ash Analysis

The chemical data from the AAS analysis of the volcanic ash magnetite (Appendix D) was evaluated by means of a step-wise discriminant analysis which evaluates the variables and determines which variables best identify and discriminate *a priori* group memberships which were based on sample elevations. In this fashion, the influence of confounding and/or non-essential variables are removed from the analysis. A combination of the remaining, significant variables is used to define the canonical discriminant functions, which are the axes by which the groups show the best separation. Six variables (Mn, Al, Ti, V, Cr, and Mg) best discriminate these ash groups (Appendix D). The graphical plot of the individual samples in Figure 5.6 illustrate the chemical interrelationships between the samples and the groupings. The accuracy of the discriminant functions can be determined by classifying the original data set to observe how many samples are correctly classified by the variables being used. The procedure for classification involves the use of a separate linear combination of discriminating variables for each group and produces a group membership probability for each sample (Klecka, 1975). The samples have high probabilities of correct group membership and appear to be related to the initial *a priori* grouping (see Appendix D).

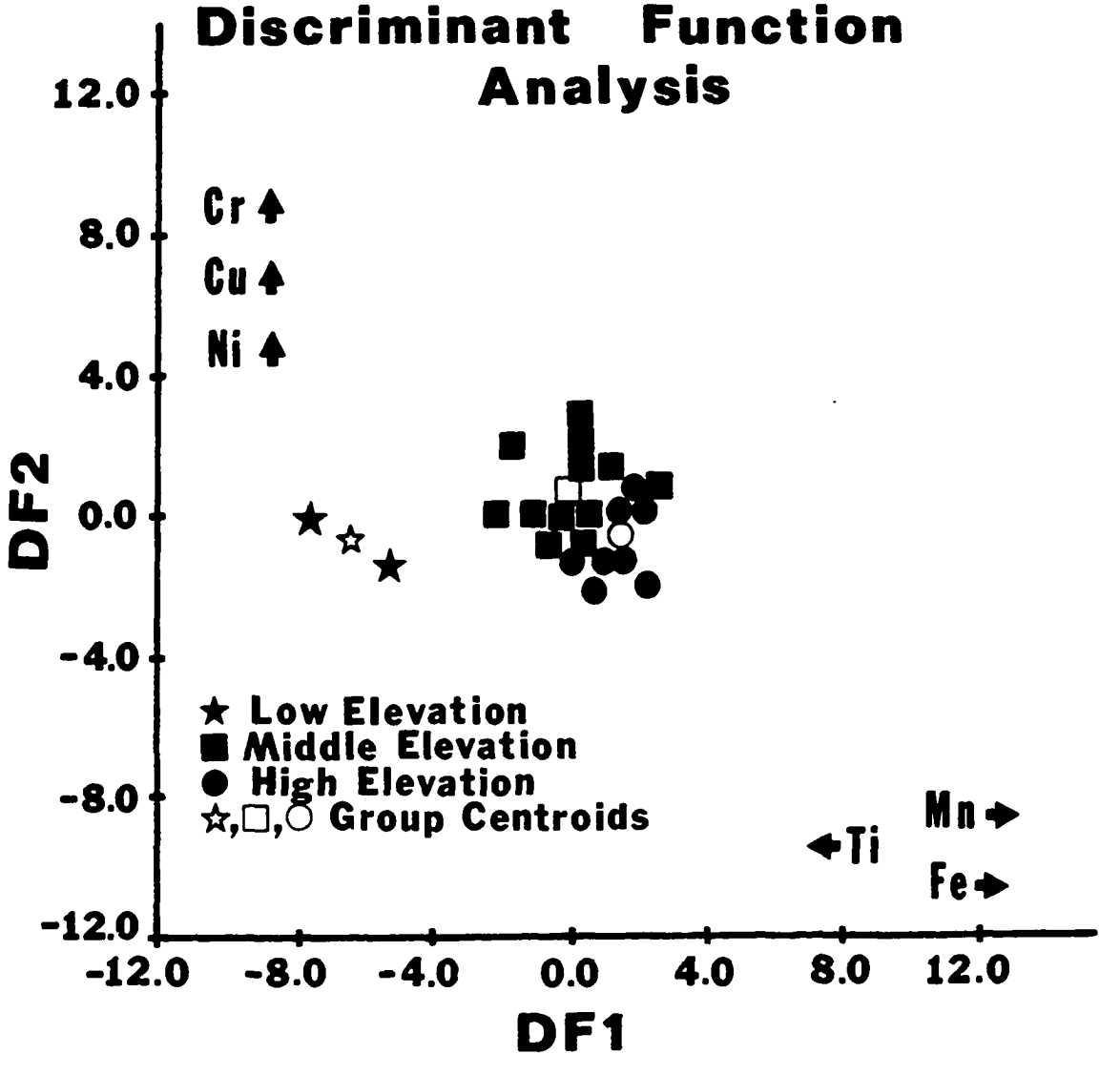

Figure 5.6 Graphical plot of the first two discriminant functions for magnetite element analysis.

The discriminant function analysis shows a separation between the three elevation groups based on the trace element content (Figure 5.6). Although the group 1 samples (ash deposits in low elevation terraces) had only two members, it is distinctly different from the other ash samples on a scatter-plot of the first two canonical discriminant functions. These group 1 samples were collected from within the sedimentary sequences at the Alcose and Panambisito Mines. The group 2 samples (ash from middle elevation terraces) occur in the Mariana, Hipolito, Blandito, Santo Domingo I, Santo Domingo II, and San Joaquin Mines. Most frequently, these ash deposits unconformably overlie a cobble gravel unit. In the canonical discriminant function plot, samples from groups 1 and 2 appear to form chemically distinct groups. However, group 2 and 3 (ash from the high elevation terraces) appear to be very close in proximity on the discriminant plot (Figure 5.6). The group 3 samples are exclusively from the San Juan and Ananias Mines. The group 3 points cluster tightly around the group 3 centroid in the principle component plot, but as a group, they plot very close to the group 2 samples.

Also of some significance to the ash stratigraphy are the ash samples which could not be analyzed due to a difficiency in magnetite. Two general types of ash fell into this category; the first is characterized by a white blocky texture, usually immediately overlying the Antigua

gravel on the higher terraces. This ash was observed in the San Joaquin and Ananias Mines and was thought to be the lower member of the San Juan Formation (Ortiz, 1982a; Darby and Whittecar, 1984). The second ash type which showed a difficiency in magnetite occurred at the surface as a reddish, clayey ash. This ash was present on all terrace surfaces. The reddish color results from weathering that formed the present-day soil. This ash corresponds to the Magui Formation of Darby and Whittecar (1984) in both stratigraphic position and appearance. In most of the mine sites the ash blanketed the high level terraces, but was inaccessible for sampling due to the near vertical slopes of the mine faces. Tree roots and thick weathered surficial soils precluded any digging on the terrace tops. However, occasional ash samples from the lower elevation terraces, where ash paraconformably overlies the Panambi gravel, indicated that this ash contained a significantly lower amount of magnetite than other ashes.

CHAPTER 6: DISCUSSION

6.1 Introduction

A close examination of the volcanic ash and the cobble gravel deposits as well as their sedimentological relationships provides some insight as to local and even regional geological processes of the area. The sequence of deposits presents a clear scenario of events which helps in our understanding of process and response models of deposition in humid alluvial fans.

6.2 Volcanic Ash Units

Volcanic ash or tephra attains considerable stratigraphic importance because it is deposited in a relatively short interval of geologic time (i.e. it is not time-transgressive). In addition, it can mantle enormous areas, allowing for the establishment of a chronology among widely separated outcrops (Blong, 1982). The tephra deposits observed within the cobble gravels appear to have been airborne, but some were clearly reworked by streams and now consist of fine-grained volcanic gravels and sands, such as those observed in the Panambisito mine, which display thin, sometimes irregular or convolute laminae (Darby and Whittecar, 1984). The bedding is

usually horizontal and conformably overlies cobble gravel units. These ash interbeds are typically less than 0.5 meter thick. The composition and thickness (often greater than 8 meters) of the volcanic ash that occurs stratigraphically above some cobble gravels indicate that the Payan area was a depositional basin, probably for the large Central Cordillera volcanic eruptions over 100 kilometers to the east (Darby and Whittecar, 1984). This interpretation of ash transport direction agrees well with the distribution pattern of volcanic ash in the east Pacific area and the present winds of the troposphere (Ninkovich and Shackleton, 1975).

In higher elevation terraces south of the Rio Magui, the ash appears to have at least two members which are separated into a lower blocky, chalky-white unit (Type B), paraconformably overlain by an upper orange-red, clayey unit (Type C), similar in appearance to the ash observed throughout the area. The sharp, but irregular nature of the contacts between the basaltic cobble gravels and the volcanic ash and the lack of weathered clasts or sands at these interfaces led Darby and Whittecar (1984) to conclude that the ash buried active depositional surfaces which preserved the paleorelief of the area.

The discriminant analysis of the magnetite chemistry from ash samples showed a clear separation of the lower terrace ashes (group 1) from the middle (group 2) and upper (group 3) elevation ashes. The group 1 samples were

collected from low elevation sedimentary sequences that are most probably fluvial in nature (Darby, 1976; Darby, 1983a; Darby and Whittecar et al., 1985) and the fine-grained "ash" deposits that occur within them are also most probably fluvial in nature, possibly derived from an earlier ash fall deposit. The middle (group 2) and upper level (group 3) terrace ash groups occur adjacent to one another on the discriminant function plot (Figure 5.6). Based on this observation, and the stratigraphic position of both volcanic ashes (overlying the basaltic cobble gravel), groups 2 and 3 are postulated to be the same ash deposit (Barringer et al., 1987). The ashes are essentially the same both chemically and mineralogically. Only elevations separate the samples; given the fact that the revelent ashes were deposited upon an irregular, possibly faulted topography, sample elevation becomes irrelevant.

The chemical analysis of the volcanic ash magnetite was undertaken because of the weathering that had altered much of the original character of the ash. Magnetite grains are more resistant to weathering processes than volcanic glass (Aomine and Wada, 1962; Ruxton, 1968). Therefore, during weathering, magnetite should be preferentially concentrated in surficial soil systems, unless weathering is sufficient to totally remove magnetite. The deficiency of magnetite in the surficial Type D ash may therefore suggest that it is different from

the magnetite-bearing Type C ash. Alternatively the ashes are separate petrographic facies caused by a change in ash chemistry emanating from one volcanic source. Theoretically, this difference could be a petrographic distinction that occurred either as a pyroclastic source chemically changed within a single eruptive event, two separate and chemically different eruptive events from the same volcanic source, or two eruptive events from completely different volcanic sources. However, given that both the Type C and Type D ashes each overlie distinctly different gravel units (described below), a significant period of time apparently elapsed between eruptions.

Multiple depositional events are apparent in the volcanic ash units in the Payan Mining District. The elemental composition of the magnetite from the ash suggested that the Type C ash layers above the Type I cobble gravels were similar throughout the area and could be distinguished from reworked Type C ash from within the Type II cobble gravel deposits (Figure 5.6). The Type C (uppermost red ash in Type I cobble gravel localities) and the Type D volcanic ash (immediately overlying the Type II cobble gravels), although similar in appearance are not correlative on the basis of their petrology. The fact that the ash above Type II cobbles is deficient in magnetite as compared to those ashes immediately above

Type I cobbles further supports two distinctly different volcanic events for these ash deposits.

6.3 Cobble Gravel Units

The lower (less than 65 meters elevation) terrace cobbles are quartz-rich and are generally restricted to lower level terraces on either side of the present-day Rio Magui and its tributary streams. These exposures include the Anguino, Panambisito, Site 6, and a section of the Clarisa Mine. These mines typically display great bedding variability (i.e. interbedded organic muds, volcanic muds, sands, and gravels), a mean clast size of 10-15 cm of predominately quartz and chert lithologies, a heavy mineral assemblage of relatively stable minerals (i.e. zircon and sphene) and capped by an ash which is mineralogically different from that observed overlying other cobble gravels in the Payan Mining District. The stratigraphy and depositional sequence of these lower elevation terraces is quite different from that observed in other mine sites at higher elevations.

The cobble gravels exposed in outcrop at the other mine sites are primarily basaltic lithologies and occur in higher elevation terraces both north and south of the Rio Magui. These cobble gravels display no obvious bedding except for the discontinuous sand lenses. These sand lenses have measured paleoslopes based on the elevation differences of their basal contact between the Piccinini

and Santo Domingo mines (I and II) and the Ananias and Santo Domingo I mines of 0.014 and 0.0107, respectively (Darby and Whittecar, 1984). The larger clast sizes, the predominance of basaltic clasts, the heavy mineral assemblage containing relatively stable and less stable constituents, the general agreement of the cobble imbrication data, and the steep paleoslopes of the sand lenses suggest a different depositional setting compared to cobble gravels of the lower elevation terraces. Hence, cobble compositions, clast sizes and terrace elevations can be used to distinguish the Type I cobble gravels from the Type II cobble gravels.

6.4 Correlation of Type Units with Previous Stratigraphy

The interpretation of three and perhaps four ash units and three cobble gravel units agrees fairly well with the work of Darby and Whittecar (1984; see also Table 3.2 and Table 6.1). The Type A ash occurs in only a few mine sites and corresponds directly to the Ananias Formation of Ortiz (1982a) and Darby and Whittecar (1984). Type A ash (Ananias Formation) shows evidence of fluvial reworking in the upper meter that is exposed in these mine sites. As this ash is quite well indurated and consistantly observed below the Type I cobble gravel unit, it is one of the more easily identified units in the Payan Mining District.

Above Type I cobble gravel exposures are additional ash units. Within a few mines two distinct members are

Table 6.1 Comparative table of the volcanic ash types (A, B, C, and D) observed in the Payan Mining District.

Type A	Type B
A blue and white dacitic volcanic arenite with intercalations of cineritic lithic tuff and lapilli of dacitic composition. Only observed in the sluiceways of mine sites and is thought to underlie all Type I cobble gravels. Total thickness is unknown, but sections in excess of 10 meters have been eastern mine sluiceways	Cinerite, partially altered to kaolinite and montmorillanite. White and blocky, this unit immediately overlies the Type I cobble gravels. This unit can contain dark gray and white laminae, with an observed fining upward in laminae. Small scale slump faulting is present in places. This unit is not always preserved, but thicknesses of greater than 10 meters are observed.
Type C	**Type D**
Cineritic units and lapilli tuffs of dacitic composition. Usually completely saprolitizeed, this unit is often red to brown in color and can display distinct layering (seen at the San Juan mine). The unit has volcanic fragments, quartz, magnetite, biotite, and hornblende. The unit paraconformably overlies the Type B ash and the Type I cobble gravels. The thickness can range between to 20 meters.	Similar to Type C ash, except for higher amounts of quartz and volcanic fragments, and much less magnetite. Usually highly oxidized when well-drained, this unit can be red to light tan in color. This unit conformably overlies the Type II cobble gravels. Blocks of this ash unit are obeserved in the upper mudstone lenses of the Type II cobble gravel in the Panambisito mine. Less than 5 meters of this unit are exposed at any one site, although as much as 10 meters may be present in some covered intervals.

observed. The lower, Type B ash unit corresponds to the lower member of the San Juan Formation as identified by Ortiz, (1982a). The Type B is a white, blocky, kaolinitic unit which is a fluvially reworked ash as evidenced from sedimentary structures at its base. The Type B ash contains irregular bedding near the base and is fine grained throughout; however, it is present only at the Ananias and San Joaquin Mines. The upper member, the red tuffaceous Type C ash is most likely an airborne ash deposit based on the bedding structures, best observed at the San Juan mine and corresponds to the upper member of the San Juan Ash of Ortiz (1982a) and the described San Juan section of Darby and Whittecar (1984). The Type C ash has distinct horizons in the San Juan mine with possibly five eruptive deposits preserved. These layers differ in texture as well as color. The lower horizons of the upper San Juan member are primarily weathered to a sticky clay, while the uppermost and thickest horizon is a mixture of clays, fine volcanic sands and lapilli agglomerates.

A later volcanic eruption of the Type D ash covered all surfaces in the Payan Mining District. It is absent only where removed by Recent erosion. This ash corresponds to the Magui Formation of Darby and Whittecar (1984). The Magui (Type D) Ash was observed in outcrop at several locations. Those lower elevation mines with Type II cobble gravels afforded the best exposures as they had

been cleared for mining up to the terrace surface. Only in the Piccinini Mine was the Magui Ash observed overlying a sequence (from bottom to top) of Type I cobble gravels, San Juan Ash (the Type C member), and a thin layer of the Type II cobble gravels.

During this time of volcanic ash deposition, fluvial cobble gravel units were periodically being deposited. The lowermost unit (Type A) was deposited after the reworking of the Ananias Formation and before emplacement of the San Juan Ash members (Types B and C). Apparently a sequence of Type I large basaltic cobble gravels accumulated in thick sequences during this time. This unit is correlative with the Antigua Formation of Darby and Whittecar (1984). Intraformational diastems and discontinuous sand lenses within the Antigua cobble gravel indicate periods of sediment reworking and entrainment sorting at lower flow regime conditions. This resulted in sand lenses with abundant wood debris usually containing placer gold accumulations vaguely similar to the modern sandy side bars of the present Rio Magui.

In the time interval between the deposition of the San Juan Ash and emplacement of the Magui Ash, a deep and widespread valley network eroded into the San Juan Formation ash deposits and the underlying Antigua Formation cobble gravels, probably as the result of some fluvial adjustment. This valley was then partially filled with sediment, mostly derived from the erosion and

reworking of the San Juan ash and Antigua gravels. Although this valley fill was also a cobble gravel, the overall clast size was smaller and dominated by chert and quartz lithologies (Type II) and corresponds directly to the Panambi Formation of Darby and Whittecar (1984). The frequent interbeds of sands, silts, and clays, with abundant logs, tree fruits, and organic debris indicate a lower gradient, meandering tropical river environment of channel fill, sidebar deposits, levee deposits, and overbank deposits (Douglas, 1977).

Following the deposition of the Magui Ash unit, the river again downcut through all previous units. The present-day Rio Magui has established fine-grained floodplain deposits on flat low-lying plains on either side of the river which are informally named the Payan Formation (Ortiz, 1983; Darby and Whittecar, 1984). The deep weathering of the exposed and surficial ash provides a ready source of fine-grained muds formerly not available during the earlier Antigua gravel deposition, but now transported in abundance by the Rio Magui and other rivers in the region (Whittecar et al., 1984).

The cobble gravel units of Darby and Whittecar (1984), (the Antigua, Panambi, and Payan Formations) correspond to the Type I, Type II, and Type III cobble gravels, respectively. The designation of these units as formations is technically valid, as they are mappable units. Despite the fact that only at Clarisa and

Piccinini Mine sites are two gravel units observed in stratigraphic sequence, the concept of two distinct episodes of gravel deposition is supported by the occurrence of ash units between the cobble gravel units.

Initial field examination of the volcanic units identified the Type B blocky white member and the Type C red clayey member of the San Juan Formation described by Ortiz (1982a). This observation is one of the few differences encountered in my stratigraphy as compared to that of Darby and Whittecar (1984). As the lower member is exposed in only two mine sites, it might be a reworked ash which was initially similar to the upper member of the San Juan Ash in character. Although this lower member has rather limited extent, it is traceable through most of the large terraces in the southeastern portion of the Payan Mining District, and deserves distinction as a separate part of the San Juan Formation, regardless of whether it is a separate ash fall event or a zone of reworking.

6.5 Alluvial Fan Model for the Payan Area

Several lines of geomorphic and stratigraphic evidence indicate that alluvial fan environments dominated the Late Quaternary history of the Payan area. The Pacific coastal basin has been identified as a large complex of confluent or coalescing alluvial fans that run along the western slope of the Western Cordillera (Bird and Schwartz, 1985). Yet, the regional geologic map of Narino (Arango

and Ponce, 1982) places the Payan Mining District within the Miocene age rocks of marine origin with fossiliferous horizons (Guapi and Naya Formations). Overlying these and other earlier formations are isolated occurrences of Tertiary/Quaternary sediments between the mountains and the sea (fluvio-volcanic terraces and fans). The surficial deposits observed in both the Payan Mining District and the Barbacoas Mining District to the south are not fossiliferous Miocene marine rocks and instead represent a deposit of Late Tertiary/Quaternary alluvial sediments with a minimum thickness of 80 meters.

Apparently the cobble gravels in the Payan Mining District are part of a much larger Quaternary fan complex. Isolated high level, flat-topped, undissected terrace surfaces visible on aerial photographs of the area form part of the drainage divide between the Rio Magui and the Rio Telembi east of Payan and may be erosional remnants of a former fan surface (Figure 3.1). Conceivably the high level basalt-rich terrace gravels near Payan (Antigua Formation) may be correlative with this large remnant fan surface, however, this cannot be confirmed without geologic examination of these larger remnant terraces.

Paleoslopes calculated from elevations of both the largest sand lenses within the Antigua cobble gravel unit and the Antigua cobble gravel/San Juan volcanic ash contacts indicate slopes of approximately 0.010

(Figure 6.1). The cobble gravel/volcanic ash contact is thought to give a more reliable slope estimate (0.010) as it is apparently a buried active depositional surface (i.e. no observed weathering or soil formation at the contact) and is observed in most mines north of the Rio Magui in an east to west trend (Darby and Whittecar, 1985). This slope figure is significantly steeper than the calculated slope (0.0029) for the present day Rio Magui (Babuin, 1985) and suggests a different depositional regime for these older (Antigua) cobble gravel units.

Stratigraphic sequences in the Payan Mining District also support an alluvial fan interpretation for the Antigua Formation. Often, there is a fining upwards of clast sizes within the higher elevation terrace cobble gravels, best observed at the San Juan mine, which commonly displays basaltic boulders and cobbles near the base and slowly grade into smaller cobble and gravel clasts to sands. This fining upward trend is often observed in a cobble gravel unit immediately beneath a sand lens. This observation, together with the abundance of cobble imbrication and clast-to-clast contact, brought about a revision of a proposed debris flow depositional process by Darby (1983a) to that of fluvial deposition on a stream-dominated alluvial fan (Darby and Whittecar, 1984). A great number of similarities exist between the Antigua Formation deposits and descriptions of stream-dominated fans elsewhere (Nilsen, 1969; McGowen and

Figure 6.1 Diagram showing the paleogradient of Antigua/San Juan Formation contact in the Payan Mining District. The large numbers denote the elevation of the contact in each mine. The "e's" designate those mines where the contact was eroded (after Darby and Whittecar, 1985).

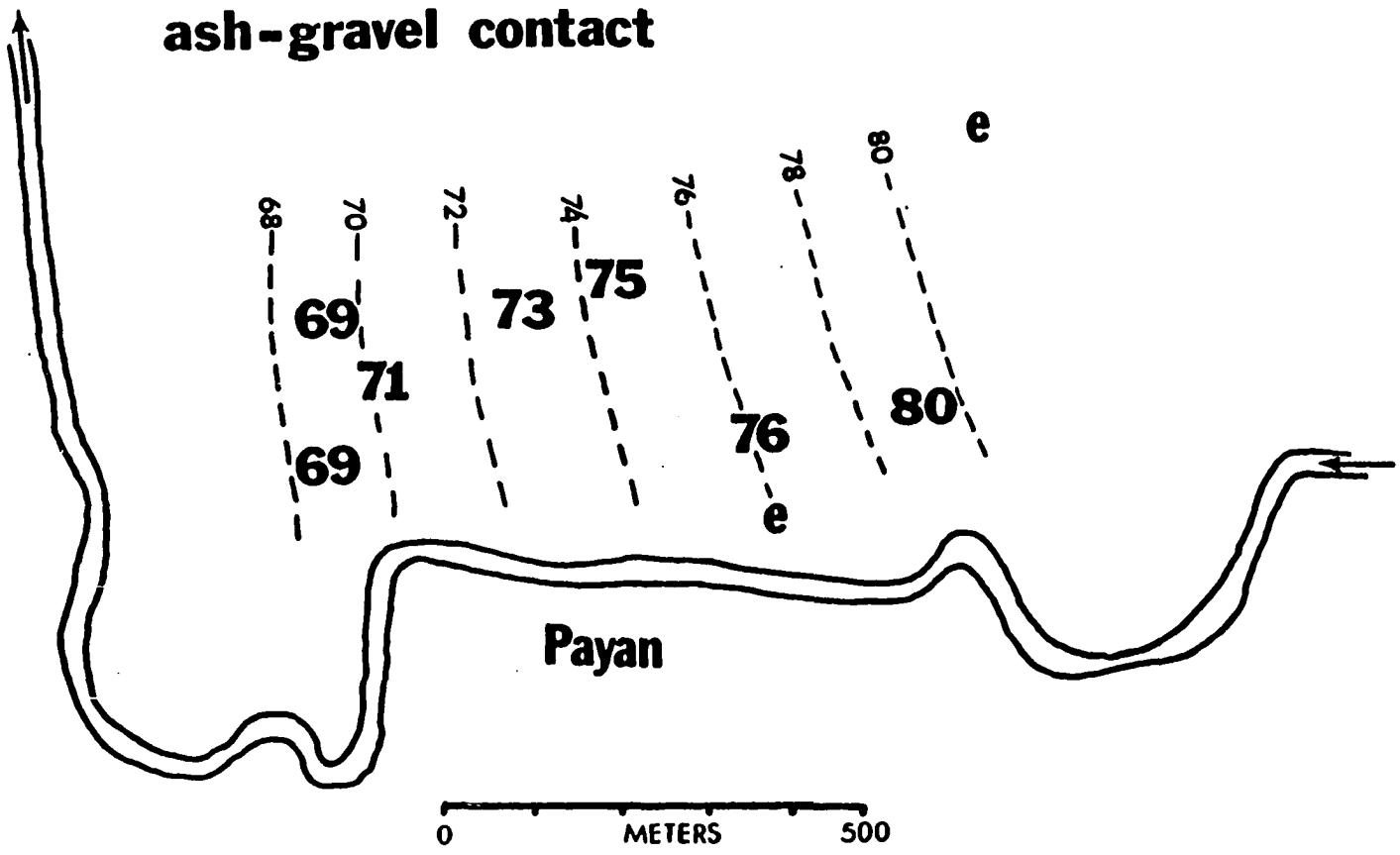

Groat, 1971; Rust, 1979; Nilsen, 1985). Alluvial fans, especially stream-dominated alluvial fans are about the only environments where very thick sequences of clast supported, imbricate cobble gravels can occur (Rust, 1979).

Depositional processes on alluvial fans fall into two types: (1) fluvial or stream flow processes, and (2) debris flow processes. It is not uncommon to find both processes on the same fan surface, but typically, conditions such as climate, vegetation, rainfall amount and intensity, and sediment type all influence which processes will dominate. Arid climates with infrequent rainfall and sheetflow and flashflooding, as well as, poor vegetation cover favor debris flow processes (Nilsen, 1982). Humid climates with more regular rainfall conditions and greater vegetation cover, favor fluvial/streamflow processes (Table 6.2). The occurrence of stratified, imbricated, clast-supported cobble gravels with discontinuous sand lenses exposed in the Payan Mining District indicates that the Antigua cobble gravel was most likely deposited by a humid climate, fluvially dominated alluvial fan. Collinson (1978) stated that because humid alluvial fans are dominated by braided channel processes, they can essentially be regarded as deposits of braided streams which develop with very little lateral confinement.

Table 6.2 List of criteria for the identification and recognition of alluvial fan deposits (after Nilsen, 1982).

FLUVIAL/STREAM FLOW PROCESSES	DEBRIS FLOW PROCESSES
suspension, saltation, traction	mudflows, gravity flows
Newtonian fluid transport	viscous fluid transport
well stratified	poorly stratified
various sedimentary structures	few sed. structures
clast supported	matrix supported
little clay	abundant clay
imbricate clasts	little or no imbrication
common in humid climate fans	commmon in arid fans
dominate distal fan facies	dominate proximal fan
typically coarse grained	reverse grading at base
typically poorly sorted	typically poorly sorted
TYPICAL SUB-ENVIRONMENTS	**TYPICAL SUB-ENVIRONMENTS**
INNER FAN CHANNEL FACIES- generally straight and entrenched channels.	**MUDFLOW FACIES-** viscous fine-grained material which range from thin wide-spread sheets with sub-horizontal margins to thick lobate bodies with thick nearly vertical margins, commonly has mudcracks.
MID AND OUTER FAN CHANNEL FACIES- generally braided channels, typically narrow, long, and coarse-grained, shallow and fine downfan, commonly conglomeratic, basal surfaces are commonly concave upward in transverse cross-section, often greater than 2 meters thick. Large channels may be difficult to recognize.	**LANDSLIDE FACIES-** includes slumps, flows, and slides and may be channelized, proximal or distal. Common where slopes are steep and weathering is deep. Often form thick and repetitive sequences. May be difficult to distinguish from debris flow or mudflow.
MID AND OUTER FAN INTER-CHANNEL FACIES- channel margin, levee and inter-channel facies often develop, but are poorly preserved. Beds thin away from channel. May not be laterally extensive or abundant.	

Table 6.2 continued

SHEETFLOOD FACIES- emerges from channelized flood. Series of low gravel bars or sand, dissected by small and shallow channels at waning flood stage.	**DEBRIS-FLOW-** type deposits generate where sediment sources provide abundant muddy material and where slopes are steep and vegetation scarce. Often form where rainfall is either seasonal or irregular. May or may not be channelized. Material ranges from clay to boulders. Typically have well-defined margins. Bedding is disorganized if present. Fabrics are usually isotropic.
SIEVE FACIES- usually in proximal fan areas, permeable lobes of well-sorted gravel, often angular, monomict, and massive with laterally extensive beds with well-developed gravel imbrication.	

Nilsen (1982) presented a general facies model for alluvial fans, both arid and humid climate types. The fan surface is divided into the following four geomorphic facies zones:

(1) the inner fan valley channel facies,
(2) the middle fan facies,
(3) the outer fan facies, and
(4) the fan fringe.

The inner fan channel valley facies is the most proximal, near the area of stream emergence from the mountain source area, and contains the coarsest sediments. The middle fan, outer fan and distal fan facies occur successively downslope from the inner fan facies, each with its own dominant depositional processes and sequences (see Table 6.3). The Antigua Formation, by virtue of its sedimentology of the thick clast-supported cobble gravels and discontinuous sand lenses would most likely fall into the middle fan facies. This is a zone of rapid sedimentation, dominated by braided channel depositional processes. The Antigua Formation, the most laterally and vertically extensive fluvial unit in the Payan Mining District, contains the rounded boulders, cobbles, gravels, and interbedded sands that are commonly observed in braided channel/humid alluvial fan deposits (Rust, 1979). Although the Panambi and Payan Formations also contain gravels, these formations both contain abundant interbedded organic-rich muds and sands (with leaves, nuts, and fruits), a facies that is not observed in the

Table 6.3 Primary facies of alluvial fans (after Nilsen, 1969).

I. Inner Fan Valley Channel	II. Middle Fan Facies
Very coarse-grained deposits in a single broad and deep channel which passes almost all the sediment deposited on the fan.	Forms the largest area of most fans and is composed of smaller distributary channels radiating outward downfan from the inner fan valley.
Finer-grained channel margin, levee, and inter-channel deposits and may include coarse-grained landslides and and debris flows derived from slopes between the major drainages.	Hundreds of these channels may be present, although most are inactive for extended periods as channels rapidly shift laterally with time.
If no longer active, inter-channel areas may form gravel topped remnant fan-terraces with soil profiles.	The channels of the middle fan are shallower and narrower than inner fan valley channels and are sites of rapid sedimentation as channels fill during the course of lateral shifting or gradual abandonment.
	Channels are commonly braided and these deposits along with less well developed inter-channel deposits make up the middle fan facies.
III. Outer Fan Facies	IV. Fan Fringe Facies
Finer-grained sheet-like deposits of non-channelized or less channelized flow which are typically not preserved in arid alluvial fans	The fine-grained deposits of the fan fringe are outer fan deposits which intertongue with other depositional systems - fluvial, aeolian, lacustrine, and marginal marine facies.
Flows emerge from channels and spread out to deposit laterally extensive sheets or bodies of sediment.	These deposits are the finest grained and most variable.
These sediments have an extememly low gradient and are often difficult to distinguish from basin-floor, alluvial plain, lacustrine, or other facies.	

Antigua Formation. Also of significance is the fact that both the Panambi and Payan Formations are confined to relatively narrow valleys within the modern drainage system.

Nilsen (1969) describes a Devonian humid alluvial fan sequence in Norway. Of the three facies, the mid-fan Vaeroy Conglomerate Member most closely compares with the Antigua gravel in the Payan Mining District. This Paleozoic conglomerate is a polymictic cobble and boulder sized unit which occurs as a very thick fan sequence (2,260 meters). The cobbles and boulders are well rounded clasts (with Powers roundness values consistently betweeen 0.6 and 0.8) and largest boulder sizes of nearly 2 meters in diameter. This unit has a well defined fabric according to the rose diagrams of the elongate clasts which show a preferred fabric reflecting a strong, persistent unidirectional current flow. The matrix material consists of finer, more angular conglomerate and fine to coarse arkosic sand. The conglomerate fabric is "closed framework" with many clasts having contact points. A finer conglomerate and sand matrix material fills the interstitial space between clasts and indicates deposition by upper flow regime. The finer sediments were deposited downfan. As in the Antigua gravels, stratification in the Vaeroy fan is generally lacking and bedding surfaces are rare, widely spaced, irregular, and discontinuous. The same is not true for the Panambi and

Payan gravels. According to Nilsen, those surfaces which are preserved must represent extended periods of non-deposition, perhaps intraformational diastems or paracoformities. Local, thin, and elongate sandstone beds in the Vaeroy Formation, typically less than 0.5 meter thick with lateral extent of as much as 20 to 30 meters in width and length, wedge out in all directions on the surface of accumulation with flat stratification, very low inclination tabular, or low plunging trough stratification, very similar to that observed in the Antigua Formation sand lenses. The strata within the sandstone interbeds range from 1 to 3 centimeters in thickness and can occur as cross-strata with amplitudes of 3 to 25 centimeters and wavelengths up to 5 or 10 meters. Paleocurrent determinations were impossible due to low inclination angles. However, the presence of preserved plant stems in the Vaeroy sandstone proved the existence of a primitive Devonian plant cover and suggest a humid climate. Preservation of abundant plant debris in thick sand and coarse gravel sequences seems to be an important criteria for recognition of humid fan paleoenvironments.

The sandstone interbeds in the Vaeroy Conglomerate occur as both beds and lenses. Nilsen states that the nature of stratification in the sandstone beds suggests deposition in the upper part of the lower flow-regime or the transition zone into the upper flow-regime and might represent periods of less intense current conditions. The

sandstone lenses are smaller and thought to resemble swale fill deposits behind bars in areas of braided stream deposition, with elongation downstream until covered again by gravel through flooding or shifting stream patterns (Figure 6.2). This interpretation of the depositional processes responsible for thin sand lenses within a thick sequence of cobble gravels agrees with that of Darby and Whittecar (1984) who related the change from cobbles to sand in the Payan Mining District as intervals of localized reworking under lower flow-regime as opposed to deposition resulting from a change in setting due to an external geomorphic threshold such as a regional reduction in gradient, or climate change.

Overall the large thickness of conglomerate and breccia in the Devonian Norway fan suggest that the source area was being uplifted contemporaneously with sedimentation (Nilsen, 1969). This situation appears to be fairly analogous to that of the Pacific Coastal Basin which has a sequence of several hundred meters of Pliocene to Recent continental sedimentary-volcanic deposits within the 3,995 meter thick section of post-Eocene strata (Bueno S. and Govea R., 1976). The coarseness of the Vaeroy conglomerate, like that of the Antigua cobble gravel in the Payan Mining District indicates high relief in the source area with both rapid erosion in the headlands and rapid deposition on the fan.

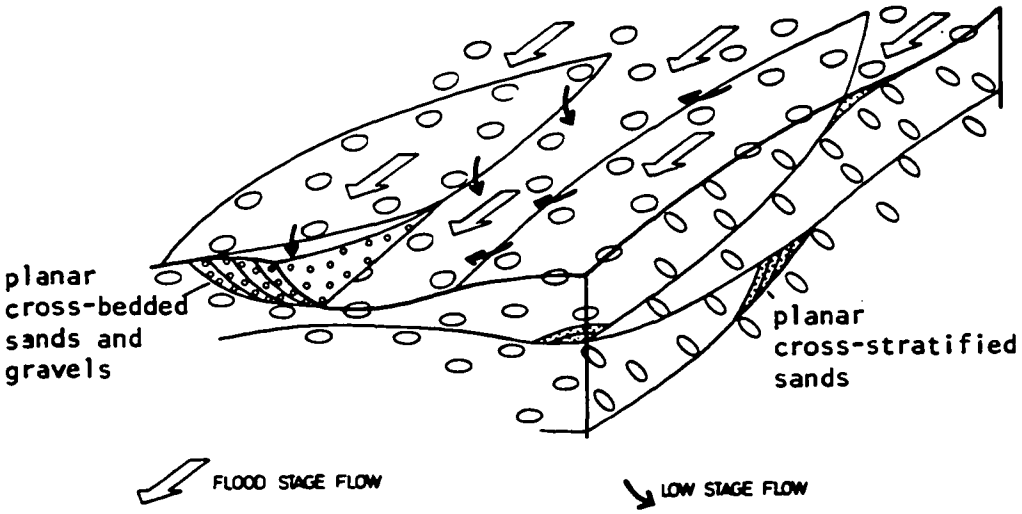

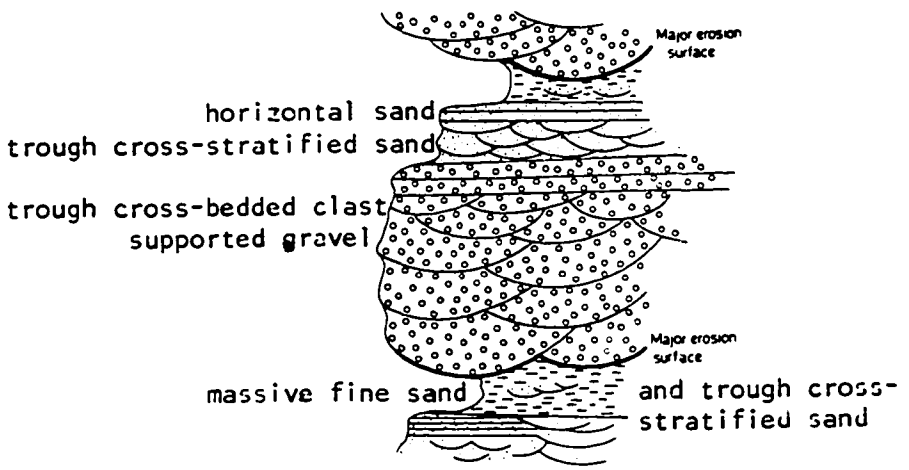

Figure 6.2 Depositional model and stratigraphic sequence of sandstone lenses within thick cobbles of braided streams/alluvial fan environments (after Rust, 1979).

6.6 Stratigraphic Variation in Gold Concentration

Although the piedmont is usually viewed as a depositional zone, it is obvious that a great deal of reworking can occur there. Even when the dominant landform is depositional, such as an alluvial fan, the great variability in fan morphology reveals that the deposition may be episodic, being interrupted by periods of fan trenching and sediment reworking.

Periodic reworking of piedmont deposits as internal geomorphic thresholds are exceeded provides a mechanism for concentration of heavy minerals within the fan deposits of the Payan area. The heavy mineral placers therefore need not be related to erosion of local heavy mineral concentrations in the rocks of the source area. Rather they are probably due to concentration by reworking of fan sediments (Schumm, 1977).

Garrett (1985) recognized that localized processes of flow velocities, entrainment sorting, and winnowing appear to be responsible for the placer gold deposits in the terraced gravel deposits in the Payan Mining District. Periodic flooding was the process which controlled the initial gold deposition in river bars. These river bars were comprised of open-fabric gravels deposited by a major flood event, with later infilling of matrix material during lower flow conditions. Entrainment sorting and concentration of this material occurred during this waning flood stage condition or subsequent smaller flood events.

He concluded by saying that these depositional processes resulted in two types of stratigraphic zones of relatively high placer concentration in the strata of the Payan Mining District. Major concentrations occurred during sustained lower-flow conditions with matrix infilling and sand layer deposition, and minor concentrations occur in zones between successive flood cobble gravels which have undergone some winnowing and entrainment sorting, but without the preservation of a sand unit. These major and minor placer concentration processes occurred periodically at many locations within the Payan area (Garrett, 1985).

In the present Rio Magui system, winnowed tops of gravel bars are common, with several other erosional and depositional features (Babuin, 1985). However, the high gold values of the Panambi (Type II) cobble gravel are not observed for the quartz-rich Payan (Type III) cobble gravel. As stated earlier (Section 3.2) the alluvial plains of the Rio Magui were explored for gold in 1937, but the gold values encountered were not economically feasible. Apparently the conditions of gradient, flood frequency and intensity and a source area buried in ash and mud, do not allow the modern Rio Magui to concentrate gold in the Payan (Type III) gravels like that found in the Panambi (Type II) gravels.

6.7 Stratigraphy and Depositional Sequence

Ultimately the cobbles in all the cobble gravel units in the Payan Mining District are most probably derived from the Diabase Group rocks which outcrop immediately to the east of the Tertiary deposits along the eastern margin of the Pacific Coastal Basin (Figure 2.2). The Diabase Group not only contains basalts, gabbros, greenstones, but also zones of metamorphic Dagua Group rocks, interstratified cherts, sheared zones, and large quartz veins. Based on the cobble terrace elevations and relative geographic distributions, two non-Recent cobble deposits can be discriminated in the Payan area (Table 6.4).

The Clarisa mine illustrates the stratigraphic relationship between the Type I gravel and the younger Type II gravel which is eroded into and justaposed against the Type I cobble gravel. This mine site had very little ash overburden, so that the Type I cobbles were totally weathered to clay, while the adjacent Type II cobble gravels showed very little weathering. The erosion of the typically thick ash overburden had permitted uninhibited weathering of the cobble gravels to the point of liesegang ring formation in the clay of the weathered cobble ghosts (Figure 6.4). The adjacent Type II cobble gravels showed a similar matrix composition, although the heavy mineral abundances typically indicated impoverishment of less stable constituents such as hornblende and biotite and

Table 6.4 Comparative table of cobble gravel Types (I and II) exposed in the terraces observed in the Payan Mining District.

Type I Cobble Gravel	Type II Cobble Gravel
Basaltic cobbles	Quartz/chert cobbles
Mean cobble size is greater than 30 centimeters	Mean cobble size is less than 20 centimeters
Carbon-14 dates range from 28,000 to greater than 40,000 YBP	Carbon-14 dates are 24,000 YBP and greater than 40,000 YBP
General lack of bedding structures of any kind, very massive unit	Frequent interbedded muds and sands within cobble gravel unit

Figure 6.4 Photograph of the completely weathered cobbles exposed within a section of the Clarisa Mine. Notice the Liesegang-like rings present in the two cobbles at the center of view. Cobbles are approximately 20 centimeters across.

enrichment of more stable minerals such as zircon and sphene (Figure 5.5). This more stable heavy mineral assemblage may be indicative of longer transport distances or perhaps a period of weathering and subsequent erosion and redeposition.

Thus both gravel types were probably initially derived from a similar, if not the same, primary source rock area in the Western Cordillera. However, differences in clast types, clast sizes, degree of clast and matrix weathering existed between Types I and II. The Clarisa Mine shows two distinct phases of cobble gravel deposition. The first, was a basalt-rich rounded boulder to cobble gravel which was later weathered in situ. Subsequently, a second rounded cobble gravel was eroded from the earlier weathered gravel and consisted of a smaller mean cobble size and predominately resistant quartz clasts. This interval of reworking is also reflected in the heavy mineral assemblages, which appear to be somewhat gradational as seen from Figure 5.5. The gravels at Anguino mine (Ang-3) and Site 6 (6-1), although having the smaller rounded quartz clasts, possess a heavy mineral assemblage with similarities to the Type I (Antigua) cobble gravels. This is primarily due to higher percentages of andalusite (45%) and biotite (5%) rather than the values observed for other Type II gravels (8-15% andalusite and 0-1% biotite). These anomalous minerals in Type II gravels might indicate shorter transport distances

for these two particular deposits, i. e., they were reworked in part from nearby, perhaps less weathered Antigua gravels.

Also supporting the concept of three episodes of cobble deposition is the fact that the boundary separating the two gravel types in the Clarisa Mine is erosional, primarily channel cut. Thus, based upon differences in cobble gravel sizes, lithologies, carbon-14 dates from wood debris (Table 6.5), and stratigraphic relationships, there appears to be at least three distinct episodes of cobble gravel deposition.

The concept of two distinct cobble gravels in the southern portion of the hill lands of Colombia°s Pacific coastal basin has been recognized in earlier investigations (Pereira-Gamba, 1909; Sandoval, 1936); however, it is not known if the two alluvial deposits they described directly correspond to the alluvial deposits observed in the Payan Mining District. Regardless, multiple depositional and erosional events within the alluvial sequences of the Tumaco Sub-Basin are not restricted to the Payan area.

6.8 Cause and Timing of Stream Incision

This repetitious sequence of cobbles, ash, and downcutting suggests that the influx of fine-grained ash deposits was the primary cause of gradient changes and not an uplift event. Apparently the relatively high gradient

Table 6.5 Carbon 14 dates from wood debris collected from sand lenses within cobble gravel sequences.

Formation	Years B.P.	Lab No.	Mine Site	Elevation
Panambi	23,850 ± 600	TX-4976	Anguino	50m
	† 40,000	TX-4975	Panambisito	48m
Antigua	26,890 ± 770	TX-4979	Magdalena	69m
	34,950 ± 630	Beta 4034	Piccinini	61(?)m
	† 40,000	TX-4977	Mariana	77m
	† 40,000	TX-4978	Epimenio	60m

(† beyond the range of radiocarbon dating)

(0.01) of the original Antigua alluvial fan was sufficient to transport sandy material through a multi-channel, humid alluvial fan/braided stream environment. An influx of abundant ash, primarily mud to this multi-channel network would tend to produce more cohesive banks and confine the river to a more narrow zone on the fan surface. Because the buried fan surface would be too steep for the single channel meandering streams now crossing it, the fluvial system would attempt to decrease its gradient (Cant, 1982). The ancestral Patia, Telembi, and Magui Rivers would downcut into the Antigua fan and San Juan Ash complex. The interfluves of the relict fan then became zones of extensive weathering of cobbles, gravels, sands, and muds. These interfluves then continued to supply sediment to the lower gradient, single channel river system, some of which was deposited in the valley cuts as the Panambi Formation. A similar type of gradient lowering event took place after the deposition of the Magui Ash, and led to the emplacement and development of the Payan Formation by the present-day Rio Magui. The Antigua gravel generally lacks mud except in its uppermost parts because of the steep gradient and general lack of available interfluve weathering. The underlying Ananias ash is extremely indurated, apparently cemented with diagenetic silica and thus was not readily available as a source of mud.

The lack of definite dates for this sequence of strata permits some leeway with the timing of events in the above interpretation. The carbon-14 dates from wood debris in the Antigua and Panambi Formations (Table 6.5) have a range from 23,000 YBP to greater than 40,000 YBP (beyond the range of Carbon-14 radiometric dating). According to Bowen (1978) direct carbon exchange with the atmosphere or more importantly, the influence of groundwater through the introduction of humic acids are a particularly serious means of contamination of organic material. He also states that quite small amounts of contamination by modern carbon can produce radiocarbon ages which may be entirely misleading by indicating much younger ages. However, assuming the late Tertiary marine deposits of Arango and Ponce (1982) are accurately dated, and assuming that the fluvial/fan deposits in the Payan Mining District do overlie these marine deposits, then the Antigua gravels are no older than Plio-Pleistocene. Quite probably, these gravels were associated with a mid-Pleistocene uplift and associated volcanism in the Andes (Burgl, 1967). A mid-Pleistocene uplift and subsequent development of an alluvial fan in the Pacific coastal basin provides a plausible scenario for the emplacement of late Quaternary Antigua fan deposits in the Payan Mining District.

CHAPTER 7: CONCLUSIONS AND FUTURE RESEARCH

7.1 Conclusions

Three gravel units and up to four ash units can be distinguished in the Payan Mining District. By evaluating the stratigraphic, sedimentologic, mineralogic, and chemical differences between units in the order of their deposition, I have developed a model for the Quaternary geologic history of the region.

The oldest unit in the Payan Mining District, the Ananias Formation probably resulted from Central Cordilleran volcanic eruptions related to Post-Andean orogenic events in the early to mid-Pleistocene (Burgl, 1967) which blanketed the Pacific Coastal Basin. Later fluvial activity partially reworked and redeposited this ash as evidenced from sedimentary structures in the upper portion of this formation. The well indurated character of this ash and the scarcity of mud beds in the overlying unit indicate that this ash became well cemented soon after reworking and certainly before the deposition of the overlying Antigua gravels.

Following this volcanic episode, a fluvial-dominated alluvial fan formed at the western edge of the Western Cordillera and prograded outward into the subsiding

Pacific Coastal Basin. A braided river depositional environment dominated this fan depositing thick sequences of large basaltic cobble gravels (Antigua Formation) derived from the western slopes of the Andes. Structures such as massive, unbedded accumulations of imbricated clasts with discontinuous sand lenses containing abundant logs and wood debris, and projected paleoslopes of depositional surfaces of approximately 0.01 suggest a humid alluvial fan/braided stream paleoenvironment. Intraformational diastems and the discontinuous sand lenses within this cobble gravel unit indicate periods of sediment reworking and entrainment sorting at lower flow regime conditions. These lower flow regime conditions resulted in sand lenses with abundant wood debris vaguely similar to the modern sandy side bars of the present Rio Magui (Babuin, 1985). These modern side bars have abundant logs and wood debris which are transported during flood events, deposited during waning flow, and are eventually buried within the bar.

Volcanic ash (the lower member of the San Juan Formation) buried this alluvial fan surface. This white, fine-grained, blocky, and kaolinitic ash unit has sedimentary structures suggesting that it was fluvially reworked. Immediately overlying the white ash is a red tuffaceous unit (the upper member of the San Juan Formation). This younger bed is most likely an airborne ash deposit, based on the bedding structures. Best

observed at the San Juan Mine, this upper member ash has as many as five distinct horizons which differ in texture as well as color. The lowest horizons in this ash are primarily weathered to a sticky clay, while the uppermost and thickest horizons are a mixture of clays, fine volcanic sands and lapilli agglomerates.

Following deposition of the San Juan Ash and in response to the abundant mud that it supplied, streams changed from braided to meandering or straight-channeled and downcut, developing valleys within the alluvial fan. The cobble gravels and ash units left as interfluve areas were extensively weathered and continued to supply mud and sand as well as stable clasts of primarily chert to the streams.

A quartz-rich fluival gravel unit, The Panambi Formation resulting from this reworking of the weathered Antigua cobble gravels and San Juan ash and was deposited within the newly downcut valleys. Within these fluvial deposits occur interbedded quartz cobble gravels, sands, logs, tree fruits, and clays. Trace element analyses indicate that the muds were probably derived from the San Juan Formation ash blanketing the interfluves. The quartzitic Panambi clasts are smaller than those observed in the basalt-rich Antigua cobble gravels. Analyses of heavy minerals in the matrices of both gravel units indicate that the Panambi Formation has higher percentages of more stable minerals such as zircon and sphene,

indicating extensive weathering which resulted in the removal of less stable minerals abundant in the Antigua gravel. The nature of the interbedded sands, muds, and gravels, their geomorphic position as a valley fill, and the smaller gravel size relative to the Antigua gravel suggests a lower gradient meandering to straight fluvial environment for the Panambi gravels.

A later volcanic eruption produced another ash unit, the Magui Formation, which covers all surfaces except the floodplain and eroded hillslopes. It forms the substrate for most present day soils. Up to 7 meters thick, the unit is distinguished from other ashes by a lack of magnetite. As in the preceding volcanic ash event, the river again downcut through the Magui ash and the Panambi gravels, leaving the Panambi gravels exposed as low (less than 65 meters) terraces along the valley sides.

The meandering Rio Magui has since established itself within the downcut valley network (Figure 7.1). This river is depositing fine-grained floodplain sediments several meters deep (Babuin, 1985) on either side of the cobble floored channel with a gradient of 0.0029. Placer gold is no longer being concentrated in economic deposits in the Payan Formation like those observed in both the Antigua and Panambi Formations. It is thought that the Rio Magui is transporting sediment derived primarily from the gold-barren ash deposits, which supplies the large volumes of mud observed at the frequent high flow or flood

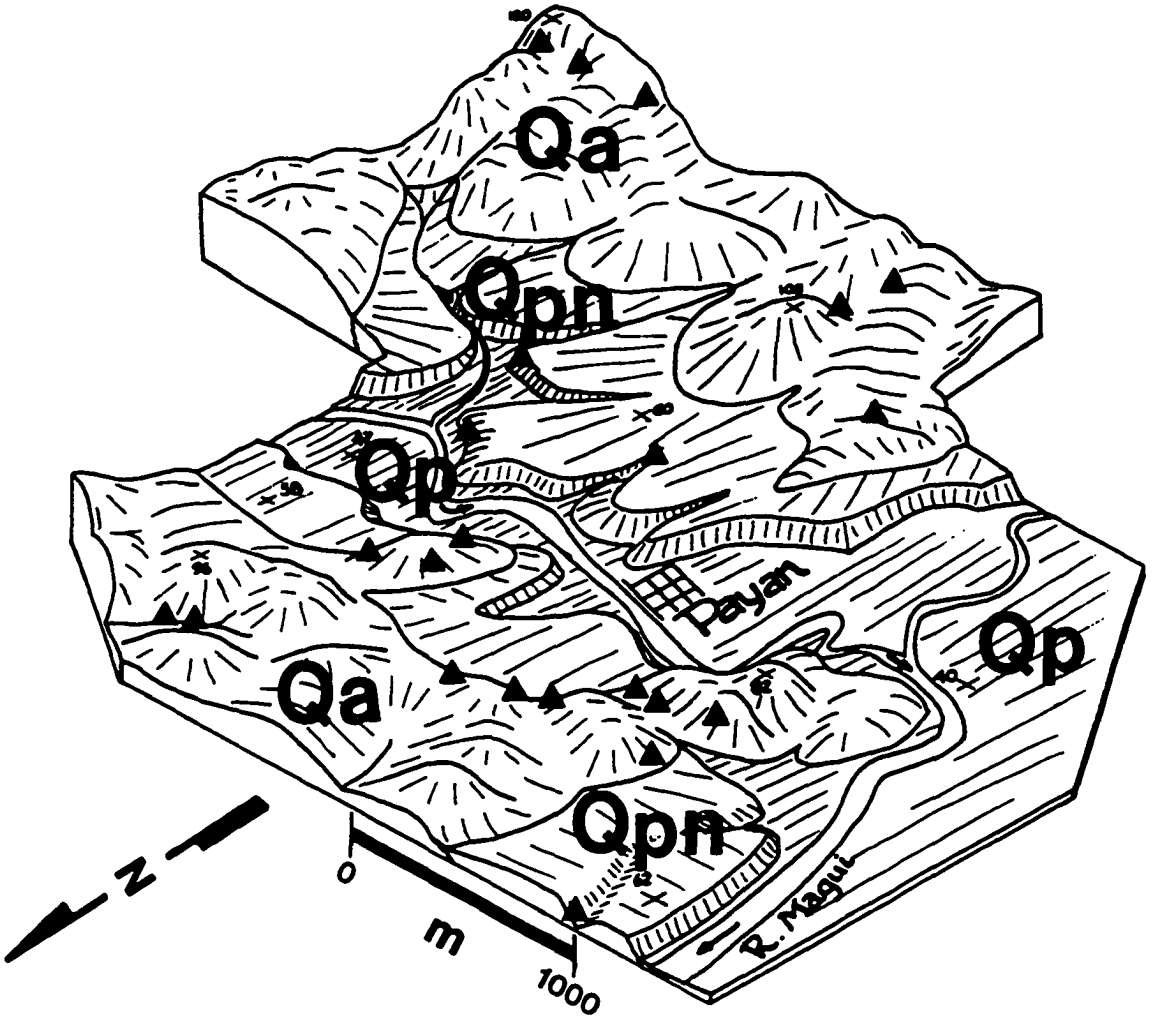

Figure 7.1 Oblique sketch of the topography and the stratigraphic relationships of the alluvial formations observed in the Payan Mining District (after Whittecar et al., 1985).

Qp Payan Fm.....Modern Alluvial Sediments

Qpn Panambi Fm...Quartz-Rich Gravelly Alluvium

Qa Antigua Fm....Basalt-Rich Gravelly Alluvium

*Note: three to ten meters of volcanic ash bury both the Panambi and Antigua Formations.

stage conditions. In addition, the much lower slope of the Rio Magui may be such that the optimum gold concentration processes simply do not occur within the 12 square kilometer area of the Payan Mining District today.

7.2 Future Research Possibilites

The Compania Minera De Colombia Y Texas, Inc. has since ceased operations due to the difficulty of mining the terraces with very thick ash overburden (sometimes greater than 20 meters). Darby and Whittecar (1984) recommend future exploration in the Panambisito Mine and the Hipolito and Mariana Mine areas as they showed higher gold values. Also suggested was an alternative mining technique similar to contour strip mining.

Garrett (1985) stated that an undiscovered primary gold deposit was likely to be found within 20 kilometers east of Payan and future explorations should proceed upstream in the Rio Magui valley, to find this primary deposit, as well as other possibly rich placer deposits. I agree with these two previous works as to areas of potential placer concentration within the field area and east of Payan. However, the number of native mine sites decreases to the east and this might indicate that Payan is located at about the optimum position on the Antigua paleofan for placer concentration (Slingerland, 1984). Like Darby and Whittecar (1984), Garrett (1985) also suggested explorations continue in the Panambisito Mine

(The Panambi Formation). Despite the discontinuous nature of the beds within this formation, the high gold values and the thin (generally less than 5 meters) of ash overburden warrant their further investigation and exploitation.

The stratigraphic framework that has been applied to the Payan Mining District should attempt to be expanded to the entire Rio Magui Basin area. Special attention should be paid to the high undissected terraces to the east, as these might contain a more complete stratigraphic record of the events that resulted in the observed sequences of Quaternary sediments.

Finally, more extensive exposures of these stream-dominated alluvial fan gravels, such as the Antigua Formation are needed in order to discern the geometry of the sand lenses and gravel units. Perhaps this would also lend to recognition of bar types preserved in these deposits and to a more complete model of their deposition.

REFERENCES CITED

Anderson, F.M., 1927. Non-marine Tertiary deposits of Colombia. Bulletin of the Geological Society of America, Vol. 38, p. 591-644.

Aomine, S., and Wada, K., 1962. Differential weathering of volcanic ash and pumice, resulting in formation of hydrated halloysite. American Mineralogy, Vol. 47, p. 1024-1048.

Arango C., J.L., and Ponce M., A., 1982. Mapa Geologico Generalizado del Departamento de Narino. Instituto Nacional de Investigaciones Geologico-Mineras, Republica de Colombia Ministerio de Minas Y Energia.

Babuin, M.L., 1985. Fluvial depositional processes of a tropical river, Colombia, South America. M.S. Thesis: Old Dominion University, Norfolk, Virginia, 139 p.

Barazangi, M., and Isacks, B., 1976. Spatial distribution of earthquakes and subduction of the Nazca plate beneath South America. Geology, Vol. 4, p. 686-692.

Barringer, R.A., Darby, D.A., Whittecar, G.R., and Garrett, J.R., 1987. The stratigraphy of Late Quaternary deposits in the Payan Mining District, Narino, Colombia, South America. The Geological Society of America Abstracts with Programs, Vol. 19, No. 2, p. 75.

Blong, R.J., 1982. The Time of Darkness. The University of Washington Press, Seattle, 257 p.

Bird, E.C.F., and Schwartz, M.L., 1985. The World°s Coastline. Van Nostrand Reinhold Company, New York, 1071 p.

Bock, R., 1979. A Handbook of Decomposition Methods in Analytical Chemistry. John Wiley and Sons, New York, 444 p.

Bowen, D.Q., 1978. Quaternary Geology - A Stratigraphic Framework for Multidisciplinary Work. Pergamon Press, New York, 221 p.

Bueno, S., R., and Govea, R., C., 1976. Potential for exploration and development of hydrocarbons in Atrato Valley and Pacific coastal and shelf basins of Colombia, in Halbouty, M.T., Maher, J.C. and Liam, H.M., eds., Circum-Pacific Energy and Mineral Resources. American Association of Petroleum Geologists, p. 318-327.

Bullman, C., 1892, Gold washing in Colombia. The Engineering and Mining Journal, Vol. 53, p. 374-375.

Burgl, H., 1967. The orogenesis in the Andean system of Colombia. Tectonophysics, Vol. 4, p. 429-443.

Campbell, C.J., 1974a. Colombian Andes, in Mesozoic-Cenozoic Orogenic Belts: Data for Orogenic Studies. Geological Society of London, Special Publication #4, p. 704-724.

Campbell, C.J., 1974b. Ecuadorian Andes, in Mesozoic-Cenozoic Orogenic Belts: Data for Orogenic Studies. Geological Society of London, Special Publication #4, p. 725-732.

Cant, D.J., 1982. Fluvial facies models and their application, in Scholle, P.A., and Spearing, D., eds., Sandstone Depositional Environments. American Association of Petroleum Geologists Memoir 31, p. 115-137

Case, J.E., Duran, S., L.G., Lopez R., A., and Moore, W.R., 1971. Tectonic investigations in Western Colombia and Eastern Panama. Geological Society of America, Vol. 82, p. 2685-2712.

Collinson, J.D., 1978. Alluvial sediments, in Reading, H.G., ed., Sedimentary Environments and Facies. Elsevier, New York, p. 15-60.

Darby, D.A., 1976. An evaluation of the auriferous gravels along the Rio Magui, Colombia, South America. Technical Report PGSTR-GE76-34, Old Dominion University, Norfolk, Virginia, 37 p.

Darby, D.A., 1983a. Geology and sedimentology of the Rio Magui terraces near Payan, Colombia, S.A. Technical Report GSTR-83-3, Old Dominion University, Norfolk, Virginia, 24 p.

Darby, D.A., 1983b. Hydrologic assessment of the planned hydraulic mining along the Rio Magui, S.W. Colombia, S.A. Technical Report GSTR-83-1, Old Dominion University, Norfolk, Virginia, 11 p.

Darby, D.A., and Whittecar, G.R., 1984. Geology and gold evaluation of the Payan Mining District, Narino, Colombia. Technical Report GSTR-84-11, Old Dominion University, Norfolk, Virginia, 98 p.

Darby, D.A., and Whittecar, G.R., 1985. A model of placer deposition in tropical alluvial fans lacking bedrock control. The Geological Society of America Abstracts with Programs, Vol. 16, No. 2, p. 87.

Douglas, I., 1977. Humid Landforms. MIT Press, Cambridge, Massachussetts, 288 p.

Garrett, J.R., 1985. A depositional model for the auriferous gravels in the Payan Mining District, Department of Nariño, Colombia, South America. M.S. Thesis: Old Dominion University, Norfolk, Virginia, 142 p.

Hall, M.L., and Wood, C.A., 1985. Volcano-tectonic segmentation of the northern Andes. Geology, Vol. 13, p. 203-207.

High, L.R., Jr., and Piccard, M.D., 1971. Mathematical treatment of orientation data, in Carver, R.E., ed., Procedures in Sedimentary Petrology. Wiley-Interscience, New York, p. 21-45.

Irving, E.M., 1975. Structural evolution of the northernmost Andes, Colombia. Geological Survey Professional Paper #846. U.S. Government Printing Office, Washington D.C., 47 p.

Isenor, A., 1941. Cross-sections thru drill lines, Magui River, Compañia Minera de Nariño, (Unpublished Report).

Jeffery, P.G., and Hutchinson, D., 1981. Chemical Methods of Rock Analysis. Pergamon Press, New York, 379 p.

Johnson R.D.O., 1912. Native placer mining in Colombia. The Engineering and Mining Journal, Vol. 94, p. 741-744.

Kim, J., 1975. Factor analysis, in Nie, N.H., ed., SPSS: Statistical Package for the Social Sciences, McGraw-Hill, Inc., New York, p. 468-514.

Klecka, W.R., 1975. Discriminant analysis, in Nie, N.H., ed., SPSS: Statistical Package for the Social Sciences, McGraw-Hill, Inc., New York, p. 434-467.

Lonsdale, P., and Klitgord, K., 1978. Structure and tectonic history of the eastern Panama Basin. Geological Society of America Bulletin, Vol. 89, p. 981-999.

Lusney, J.E., 1981. Report on Rio Magui Placer Properties for Cal-Colombian Mines, Ltd., 16 p. (Unpublished Report).

Miller, B.L., and Singewald, J.T., Jr., 1919. The Mineral Deposits of South America. McGraw-Hill, Inc., New York, 598 p.

Mooney, W.D., 1980. An east Pacific-Caribbean ridge during the Jurassic and Cretaceous and the evolution of western Colombia, in Pichler, R.H., Jr., ed., The Origin of the Gulf of Mexico and the Early Openings of the Central North Atlantic Ocean. Louisiana State University Press, Baton Rouge, Louisiana, p. 55-74.

Nicholas, F.C., 1897. Explorations in the gold fields of western Colombia. The School of Mines Quarterly, Vol. 18, p. 259-265.

Nilsen, T.H., 1969. Old Red sedimentation in the Buelandet-Vaerlandet Devonian District, Western Norway. Sedimentary Geology, Vol. 3, p. 35-57.

Nilsen, T.H., 1982. Alluvial fan deposits, in Scholle, P.A., and Spearing, D., eds., Sandstone Depositional Environments. American Association of Petroleum Geologists Memoir 31, p. 49-86

Ninkovich, D., and Shackleton, N.J., 1975. Distribution, stratigraphic position, and age of ash layer "L" in the Panama Basin region. Earth and Planetary Science Letters, Vol. 27, p. 20-34.

Oppenheim, V., 1949. Geologia de la costa sur del Pacifico de Colombia. Instituto Geofisico De Los Andes Colombianos, Boletin, Vol. 1, 23 p.

Ortiz, H.D., 1982a. Projecto Payan, reconocimiento geologico de depositos de placer: Informe de progresso No. 1, para Compania Minera de Colombia Y Texas, S.A., Inc., 13 p. (Unpublished Report).

Ortiz, H.D., 1982b. Development and mining project for the area of exloration license 8705, municipality of Magui (Payan), Department of Narino: for Compania Minera de Colombia Y Texas, S.A., Inc., 30 p. (Unpublished Report).

Ortiz, H.D., 1983. Projecto Payan, exploracion geologia de depositos de placer: Informe de progresso No. 2, para Compania Minera de Colombia Y Texas, S.A., Inc., 13 p. (Unpublished Report).

Pereira-Gamba, F., 1909. Mineral resources of the south of Colombia, South America. The Engineering and Mining Journal, Vol. 88, p. 312-313.

Radelli, L., 1965. Metallogenic belts and igneous rocks of the Colombian Andes. Travaux du Laboratoire de Geologie de la Faculte des Sciences de Grenoble, Tome 41, p. 219-228.

Ramirez, J.E., and Aldrich, L.T., 1977. The Ocean-Continent Transition in SW-Colombia. Instituto Geofisico Universidad Javeriana, Bogota, Colombia, 313 p.

Reeves, R.D., and Brooks, R.R., 1978. Trace Element Analysis of Geological Materials. John Wiley and Sons, Inc., New York, 421 p.

Restrepo, V., 1886. A Study of the Gold and Silver Mines of Colombia. C. Jourgensen, New York, 320 p.

Rodriguez Guerrero, I., 1961. Geografia Economica De Narino, Tomo IV. Editorial Sur Colombiana, Pasto, 362 p.

Rust, B.R., 1979. Facies models 2: coarse alluvial deposits, in Walker, R.G., ed., Facies Models. Geoscience Canada, Reprint Series No. 1., p. 9-21.

Ruxton, B.P., 1968. Rates of weathering of Quaternary volcanic ash in north-east Papua. Ninth International Congress of Soil Science Transactions, Vol. 4, Paper 38, p. 367-376.

Sandoval, J., 1936. Estudios mineros de algunas regiones del Departmento de Narino. Boletin de Minas Y Petroleos, Nos. 91-96, p. 368-378.

Schumm, S.A., 1977. The Fluvial System. John Wiley & Sons, New York, 338 p.

Slingerland, R., 1984. The role of hydraulic sorting in the origin of fluvial placers. Journal of Sedimentary Petrology, Vol. 54, No. 1, p. 137-150.

Steen-McIntyre, V., 1977. A Manual for Tephrochronology. Ph.D. Dissertation: University of Idaho, Moscow, Idaho, 167 p.

Tricart, J., 1972. The Landforms of the Humid Tropics, Forests and Savannas. St. Martin°s Press, Inc., New York, 306 p.

Tsang, Y.W., 1985. The use of ilmenite element composition for determination of provenance. M.S. Thesis: Old Dominion University, Norfolk, Virginia, 99 p.

Utter, T., 1984. Geological settings of primary gold deposits in the Andes of Colombia (South America), in Gold °82: Geology, Geochemistry, and Genesis of Gold Deposits, A.A. Balkema, Rotterdam, The Netherlands, p. 731-753.

Van Houten, F.B., and Travis, R.B., 1968. Cenozoic deposits, Upper Magdalena Valley, Colombia. American Association of Petroleum Geologists Bulletin, Vol. 52, p. 675-702.

Ward, W.F., 1913. Nechi River placer mining, Colombia. The Engineering and Mining Journal, Vol. 96, p. 297-299.

West, R.C., 1952a. Colonial Placer Mining in Colombia. Louisiana State University Press, Baton Rouge, Louisiana, 157 p.

West, R.C., 1952b. Folk mining in Colombia. Economic Geography, Vol. 28, p. 323-330.

West, R.C., 1957. The Pacific Lowlands of Colombia. Louisiana State University Press, Baton Rouge, Louisiana, 278 p.

Whittecar, G.R., Darby, D.A., Barringer, R.A., Garrett, J.R., and Babuin, M.L., 1984. Changes of Quaternary fluvial systems in a high relief humid tropical environment. The Geological Society of America Abstracts with Programs, Vol. 16, No. 6, p. 693.

Whittecar, G.R., Babuin, M.L., Barringer, R.A., and Darby, D.A., 1985. Tectonic geomorphology on the coastal plain of southwest Colombia. The Geological Society of America Abstracts with Programs, Vol. 17, No. 7, p. 750.

Zeil, W., 1979. The Andes: A Geological Review. Gebruder Borntraeger, Berlin, 260 p.

Appendix A

Stratigraphic Description of Mines

(after Darby and Whittecar, 1984)

APPENDIX A. STRATIGRAPHIC DESCRIPTIONS OF MINES, PAYAN MINING DISTRICT

EXPLANATION OF SYMBOLS

	volcanic ash, both pyroclastic and reworked
	highly weathered volcanic ash (clay)
	volcanic gravel or volcanic conglomerate
	laminated volcanic ash
	mud or mudstone
	cobble to boulder gravel with sandy matrix
	pebble to cobble gravel with sandy matrix
	sand
	wood debris
	cross-bedding
	cobble imprication
	grab sample
	0.25m^3 sample for Au content
	0.5 m^3 sample for Au content
	1.0 m^3 sample for Au content

TYPED DESCRIPTIONS

σ	sorting
Mz	average size of matrix
Max	maximum clast size in matrix
V	volcanic fragment or aggregate
Q	quartz
Q/	bipyramidal quartz
M	mica (mostly leached biotite)
B	biotite
Mag	magnetite and other opaques
H	hematite (coating)
L	lithic fragment (mostly volcanic)
G	garnet
Py	pyrite
H	hornblende
( )	minerals in order of abundance

DISTANCE AND DIRECTION TO MINE SITE BASED UPON BRASS MARKER IN FRONT OF PAYAN CHURCH.

ALCOSE (1000 meters, N22W)

DESCRIPTIONS OF STRATIGRAPHIC SECTIONS

GOLD CONTENT (oz/yd^3)

-cobble to boulder gravel with red-brown to gray sand matrix (0.25-2mm) mostly weathered to clay; average clast is 8-10cm; maximum clast is 45 cm.

-sand lense with laminae of gray, brown or red sand (0.2-2mm), mostly weathered to clay; convolute bedding & liesegang rings; laminations dip N30°W at 19°.

-? ash

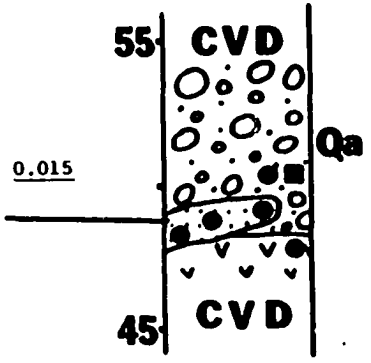

DESCRIPTIONS OF ANALYZED SAMPLES

ALC-3	Mz=0.2mm Max=0.8mm(Q,V,M)
ALC-4,2, and 1	Mz=0.14mm Max=2mm(V,Q',L,M,B)
ALC-5	Mz=0.3mm Max=2mm σ=poor(V,Q,B,M)

ANANIAS (1400 meters, S51E)

DESCRIPTIONS OF STRATIGRAPHIC SECTIONS

GOLD CONTENT (oz/yd^3)

-red ash and fine-grained volcanic gravel mostly weathered to clay.

-white ash, very blocky with iron concretions, laminated at the base; pyroclastic debris is finer than 0.08mm. Sharp contact with sand below dips to south (7°).

-dark gray fine sand (0.13-0.25mm)

-cobble to boulder gravel with fine to coarse sand matrix (0.12-1mm); charred wood debris in upper meter; average clast is 12cm and largest boulder is 35cm.

-buff colored volcanic sand, fine conglomerate & ash, well indurated.

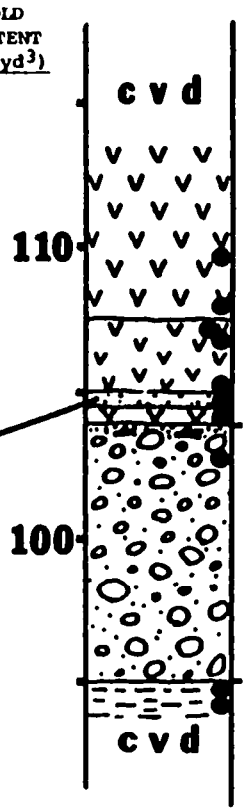

DESCRIPTIONS OF ANALYZED SAMPLES

ANA-4	Mz=0.21mm Max=2.1mm σ=good(V,L,Mag,Q,B)
ANA-8	Mz=0.25mm Max=1.2mm σ=mod.(Q,V,Mag,M)
ANA-2	
ANA-3	Mz=0.33mm Max=4.3mm σ=poor(H,Basalt,Q,B)
ANA-6	Mz=0.2mm Max=0.7mm σ=good(Mag,V,Q)
ANA-7	Mz=0.1mm Max=0.9mm σ=good(V,Q,B,Mag)
ANA-5	Mz=0.3mm Max=1.6mm σ=mod.(V,Q,Mag,B)
ANA-1	MZ=0.18mm Max=0.5mm(V,Q,M,H,L)
ANA-9	Mz=0.3mm Max=0.9mm(V,Q,M)
ANA-10	MZ=0.1mm Max=0.6mm(V,Q,Mag,L)

ANGUIÑO (280 meters, S51E)

DESCRIPTIONS OF STRATIGRAPHIC SECTIONS

GOLD CONTENT (oz/yd^3)

-ash

-interbedded light gray mudstone lenses & brown or gray sand with wood debris in both. Sand is also lense-shaped with irregular contacts with mudstone.

-pebble gravel with gray, fine sandy matrix, moderately sorted & lacking wood debris. Chert pebbles abundant. Iron-rich concretions along contact between gravels.

-pebble gravel with red-brown, very fine to coarse sand matrix; no wood debris; abundant chert cobbles; many coated with iron.

-light gray massive mudstone exposed in sluice.

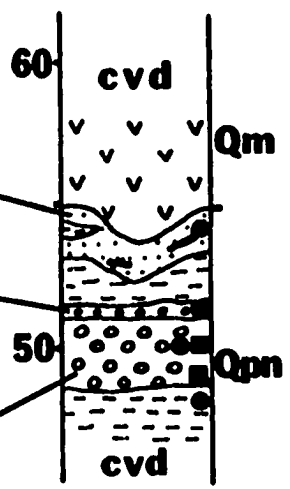

DESCRIPTIONS OF ANALYZED SAMPLES

ANG-1	Mz=0.18mm Max=2mm(L,Q',L,M)
ANG-2	Mz=0.1mm Max=0.37mm(Q,V,G,L)
ANG-3	Mz=0.5mm Max=2mm(Q,V,Mag)
ANG-4	Mz=0.4mm Max=0.7mm(Q,V,L,M)

BLANDITO (850 meters, S17E)

DESCRIPTIONS OF STRATIGRAPHIC SECTIONS

GOLD CONTENT (oz/yd^3)

-red ash & fine-grained volcanic gravel. very clayey with many 3-5cm clases weathered to clay. Irregular indistinct boundary.

0.012

-pebble to boulder gravel with white-to-red clayey matrix. Nearly all clasts weathered to clay. No wood observed. Contains one-meter-thick lens of thorougly weathered fine-to-coarse sand. Average clasts are 6cm, maximum clasts are 35 cm. Matrix contains 0.5-2mm grains weathered to clay.

-fine red ash, reworked.

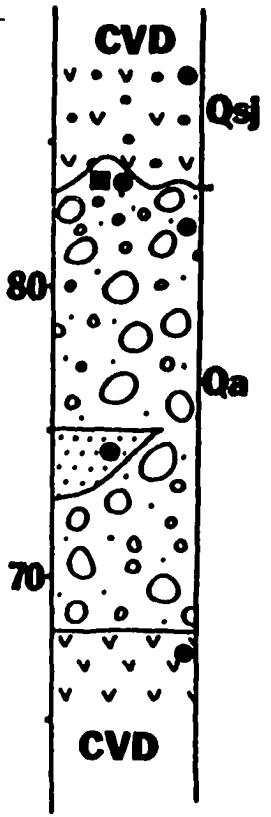

DESCRIPTIONS OF ANALYZED SAMPLES

BLA-5 Mz=0.2mm Max=0.9mm σ=good(Q,Mag,V,H,M)

BLA-4

BLA-3 Mz=0.12mm Max=35cm(V,Q,M)

BLA-2 Mz=0.12mm Max=2mm(V,Q,M,Mag)

BLA-1 Mz=0.13mm Max-0.6mm σ=good(Q,Mag,V,M)

CLARISA (890 meters, N32E)

DESCRIPTIONS OF STRATIGRAPHIC SECTIONS

GOLD CONTENT (oz/yd^3)

-ash

-pebble gravel with fine sandy matrix poorly sorted (CLA-2). Firm chert pebbles abundant.

-UNCONFORMITY

-red medium to coarse sand, entirely weathered to clay.

-brown & red cobble-to-pebble gravel with sandy matrix. Thoroughly weathered to clay: Lens of medium-coarse contains wavy laminations and cross-bedding dipping S30E, N70E, & N55E.

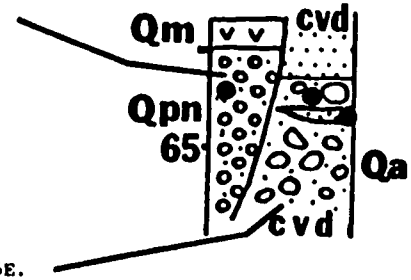

DESCRIPTIONS OF ANALYZED SAMPLES

CLA-2	Mz=0.25mm Max-2.0mm(V,Q/)
CLA-1	Mz=0.25mm Max-1.0mm(V,Q,M)
CLA-3	Mz=0.12mm Max-2.0mm(V,L,Q,M)

EPIMENIO (530 meters, N13W)

DESCRIPTIONS OF STRATIGRAPHIC SECTIONS

GOLD CONTENT (oz/yd^3)

-red to white ash weathered to clay.

-intercalated medium sand & mudstone with occasional wood debris especially concentrated at base of unit.

-cobble to boulder gravel with light gray, medium sand (0.35mm) matrix; average clast is 6cm & maximum clast is 30cm; varying degrees of weathering in cobbles.

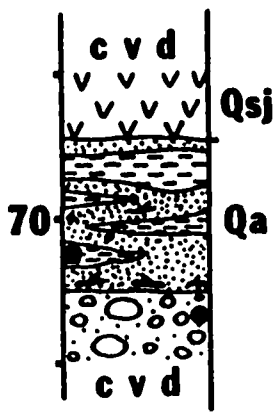

DESCRIPTIONS OF ANALYZED SAMPLES

EPI-2 Mz=0.2mm Max=0.3mm(V,Q,Mag,L)

EPI-1 Mz=0.35mm Max=0.5mm(Q,V,L,M,H,B)

HIPOLITO (440 meters, N40E)

DESCRIPTIONS OF STRATIGRAPHIC SECTIONS

	GOLD CONTENT (oz/yd^3)
-red & white mottled ash & fine-grained volcanic gravel. Many banded rock fragments weathered to clay.	
-very fine-grained mudstone. Blocky and massive.	
-cobble gravel with blue-gray matrix interbedded with sand lenses. Cobbles well-rounded with moderately thick weathering rinds. Some imbrication visible. Lowest blue-gray sand lens contains poorly sorted coarse sand with some thin cobble beds and no wood. Middle sand lens deposited behind 2-meter boulder & contains medium-to-coarse sand with weathered pebble ghosts & no sedimentary structures. The upper sand lens contains medium-to-coarse sand with abundant wood debris & no sedimentary structures. All sand lenses partly weathered to clay.	0.010 0.008 0.002
-fine-grained compact mudstone & medium sand.	

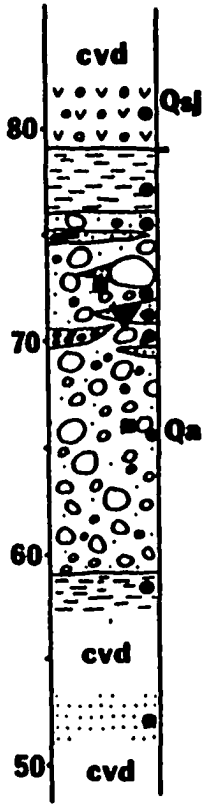

DESCRIPTIONS OF ANALYZED SAMPLES

HIP-10	Mz=0.1mm Max=1.7mm(Q,V,Mag,M)
HIP-2	Mz=0.18mm Max=0.4mm(Q,V,Mag,B)
HIP-4	Mz=0.1mm Max=0.37mm(V,Q,L,M)
HIP-5	Mz=0.1mm Max=2mm(Q/,V,Mag,M,L)
HIP-7	Mz=0.09mm Max=2mm(Q,V,M,Mag,L.)
HIP-3	Mz=0.2mm Max=0.8mm(Q,V,L,M)
HIP-8	Mz=0.09mm Max=1mm(Q/,V,Mag,L)
HIP-9	Mz=0.2mm Max=2mm(V,Q/,Mag,L,Py)
HIP-6	Mz=0.37mm Max=2mm(V,Q,Mag,B,G,Py)
HIP-1	Mz=0.2mm Max=0.9mm(Q,V,Mag,L)
MAG-3	Mz=0.3mm Max=0.4mm(Q,Mag,V,M,L)

LA JUNTA (540 meters, N45W)

DESCRIPTIONS OF STRATIGRAPHIC SECTIONS

DESCRIPTIONS OF ANALYZED SAMPLES

GOLD CONTENT (oz/yd^3)

-red to red-gray, highly weathered ash; some laminae 5m above the base of unit.

-greenish, gray cobble gravel (average clast is 10cm, maximum size is 20cm) with coarse sand (.8-1mm) matrix; mostly weathered to clay except for cobbles.

-gray, compact, fine sand mostly weathered to clay.

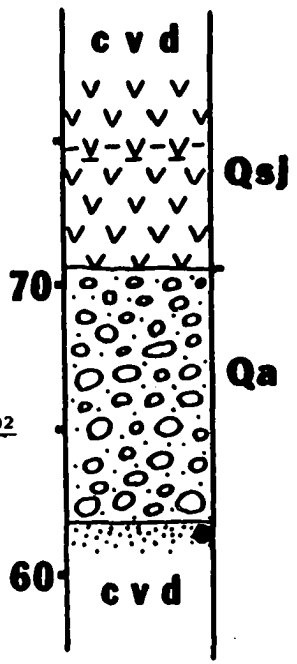

0.00002
0.002
0.008
0.009
0.010
0.013
0.082
0.029
0.005

LAJ-1 Mz=0.13mm Max=0.7mm(V,L,Q,M,Mag)

Average value (±0.082) from 50-55 level.
in nearby drill hole (Ortiz, 1983).
49m level (Ortiz, 1983).
48m level (Ortiz, 1983).
Average (±0.005) from 40-47m level).

LUIS (430 meters, N51W)

DESCRIPTIONS OF STRATIGRAPHIC SECTIONS

GOLD CONTENT (oz/yd^3)

-red-brown volcanic ash; colluvium. Irregular contact.

-cobble gravel with grey-brown coarse sandy matrix. Cobbles average 8cm diameter, maximum 15 cm.

-coarse sand with interbedded pebble lens. Sand is bluish-gray with scattered wood fragments & many pyrite grains visible. Iron staining present along fractures. Pebbles in lens are 3-5cm & weathered to clay. Troughs filled with pebbles are 30 to 70cm long. Carbonized wood & no pebbles lie in sand below pebble lens. Sharp undulatory contact at base of sand.

-cobble gravel with grayish-brown sand matrix.

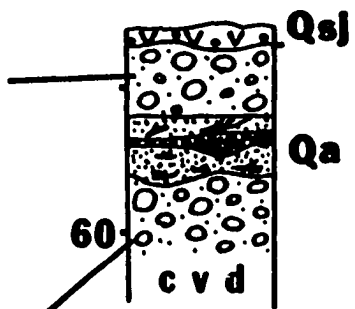

DESCRIPTIONS OF ANALYZED SAMPLES

LUI-1 Mz=0.13mm Max=3-5cm(V,Q,M,L,Mag,B,Py)

MAGDALENA (340 meters, N46E)

DESCRIPTIONS OF STRATIGRAPHIC SECTIONS

GOLD CONTENT (oz/yd^3)

-tan -to-orange volcanic ash, clayey. Many liesegang rings 1 to 3mm thick.

-orange-to-white volcanic ash & volcanic sand with black-to-rust iron concretionary layers. Clasts in volcanic gravel are medium-to-coarse sand.

-cobble to boulder gravel with coarse, poorly-sorted sand matrix. Clasts average 15cm in outcrop, maximum 36cm. 60cm boulder seen in tailings. Many cobbles in contact with cobbles while others float in matrix. Cobbles fine upwards & have notable imbrication. Minor amounts of wood present. Matrix well-weathered to clay, bottled from white-to-red.

-compact gray mudstone, exposed in sluice.

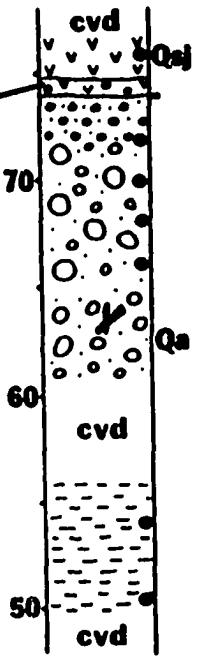

DESCRIPTIONS OF ANALYZED SAMPLES

MAG-9	Mz=0.12mm Max=1.1mm(Q,V,Mag,M)
MAG-6	Mz=0.25mm Max=3mm(V,Q,Mag,B)
MAG-7	Mz=0.25mm Max=0.5mm(V,Q,M)
MAG-2	Mz=0.25mm Max=0.5mm(V,Q,M)
MAG-1	Mz=0.25mm Max=1mm(V,Q,M)
MAG-5	Mz=0.2mm Max=0.5mm(V,Q,B)
MAG-4	Mz=0.1mm Max=0.4mm(Q,L,Mag,V,M)
MAG-8	Mz=0.3mm Max=1.9mm(Q,V,L,M,H)

MARIANNA (470 meters, N47E)

DESCRIPTIONS OF STRATIGRAPHIC SECTIONS

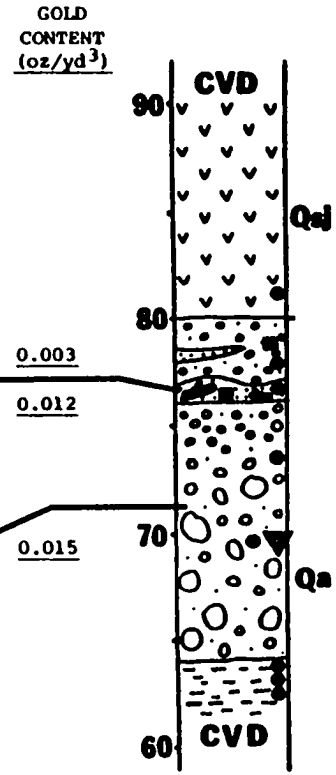

-red ash & volcanic sand, highly weathered.

-cobble to boulder gravel (average size of clasts is 10cm, maximum size is 35cm) with red & gray, mottled, coarse sand (0.5-0.8mm) matrix & lenses of mud & sand; mostly weathered to clay.

-gray, coarse sand (0.5-0.8mm) with wood debris (up to 0.8m) especially concentrated near top of unit; weathered to sticky clay; alternating coarse & fine-grained laminae & trough cross-bedding dipping 8° to west (N86°W).

-cobble to boulder gravel (average clast is 20cm, maximum clast is 80 cm) with blue-gray, weathered coarse to medium sand matrix; cobbles fine upward.

-compact, gray to brown mudstone with small amount of medium to coarse sand.

DESCRIPTIONS OF ANALYZED SAMPLES

MAR-1 Mz=0.2mm Max=1.4mm σ =mod.(Q,V,Mag)

MAR-8 Mz=0.25mm Max=0.5mm(V,Q,M)
MAR-5 Mz=0.09mm Max=0.5mm(L,Q,M,Mag)

MAR-3 Mz=0.25mm Max=0.5mm(V,Q,M,L)

MAR-4 Mz=0.25mm Max=0.5mm(Q,V,M,H)

MAR-6 Mz=0.06mm Max=0.7mm(Q,V,L,Mag)
MAR-2 Mz=0.1mm Max=1.3mm(V,Q,M,L,Mag)
MAR-7 Mz=0.1mm Max=0.7mm(Q,V,M,Mag,L)

MARTA (880 meters, N31E)

DESCRIPTIONS OF STRATIGRAPHIC SECTIONS

GOLD CONTENT (oz/yd^3)

-red volcanic ash.

-red-brown to gray coarse sand; many weathered ghost grains. Scattered wood debris. No sedimentary structures visible. Contains poorly sorted pebble gravel lens with wood debris.

0.012

0.040

-cobble-to-boulder gravel with sandy matrix. Cobbles average 10 cm in outcrop, maximum 45 cm. Many weathered clay ghosts of pebbles.

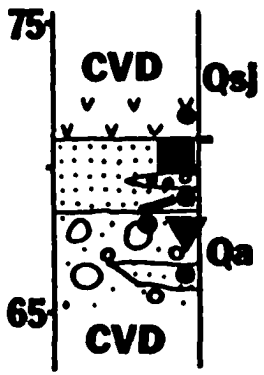

DESCRIPTIONS OF ANALYZED SAMPLES

MAT-1 Mz=0.2mm Max=1.6mm(Q,V,Mag)

MAT-2 Mz=0.1mm Max=5mm(Q,L,M.Mag)

MAT-3 Mz=0.2mm Max=0.8mm(L,Q,M,H)

MAT-4 Mz=0.13mm Max=4mm(Q,L,Mag)

PAÑAMBISITO (690 meters, S50E)

DESCRIPTIONS OF STRATIGRAPHIC SECTIONS

GOLD CONTENT (oz/yd^3)

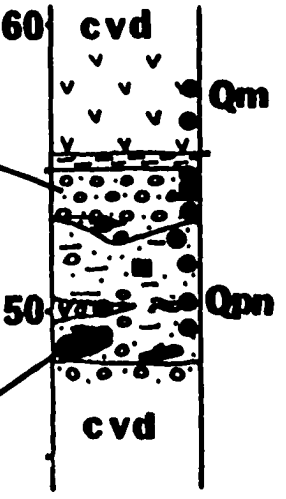

-red volcanic ash, very sticky.

-grey mudstone.

-pebble gravel with grey clayey matrix. Pebbles predominately white chert. Lens of coarse sand & gravel interbedded at base of unit; irregular abrupt contact.

-interbedded sands, mudstones, clays & pebbly gravel in extremely variable bedding pattern. Half-meter long logs & stumps, nuts & leaves present in organic-rich mudstone & medium sand. Agglomerate lens 25cm thick also interbedded.

-pebble conglomerate with very large basalt boulders visible in sluice.

DESCRIPTIONS OF ANALYZED SAMPLES

PAN-9	Mz=0.2mm Max=0.6mm(Q,V,Mag,M)
PAN-7	Mz=0.2mm Max=1.0mm(Q,V,Mag,M,B)
PAN-10	Mz=0.2mm Max=1.9mm(L,Q,M)
PAN-3	Mz=0.25mm Max=0.8mm(Q/,V,L,M)
PAN-2	Mz=0.25mm Max=0.5mm(V,Q/,L,M)
PAN-6	Mz=0.9mm Max=2mm(Q,L,Mag,M)
PAN-1	Mz=0.05mm Max=0.2mm(Q,V,Mag,L)
PAN-4	Mz=0.25mm Max=1.5cm(L,Q,Mag,M)
PAN-8	Mz=0.09mm Max=1.2cm(L,Q,Mag)
PAN-5	Mz=0.2mm Max=1.4mm(Q,V,Mag,B)
PAN-11	Mz=0.2mm Max=0.6mm(V,Q,H,wood debris)

PICCININI (580 meters, N44W)

DESCRIPTIONS OF STRATIGRAPHIC SECTIONS

	GOLD CONTENT (oz/yd^3)
-red to reddish, gray ash, highly weathered to a sticky mud. Volcanic gravel at base.	
-red to gray ash, weathered to sticky mud.	
-cobble gravel (average size is 8-10cm, maximum size is 18cm) with a greenish-gray, coarse sand (1-2mm) matrix; mostly weathered to clay.	
	0.0005
	0.0003
-discontinuous medium sand lense without wood debris.	0.003-0.05
-medium to coarse sand (0.3-0.5mm) with subangular grains & abundant wood debris; ripple cross beds dipping nearly due west; inter-bedded sand & organic-rich mud in places; weathered to clay.	0.009-0.07
	0.03-0.07
-cobble to boulder gravel (average size is 15cm, maximum size is 50cm) with green-gray, coarse sand matrix weathered to clay; cobbles imbri-cated indicating a flow direction to west.	0.007-0.01
	0.002
	0.004
	0.006
	0.003
	0.02

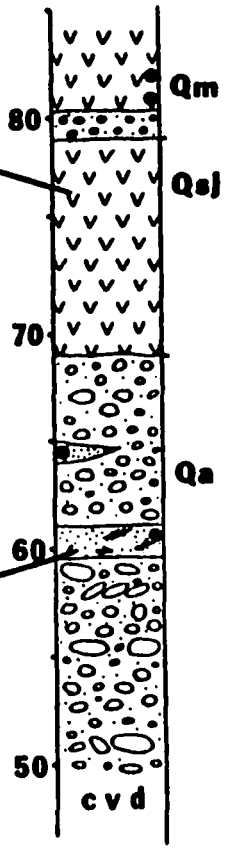

DESCRIPTIONS OF ANALYZED SAMPLES

PIC-2 Mz=0.12mm Max=1.9mm σ =mod./poor(Q,Fe,V,Mag,M)
PIC-3 Mz=0.2mm Max=0.3mm σ =good(Q,V,M,B,H,Mag)

PIC-4 Mz=0.18 mm Max=2.0mm(Q,L,M,Mag)

PIC-1 Mz=0.18mm Max=0.5mm(Q,L,Mag,B)

SAN JUAN (1220 meters, S50E)

DESCRIPTIONS OF STRATIGRAPHIC SECTIONS

GOLD CONTENT (oz/yd^3)

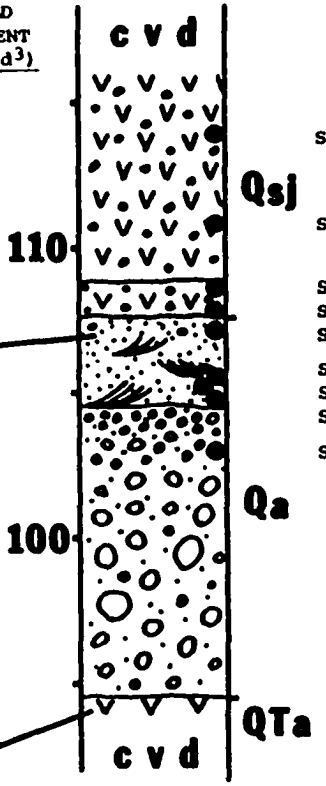

-red-brown volcanic ash & volcanic gravel; contains weathered pebbles & some cobbles. Sharp lower contact.

-dark red to white-&-purple volcanic ash & volcanic gravel; granules & pebbles up to 0.5cm present. Sharp lower contact.

-red medium sand with black sand laminae. Ripples up to 15cm amplitude present with dip directions at N20°W(21°) & S50°W(6°). Very little black sand present in upper 0.5 m of sand; some isolated 1cm pebbles present. Red clay laminations 5-8cm thick present throughout unit. Sand coarsens towards base. Sharp undulatory contact.

-pebble to cobble gravel with red-to-white sandy matrix. Clasts average 3cm at the top, 10cm at the base; maximum 35cm. Matrix & many cobbles extensively weathered to clay. Matrix ghost textures show medium-to-coarse sand.

-dark blue to buff colored volcanic sand, fine conglomerate & ash; well indurated.

DESCRIPTIONS OF ANALYZED SAMPLES

SJU-6	Mz=0.15mm Max=0.7mm σ=mod.(Q,F,V,M)
SJU-9	Mz=0.12mm Max=1.0mm σ=mod.(V,Q,Mag,M)
SJU-8	Mz=0.3mm Max=1.0mm σ=mod.(V,Q,Mag,M)
SJU-7	Mz=0.1mm Max=0.9mm σ=good(Q,V,Mag,M)
SJU-10	Mz=0.13mm Max=4.0mm(L,Q,M,Mag)
SJU-2	Mz=0.09mm Max=2.0mm(L,Q,Mag,M,L,B)
SJU-3	Mz=0.09mm Max=2.0mm(L,Q,Mag,M,L,B)
SJU-11	Mz=0.13mm Max=2.0mm(L,Q,Mag,M)
SJU-3/4	Mz=0.13mm Max=0.5mm(Q,L,H,Mag,M)

SANTA ANA TERRACE (ORTIZ) (300-600 meters west of Payan)

DESCRIPTIONS OF STRATIGRAPHIC SECTIONS

GOLD CONTENT (oz/yd^3)

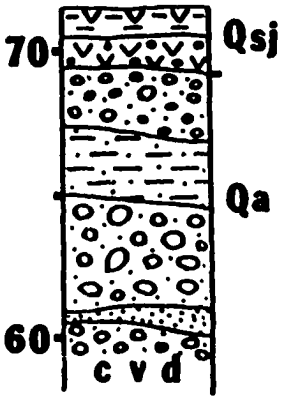

0.000025

0

0.0001
0.0015
0.0001
0.003
0.005
0.009

-weathered ash.
-weathered volcanic gravel & ash.

-cobble gravel (average clast is ∿6cm, with coarse sand matrix, mostly weathered to clay.
-blue-gray mudstone, finely laminated with leaf debris in places along laminae.

-cobble to boulder gravel (average clast is ∿10cm, maximum clast is 35cm) with coarse sand matrix, mostly weathered to clay.
-gray medium-coarse sand with minor wood debris, mostly weathered to clay.

-cobble to boulder gravel (average clast is ∿10cm, maximum clast is ∿30cm) with coarse sand matrix, mostly weathered to clay.

SANTO DOMINGO I (480 meters, S9E)

DESCRIPTIONS OF STRATIGRAPHIC SECTIONS

-red-brown ash & volcanic gravel (up to 10cm clasts) weathered to clay.

-red-brown, blocky ash, weathered to clay.

-white ash.

-lense of gray, medium sand (0.25-0.35mm) mostly weathered to clay.

-cobble to small boulder gravel (average clast is 10cm, maximum clast is 30cm) with brown to tan coarse sand matrix mostly weathered to clay. 1.5m boulders at 74m elevation.

-*compact mudstone exposed* in sluice.

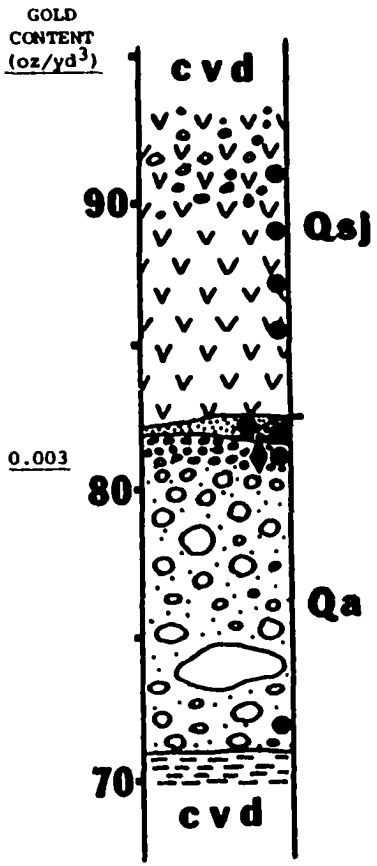

DESCRIPTIONS OF ANALYZED SAMPLES

SD1-1 Mz=0.25mm Max=0.7mm σ=good(V,Q,Mag,M)

SD1-8 Mz=0.14mm Max=2.0mm σ=poor(V,Q,Mag,M)

SD1-7 Mz=0.12mm Max=0.9mm σ=mod/good(V,Q,Mag,M)

SD1-4 Mz=0.13mm Max=1.4mm σ=mod/good(V,Q,Mag,M,H)

SD1-5 Mz=0.25mm Max=8.0mm(L,Q,M,B,Mag)

SD1-6 Mz=0.35mm Max=5.0mm(L,Q,M,Mag)

SD1-3 Mz=0.3mm Max=0.5mm(V,Q,L,M)

SD1-2 Mz=0.18mm Max=0.5mm(Q,V,M,H,L)

SANTO DOMINGO ii (670 meters, S21E)

DESCRIPTIONS OF STRATIGRAPHIC SECTIONS

GOLD CONTENT (oz/yd^3)

-ash

-dark blue-gray, blocky, & massive mudstone, well-indurated with iron staining along fractures

-cobble to boulder gravel (avg. clast is 12cm, max.40cm) with gray, coarse sand matrix; pebble gravel at top of unit at contact with mudstone; medium to coarse sand lense with charred wood debris; fine pebble gravel at base of unit in contact with underlying mudstone.

0.027

-light grey, compact mudstone.

-cobble gravel, clasts fine upward; brown coarse sand matrix.

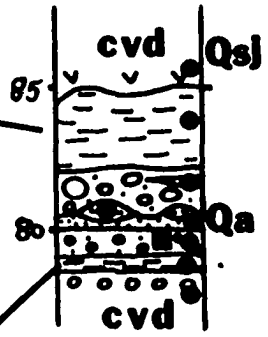

DESCRIPTIONS OF ANALYZED SAMPLES

SD2-5	Mz=0.1mm Max=1.1mm(V,Q,Mag,M)
SD2-4	Mz=0.3mm Max=0.4mm(V,M,H,Q)
SD2-3	Mz=0.24mm Max=0.7mm σ=good(Q/,V,B,M,Mag,H)
SD2-1	Mz=0.3mm Max=1.7mm(V,Q,M,Mag)
SD2-2	Mz=0.22mm Max=3mm(L,Q,H,Mag,M,B,wood debris)
SD2-9	Mz=0.1mm Max=0.2mm(V,Q,B,M,H)
SD2-6	Mz=0.4mm Max=0.12mm(V,M,Q)
SD2-7	Mz=0.1mm Max=0.37mm(Q,V,H)

SAN JOAQUIN (1190 meters, S47E)

DESCRIPTIONS OF STRATIGRAPHIC SECTIONS

-brown-red, highly weathered ash.

-white, chalky ash (weathered), with occasional dark gray & white laminae; fining upward in laminae; small-scale slump faulting present in places.

-cobble to boulder gravel with coarse sand & pebble matrix; unweathered.

-white ash.

-cobble to boulder gravel with coarse sand & pebble matrix; unweathered.

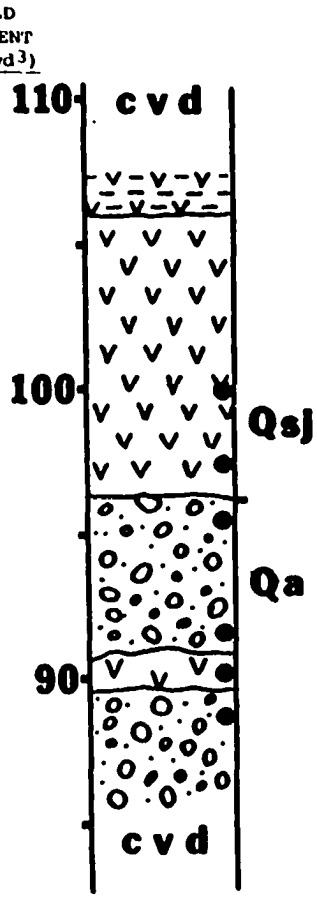

DESCRIPTIONS OF ANALYZED SAMPLES

SJO-1 Mz=0.07mm Max=0.8mm σ=mod.-good(V,Q,Mag,B)

SJO-2 Mz=0.2mm Max=2.0mm(V,Q,Mag)

SJO-5 Mz=0.25mm Max=1.0mm(Q,V,L,B,M)

SJO-4 Mz=0.8mm Max=0.5mm (V,Q,L,M,H)

SJO-6 Mz=0.25mm Max=2.5mm σ=mod.-good(Q,V,Mag,B)

SJO-3 Mz=0.25mm Max=0.7mm(V,Q,L,B)

SITE 6 (DARBY, 1976) (560 meters, S87E)

DESCRIPTIONS OF STRATIGRAPHIC SECTIONS

GOLD CONTENT (oz/yd^3)

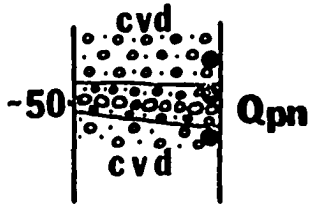

S6-2

S6-1

-pebble gravel with gray sandy matrix (Max: 10cm).

-gray fine pebble gravel (Max: 4cm) with fine sand matrix. Cobble lag interbedded in unit.

-red pebble gravel (Max: 3cm) with fine sand matrix.

TRAVESIA (560 meters, N3W)

DESCRIPTIONS OF STRATIGRAPHIC SECTIONS

GOLD CONTENT (oz/yd^3)

-pink and gray mottled ash.

-bluish-gray compact sand & mud lenses & interlaminae, fines upward; isolated cobbles, pebbles & wood debris; irregular ripple lamination & cut & fill troughs of coarse sand (0.25-0.35mm); weathers to red brown clay.

-basal coarse sand (0.25-0.5mm) with localized concentrations of black sand & large wood debris (up to 2m long); mostly weathered to clay.

0.015

0.018

-cobble to small boulder gravel with light gray, coarse sand (0.5-0.8mm) matrix; average clast is 6cm & maximum boulder size is 28cm; all degrees of cobble weathering.

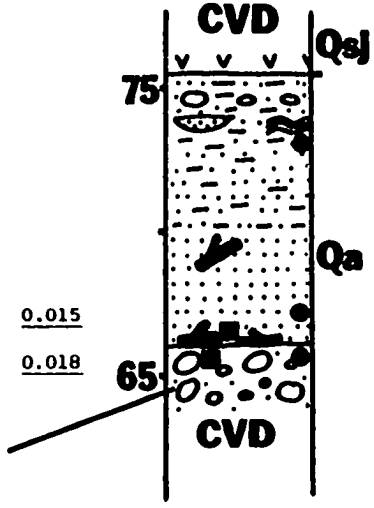

DESCRIPTIONS OF ANALYZED SAMPLES

TRA-1 Mz=0.3mm Max=0.6mm(V,Q,Mag,M,L)

TRA-2 Mz=0.1mm Max=2mm(L,Q,M,Mag,B)

TRA-3 Mz=0.1mm Max=0.8mm(V,Q,L)

Appendix B

Central Tendency of Cobble Gravel Exposures with Tests of Significance of the Resulting Rose Diagrams

GRAPHIC PLOT OF IMBRICATION DATA IN THE ALCOSE MINE

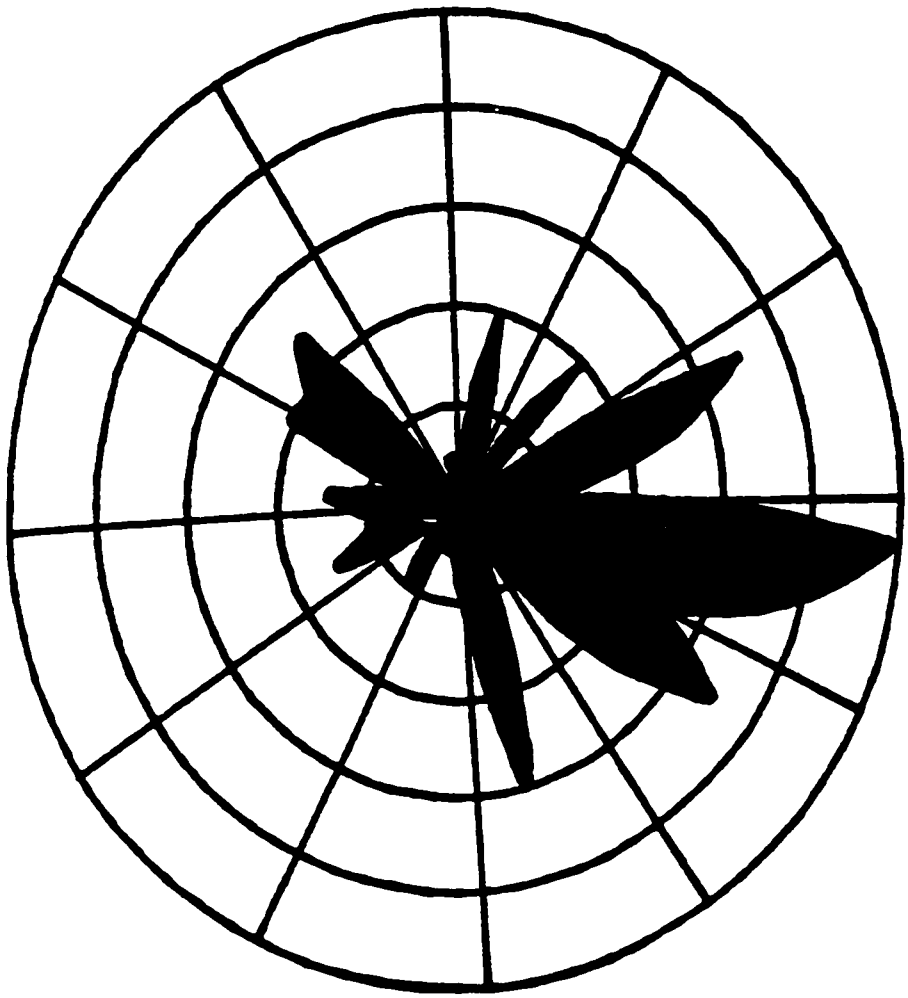

Cobble Orientation Data and Chi-Square Test Results for the Alcose Mine

Azimuth Interval	Frequency	Azimuth Interval	Frequency
0 - 9	1	180-189	0
10 - 19	4	190-199	1
20 - 29	1	200-209	1
30 - 39	1	210-219	2
40 - 49	4	220-229	1
50 - 59	0	230-239	0
60 - 69	7	240-249	3
70 - 79	5	250-259	2
80 - 89	2	260-269	2
90 - 99	10	270-279	3
100-109	8	280-289	1
110-119	5	290-299	4
120-129	7	300-309	4
130-139	4	310-319	5
140-149	0	320-329	0
150-159	2	330-339	0
160-169	6	340-349	1
170-179	2	350-359	1

Chi-Square Test Results

The expected number of observations per interval = 2.8

The tangent Theta = -7.19

The calculated value of Chi-Square = 15.48

Exceeds the value 9.21 at the 99.0 level.

The null hypothesis which states "the distribution of the cobbles is random and has no preferred orientation" is rejected.

The preferred orientation is 97.9 degrees.

GRAPHIC PLOT OF IMBRICATION DATA IN THE ANANIAS MINE

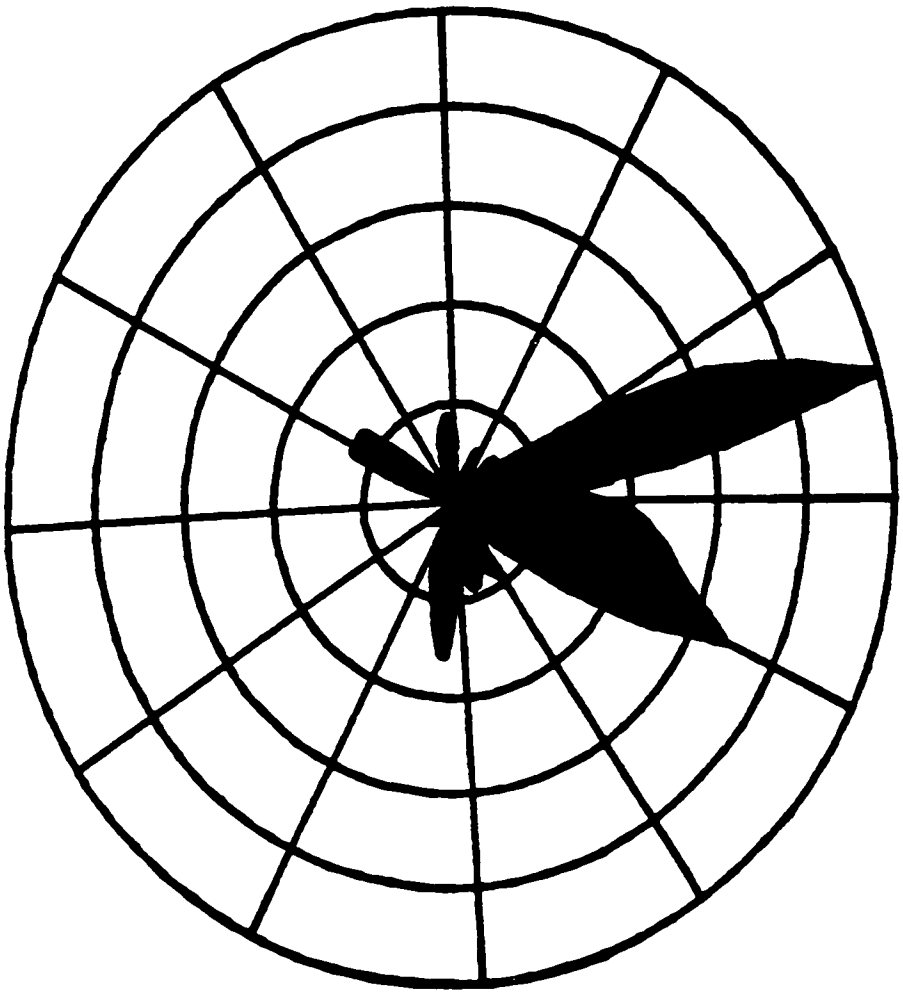

Cobble Orientation Data and Chi-Square Test Results
for the Ananias Mine

Azimuth Interval	Frequency	Azimuth Interval	Frequency
0 - 9	0	180-189	5
10 - 19	0	190-199	3
20 - 29	2	200-209	0
30 - 39	0	210-219	0
40 - 49	2	220-229	1
50 - 59	2	230-239	1
60 - 69	10	240-249	0
70 - 79	16	250-259	0
80 - 89	4	260-269	0
90 - 99	7	270-279	0
100-109	8	280-289	0
110-119	11	290-299	4
120-129	5	300-309	4
130-139	0	310-319	0
140-149	3	320-329	0
150-159	2	330-339	0
160-169	3	340-349	4
170-179	2	350-359	4

Chi-Square Test Results

The expected number of observations per interval = 2.8

The tangent Theta = -14.93

The calculated value of Chi-Square = 56.16

Exceeds the value 9.21 at the 99.0 level.

The null hypothesis which states "the distribution of the cobbles is random and has no preferred orientation" is rejected.

The preferred orientation is 93.8 degrees.

GRAPHIC PLOT OF IMBRICATION DATA IN THE ANGUINO MINE

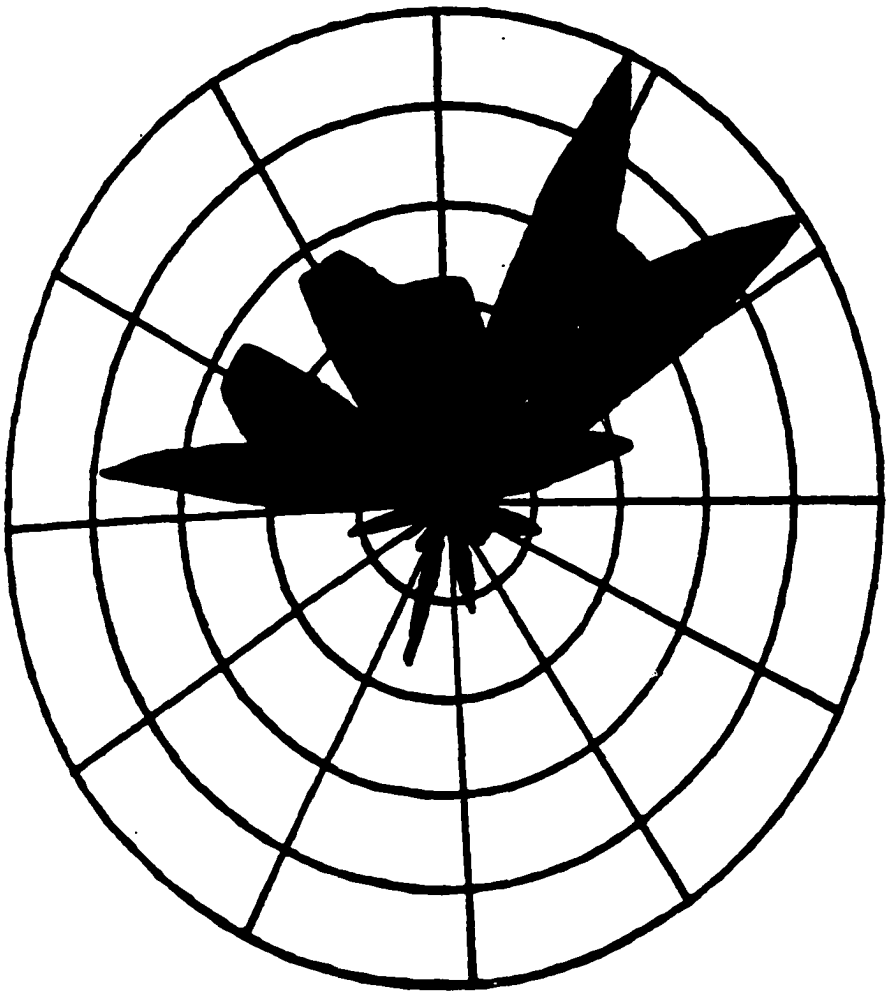

Cobble Orientation Data and Chi-Square Test Results for the Anguino Mine

Azimuth Interval	Frequency	Azimuth Interval	Frequency
0 - 9	4	180-189	0
10 - 19	3	190-199	3
20 - 29	9	200-209	0
30 - 39	6	210-219	1
40 - 49	6	220-229	0
50 - 59	9	230-239	1
60 - 69	3	240-249	0
70 - 79	4	250-259	2
80 - 89	0	260-269	0
90 - 99	1	270-279	7
100-109	2	280-289	4
110-119	1	290-299	5
120-129	1	300-309	5
130-139	1	310-319	2
140-149	0	320-329	5
150-159	1	330-339	5
160-169	3	340-349	4
170-179	0	350-359	4

Chi-Square Test Results

The expected number of observations per interval = 2.8

The tangent Theta = 0.03

The calculated value of Chi-Square = 42.36

Exceeds the value 9.21 at the 99.0 level.

The null hypothesis which states "the distribution of the cobbles is random and has no preferred orientation" is rejected.

The preferred orientation is 1.9 degrees.

GRAPHIC PLOT OF IMBRICATION DATA IN THE BLANDITO MINE

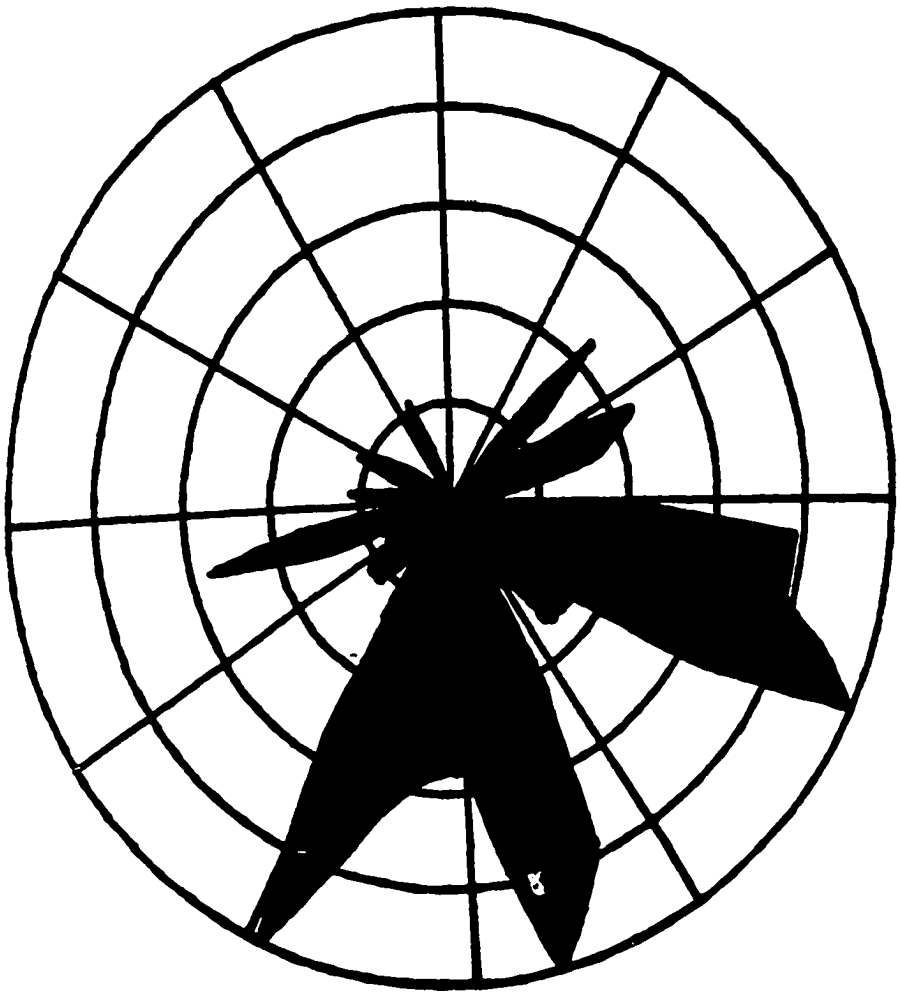

Cobble Orientation Data and Chi-Square Test Results for the Blandito Mine

Azimuth Interval	Frequency	Azimuth Interval	Frequency
0 - 9	0	180-189	5
10 - 19	0	190-199	6
20 - 29	0	200-209	9
30 - 39	0	210-219	1
40 - 49	4	220-229	2
50 - 59	1	230-239	2
60 - 69	4	240-249	1
70 - 79	3	250-259	5
80 - 89	0	260-269	1
90 - 99	7	270-279	2
100-109	7	280-289	0
110-119	9	290-299	2
120-129	3	300-309	1
130-139	3	310-319	0
140-149	0	320-329	0
150-159	7	330-339	2
160-169	9	340-349	0
170-179	5	350-359	0

Chi-Square Test Results

The expected number of observations per interval = 2.8

The tangent Theta = -0.46

The calculated value of Chi-Square = 48.49

Exceeds the value 9.21 at the 99.0 level.

The null hypothesis which states "the distribution of the cobbles is random and has no preferred orientation" is rejected.

The preferred orientation is 155.2 degrees.

GRAPHIC PLOT OF IMBRICATION IN THE HIPOLITO MINE

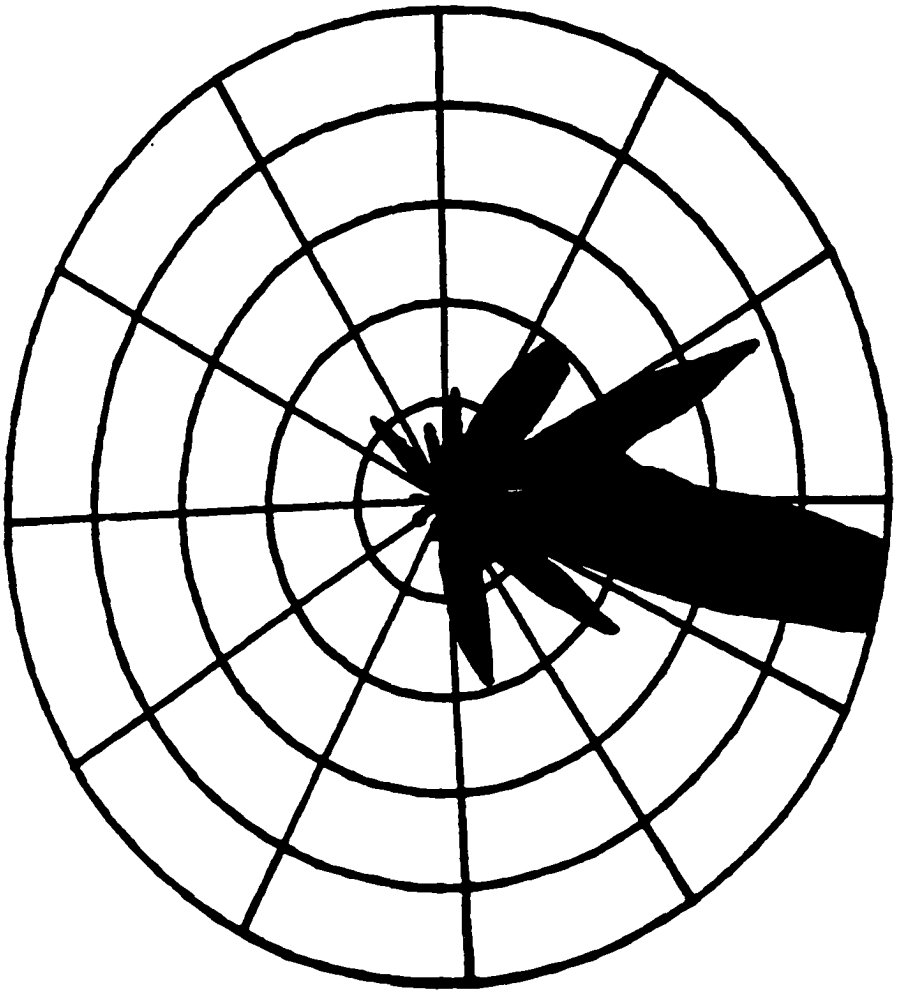

Cobble Orientation Data and Chi-Square Test Results for the Hipolito Mine

Azimuth Interval	Frequency	Azimuth Interval	Frequency
0 - 9	3	180-189	1
10 - 19	1	190-199	1
20 - 29	3	200-209	1
30 - 39	5	210-219	0
40 - 49	5	220-229	0
50 - 59	2	230-239	0
60 - 69	10	240-249	1
70 - 79	5	250-259	0
80 - 89	6	260-269	0
90 - 99	13	270-279	1
100-109	13	280-289	0
110-119	2	290-299	0
120-129	6	300-309	0
130-139	2	310-319	3
140-149	2	320-329	1
150-159	2	330-339	0
160-169	5	340-349	2
170-179	3	350-359	1

Chi-Square Test Results

The expected number of observations per interval = 2.8

The tangent Theta = 22.63

The calculated value of Chi-Square = 74.39

Exceeds the value 9.21 at tne 99.0 level.

The null hypothesis which states "the distribution of the cobbles is random and has no preferred orientation" is rejected.

The preferred orientation is 87.5 degrees.

GRAPHIC PLOT OF IMBRICATION DATA IN THE LA JUNTA MINE

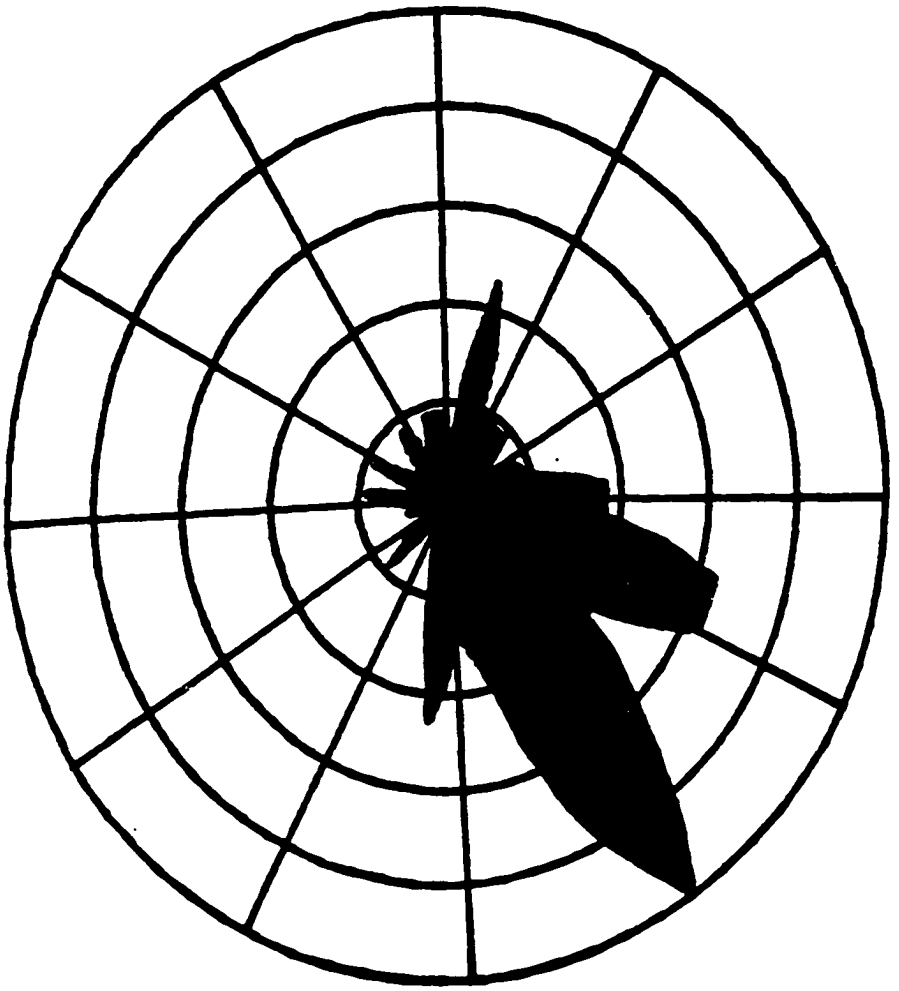

Cobble Orientation Data and Chi-Square Test Results
for the La Junta Mine

Azimuth Interval	Frequency	Azimuth Interval	Frequency
0 - 9	1	180-189	5
10 - 19	5	190-199	1
20 - 29	2	200-209	1
30 - 39	2	210-219	0
40 - 49	2	220-229	2
50 - 59	1	230-239	0
60 - 69	2	240-249	0
70 - 79	2	250-259	1
80 - 89	4	260-269	1
90 - 99	4	270-279	2
100-109	7	280-289	0
110-119	7	290-299	2
120-129	4	300-309	1
130-139	7	310-319	1
140-149	11	320-329	2
150-159	8	330-339	1
160-169	4	340-349	2
170-179	3	350-359	2

Chi-Square Test Results

The expected number of observations per interval = 2.8

The tangent Theta = -1.68

The calculated value of Chi-Square = 38.19

Exceeds the value 9.21 at the 99.0 level.

The null hypothesis which states "the distribution of the cobbles is random and has no preferred orientation" is rejected.

The preferred orientation is 120.8 degrees.

GRAPHIC PLOT OF IMBRICATION DATA IN THE PANAMBISITO MINE

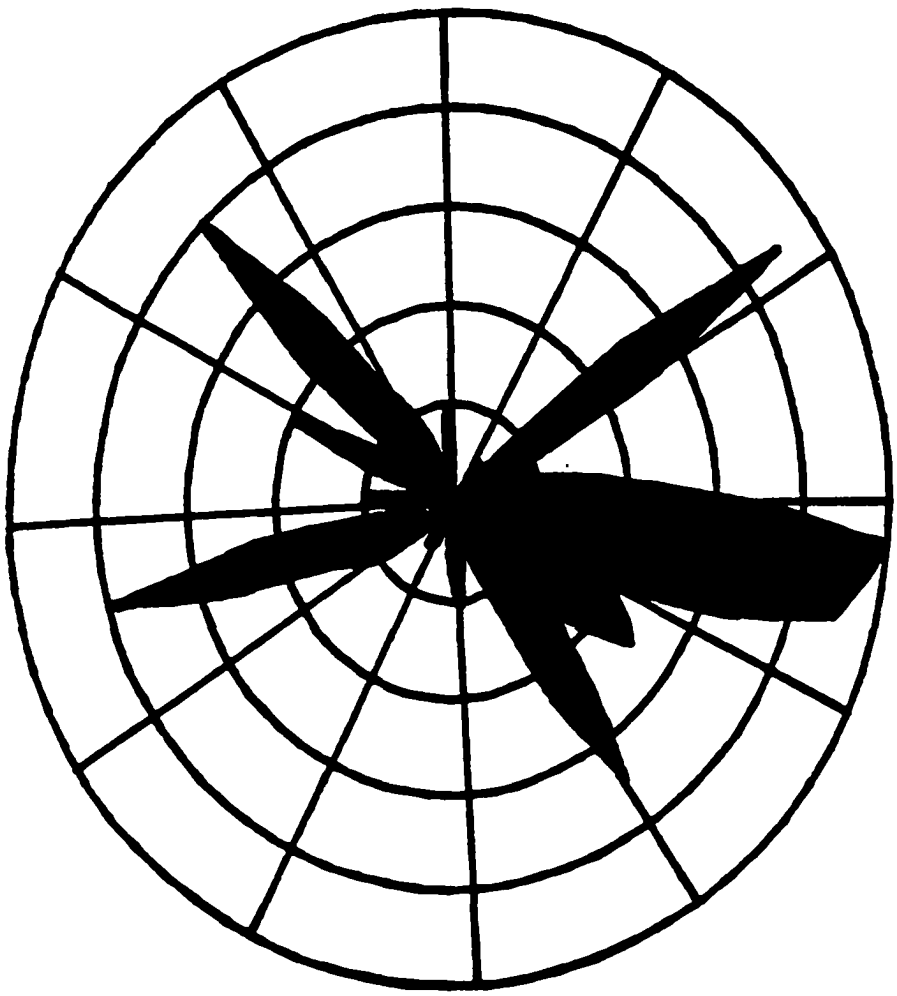

Cobble Orientation Data and Chi-Square Test Results for the Panambisito Mine

Azimuth Interval	Frequency	Azimuth Interval	Frequency
0 - 9	0	180-189	1
10 - 19	0	190-199	0
20 - 29	0	200-209	1
30 - 39	1	210-219	1
40 - 49	1	220-229	0
50 - 59	9	230-239	2
60 - 69	2	240-249	3
70 - 79	2	250-259	8
80 - 89	4	260-269	1
90 - 99	10	270-279	2
100-109	9	280-289	0
110-119	4	290-299	4
120-129	5	300-309	1
130-139	3	310-319	8
140-149	7	320-329	3
150-159	2	330-339	2
160-169	0	340-349	0
170-179	2	350-359	2

Chi-Square Test Results

The expected number of observations per interval = 2.8

The tangent Theta = -5.29

The calculated value of Chi-Square = 9.06

Exceeds the value 7.38 at the 97.5 level.

The null hypothesis which states "the distribution of the cobbles is random and has no preferred orientation" is rejected.

The preferred orientation is 100.7 degrees.

GRAPHIC PLOT OF IMBRICATION DATA IN THE PICCININI MINE (UPPER)

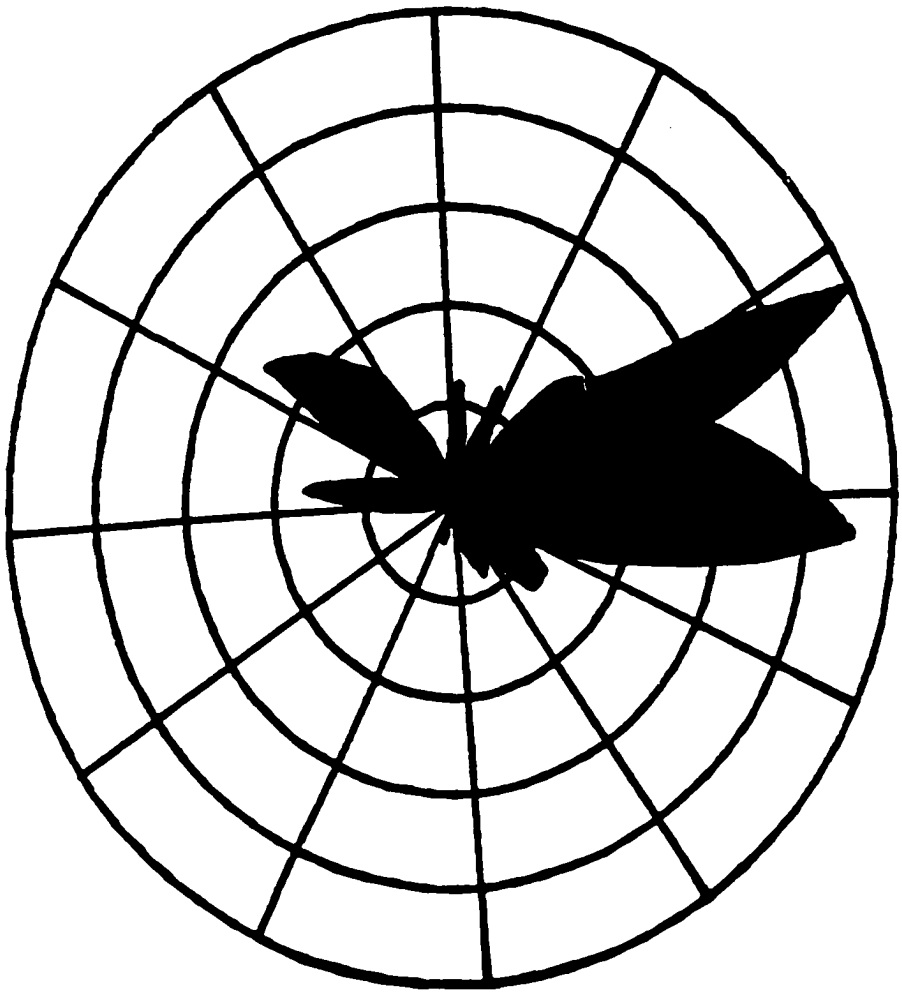

Cobble Orientation Data and Chi-Square Test Results
for the Piccinini Mine (upper cobble layer)

Azimuth Interval	Frequency	Azimuth Interval	Frequency
0 - 9	3	180-189	0
10 - 19	0	190-199	1
20 - 29	3	200-209	0
30 - 39	1	210-219	0
40 - 49	4	220-229	0
50 - 59	5	230-239	0
60 - 69	12	240-249	0
70 - 79	7	250-259	0
80 - 89	9	260-269	1
90 - 99	11	270-279	4
100-109	6	280-289	2
110-119	2	290-299	1
120-129	3	300-309	6
130-139	3	310-319	5
140-149	1	320-329	4
150-159	2	330-339	2
160-169	1	340-349	0
170-179	0	350-359	1

Chi-Square Test Results

The expected number of observations per interval = 2.8

The tangent Theta = 1.82

The calculated value of Chi-Square = 43.15

Exceeds the value 9.21 at the 99.0 level.

The null hypothesis which states "the distribution of the cobbles is random and has no preferred orientation" is rejected.

The preferred orientation is 61.2 degrees.

GRAPHIC PLOT OF IMBRICATION DATA IN THE PICCININI MINE (LOWER)

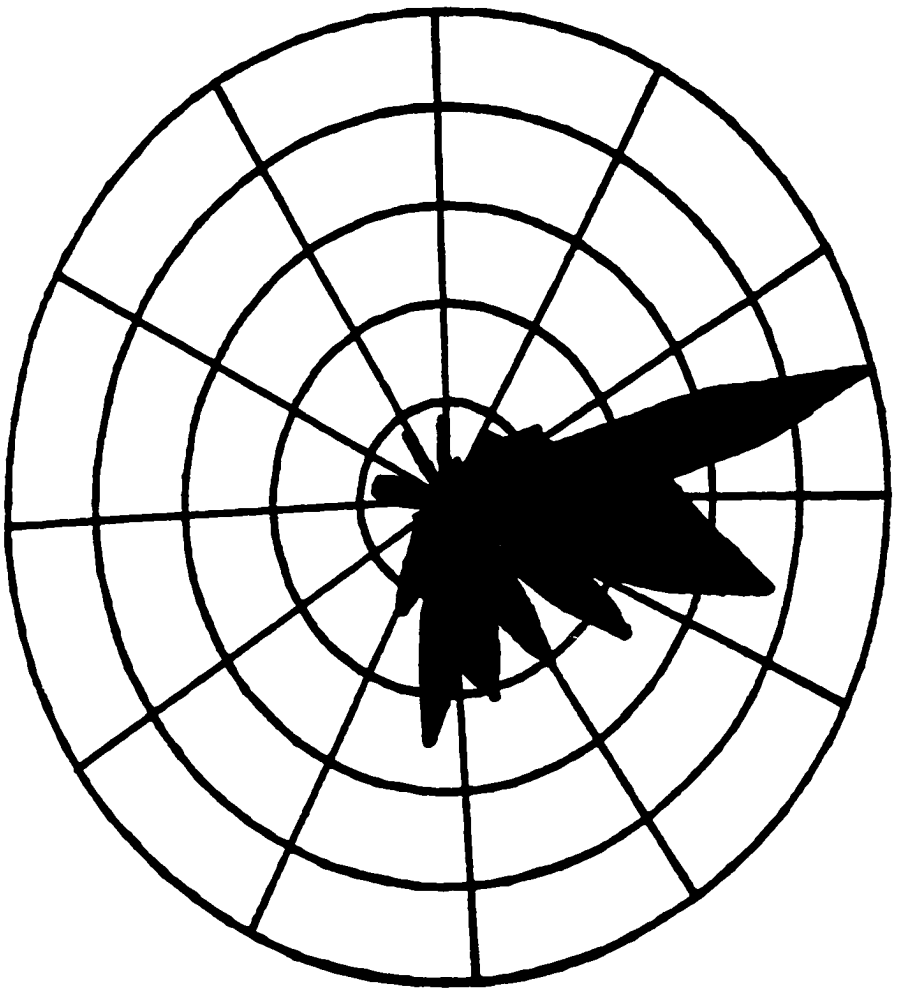

Cobble Orientation Data and Chi-Square Test Results
for the Piccinini Mine (lower cobble layer)

Azimuth Interval	Frequency	Azimuth Interval	Frequency
0 - 9	0	180-189	6
10 - 19	1	190-199	2
20 - 29	0	200-209	3
30 - 39	2	210-219	2
40 - 49	2	220-229	1
50 - 59	3	230-239	1
60 - 69	3	240-249	1
70 - 79	12	250-259	0
80 - 89	6	260-269	1
90 - 99	7	270-279	2
100-109	9	280-289	2
110-119	4	290-299	1
120-129	6	300-309	0
130-139	2	310-319	0
140-149	5	320-329	2
150-159	3	330-339	0
160-169	5	340-349	0
170-179	4	350-359	2

Chi-Square Test Results

The expected number of observations per interval = 2.8

The tangent Theta = -1.85

The calculated value of Chi-Square = 49.91

Exceeds the value 9.21 at the 99.0 level.

The null hypothesis which states "the distribution of the cobbles is random and has no preferred orientation" is rejected.

The preferred orientation is 118.4 degrees.

GRAPHIC PLOT OF IMBRICATION DATA IN THE MAGDALENA MINE

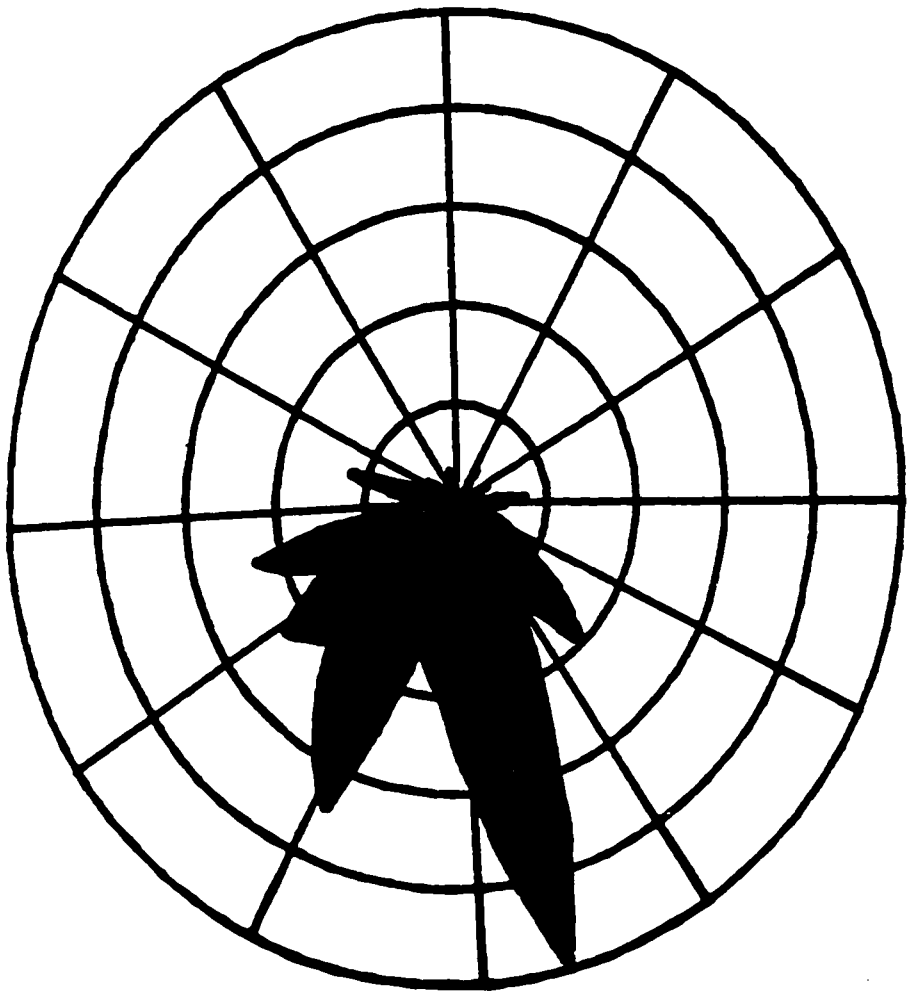

Cobble Orientation Data and Chi-Square Test Results for the Magdalena Mine

Azimuth Interval	Frequency	Azimuth Interval	Frequency
0 - 9	0	180-189	5
10 - 19	0	190-199	4
20 - 29	0	200-209	9
30 - 39	1	210-219	7
40 - 49	0	220-229	5
50 - 59	0	230-239	6
60 - 69	1	240-249	4
70 - 79	0	250-259	6
80 - 89	2	260-269	2
90 - 99	1	270-279	1
100-109	1	280-289	3
110-119	2	290-299	0
120-129	3	300-309	1
130-139	5	310-319	0
140-149	3	320-329	0
150-159	6	330-339	0
160-169	13	340-349	1
170-179	8	350-359	0

Chi-Square Test Results

The expected number of observations per interval = 2.8

The tangent Theta = 0.20

The calculated value of Chi-Square = 85.54

Exceeds the value 9.21 at the 99.0 level.

The null hypothesis which states "the distribution of the cobbles is random and has no preferred orientation" is rejected.

The preferred orientation is 191.1 degrees.

GRAPHIC PLOT OF IMBRICATION DATA IN THE MARIANA MINE (UPPER)

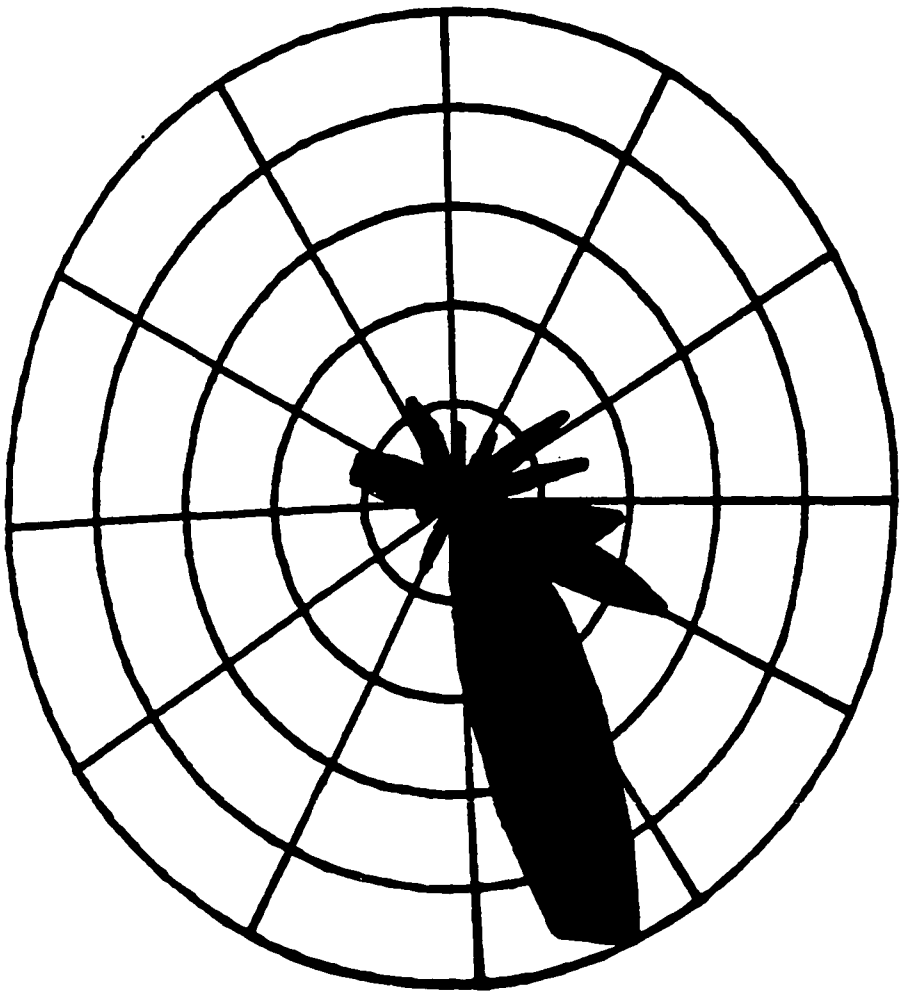

Cobble Orientation Data and Chi-Square Test Results
for the Mariana Mine (upper cobble layer)

Azimuth Interval	Frequency	Azimuth Interval	Frequency
0 - 9	2	180-189	0
10 - 19	0	190-199	0
20 - 29	1	200-209	2
30 - 39	2	210-219	1
40 - 49	1	220-229	0
50 - 59	4	230-239	0
60 - 69	1	240-249	1
70 - 79	4	250-259	1
80 - 89	0	260-269	1
90 - 99	5	270-279	2
100-109	4	280-289	3
110-119	7	290-299	3
120-129	3	300-309	2
130-139	5	310-319	1
140-149	8	320-329	1
150-159	13	330-339	3
160-169	12	340-349	2
170-179	5	350-359	0

Chi-Square Test Results

The expected number of observations per interval = 2.8

The tangent Theta = -0.97

The calculated value of Chi-Square = 33.83

Exceeds the value 9.21 at the 99.0 level.

The null hypothesis which states "the distribution of the cobbles is random and has no preferred orientation" is rejected.

The preferred orientation is 135.7 degrees.

GRAPHIC PLOT OF IMBRICATION DATA IN THE MARIANA MINE (LOWER)

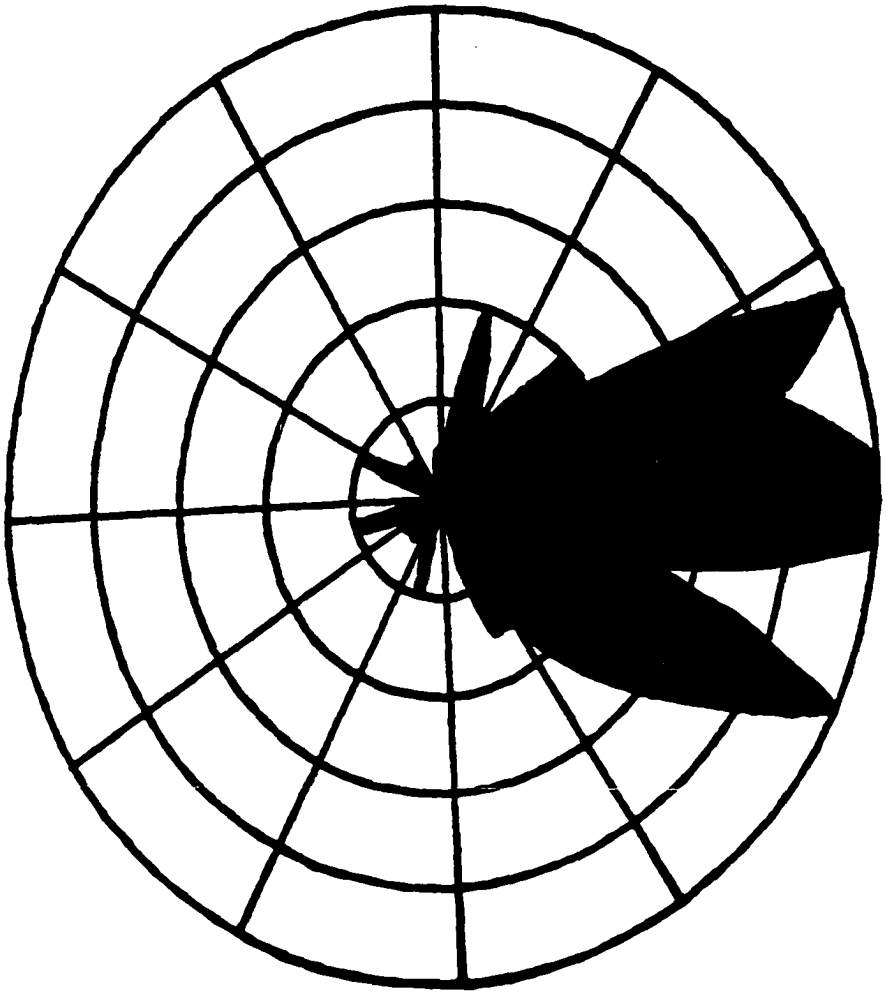

Cobble Orientation Data and Chi-Square Test Results
for the Mariana Mine (lower cobble layer)

Azimuth Interval	Frequency	Azimuth Interval	Frequency
0 - 9	1	180-189	0
10 - 19	4	190-199	2
20 - 29	2	200-209	0
30 - 39	2	210-219	1
40 - 49	4	220-229	1
50 - 59	4	230-239	1
60 - 69	10	240-249	1
70 - 79	8	250-259	2
80 - 89	10	260-269	0
90 - 99	10	270-279	0
100-109	5	280-289	0
110-119	10	290-299	2
120-129	7	300-309	1
130-139	5	310-319	1
140-149	3	320-329	1
150-159	3	330-339	0
160-169	0	340-349	0
170-179	0	350-359	1

Chi-Square Test Results

The expected number of observations per interval = 2.8

The tangent Theta = 138.44

The calculated value of Chi-Square = 76.92

Exceeds the value 9.21 at the 99.0 level.

The null hypothesis which states "the distribution of the cobbles is random and has no preferred orientation" is rejected.

The preferred orientation is 89.6 degrees.

GRAPHIC PLOT OF IMBRICATION IN THE MARTA MINE

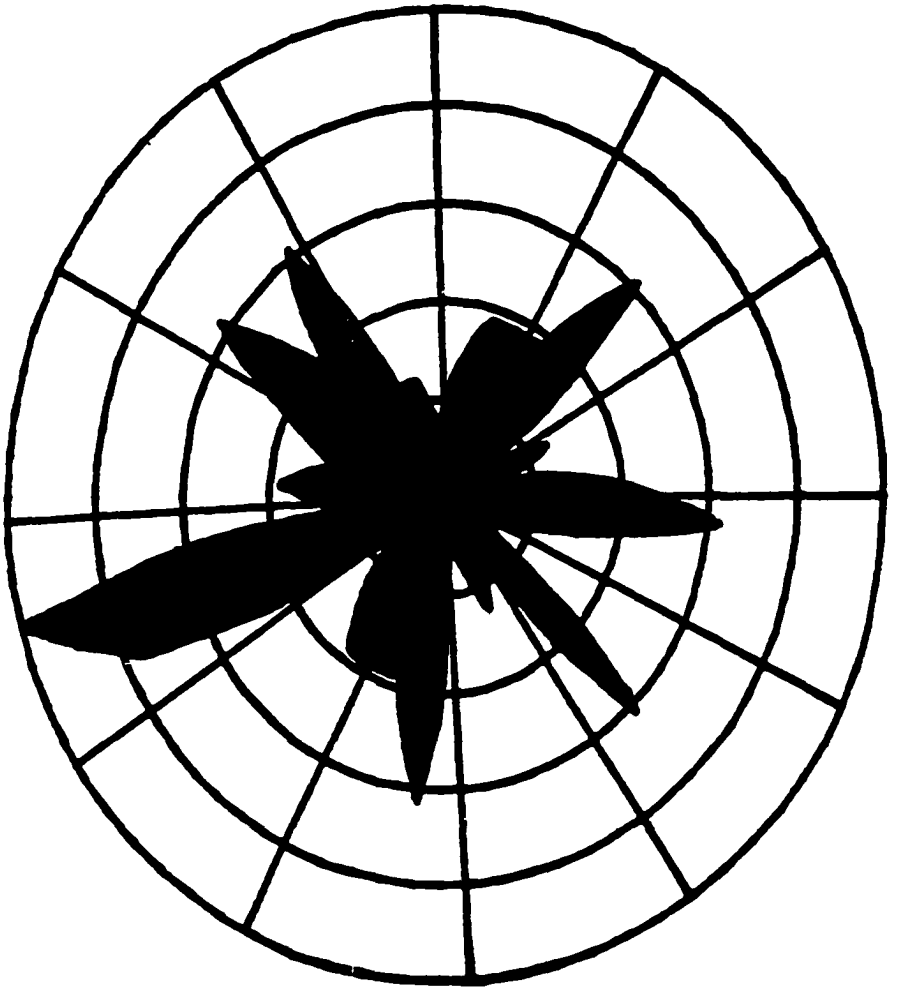

Cobble Orientation Data and Chi-Square Test Results for the Marta Mine

Azimuth Interval	Frequency	Azimuth Interval	Frequency
0 - 9	2	180-189	5
10 - 19	3	190-199	3
20 - 29	3	200-209	3
30 - 39	3	210-219	3
40 - 49	5	220-229	2
50 - 59	1	230-239	1
60 - 69	2	240-249	6
70 - 79	1	250-259	8
80 - 89	3	260-269	2
90 - 99	5	270-279	3
100-109	2	280-289	2
110-119	1	290-299	3
120-129	1	300-309	5
130-139	5	310-319	3
140-149	1	320-329	5
150-159	2	330-339	2
160-169	1	340-349	2
170-179	1	350-359	1

Chi-Square Test Results

The expected number of observations per interval = 2.8

The tangent Theta = -7.79

The calculated value of Chi-Square = 2.79

It is less than the value 4.61 at the 90.0 level.

The null hypothesis which states "the distribution of the cobbles is random and has no preferred orientation" cannot be rejected.

The orientation of the cobbles may therefore be random.

GRAPHIC PLOT OF IMBRICATION DATA IN THE SAN JOAQUIN MINE

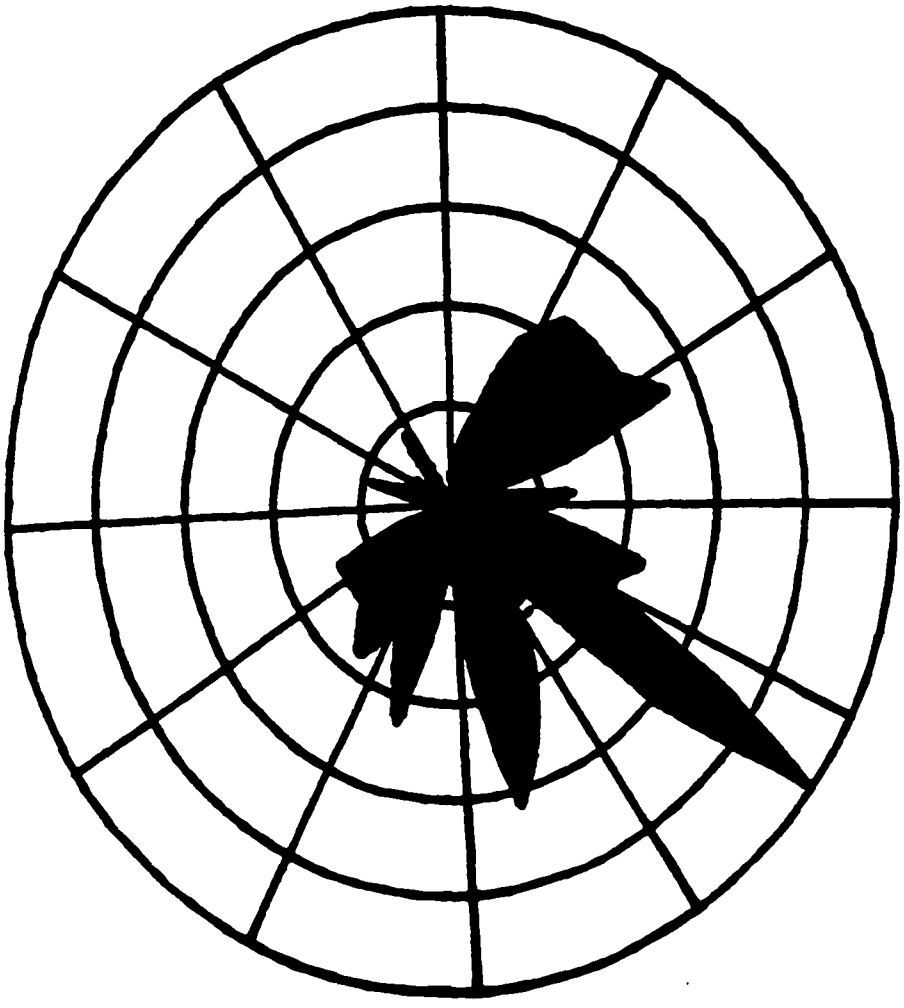

Cobble Orientation Data and Chi-Square Test Results
for the San Joaquin Mine

Azimuth Interval	Frequency	Azimuth Interval	Frequency
0 - 9	1	180-189	1
10 - 19	2	190-199	5
20 - 29	4	200-209	3
30 - 39	5	210-219	4
40 - 49	5	220-229	3
50 - 59	5	230-239	3
60 - 69	6	240-249	3
70 - 79	0	250-259	0
80 - 89	3	260-269	0
90 - 99	2	270-279	0
100-109	5	280-289	2
110-119	4	290-299	0
120-129	11	300-309	1
130-139	3	310-319	0
140-149	3	320-329	2
150-159	5	330-339	0
160-169	7	340-349	0
170-179	2	350-359	0

Chi-Square Test Results

The expected number of observations per interval = 2.8

The tangent Theta = -1.50

The calculated value of Chi-Square = 30.50

Exceeds the value 9.21 at the 99.0 level.

The null hypothesis which states "the distribution of the cobbles is random and has no preferred orientation" is rejected.

The preferred orientation is 123.7 degrees.

GRAPHIC PLOT OF IMBRICATION DATA IN THE SAN JUAN MINE

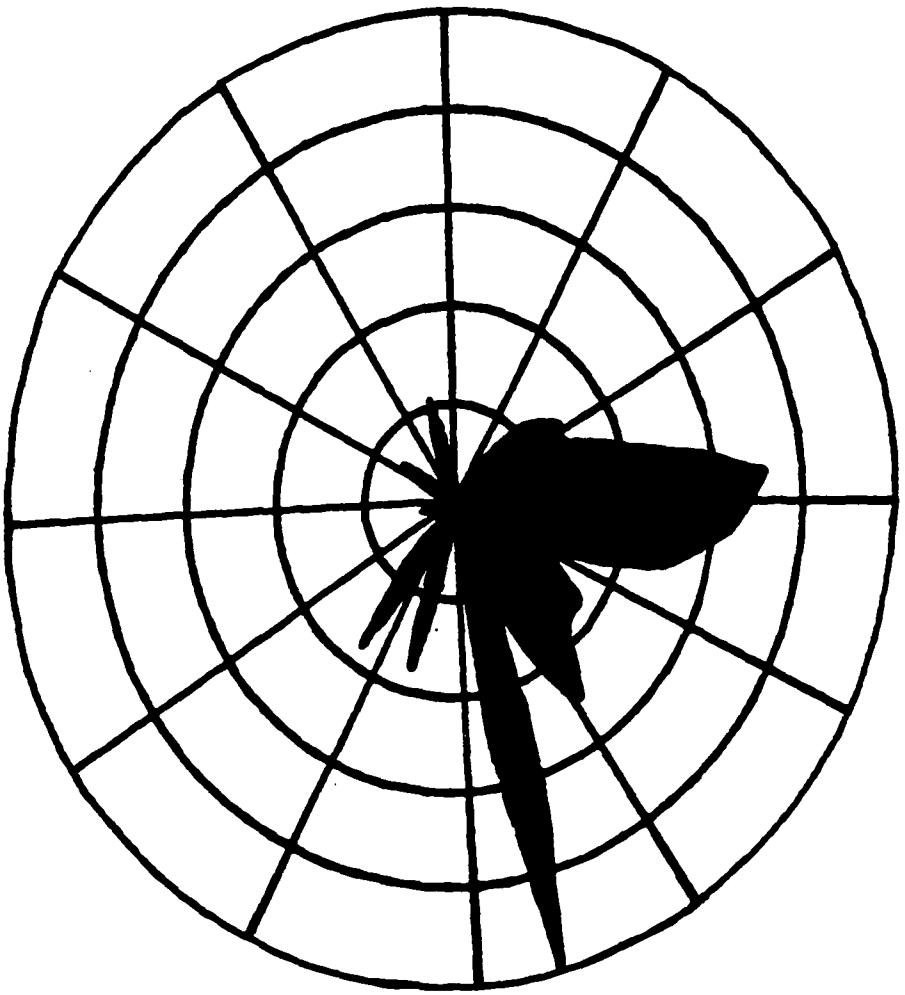

Cobble Orientation Data and Chi-Square Test Results for the San Juan Mine

Azimuth Interval	Frequency	Azimuth Interval	Frequency
0 - 9	0	180-189	0
10 - 19	0	190-199	5
20 - 29	0	200-209	0
30 - 39	1	210-219	5
40 - 49	3	220-229	0
50 - 59	4	230-239	0
60 - 69	4	240-249	0
70 - 79	6	250-259	1
80 - 89	10	260-269	1
90 - 99	9	270-279	0
100-109	7	280-289	0
110-119	3	290-299	1
120-129	5	300-309	2
130-139	5	310-319	0
140-149	7	320-329	0
150-159	3	330-339	0
160-169	14	340-349	3
170-179	0	350-359	1

Chi-Square Test Results

The expected number of observations per interval = 2.8

The tangent Theta = -1.90

The calculated value of Chi-Square = 65.88

Exceeds the value 9.21 at the 99.0 level.

The null hypothesis which states "the distribution of the cobbles is random and has no preferred orientation" is rejected.

The preferred orientation is 117.7 degrees.

GRAPHIC PLOT OF IMBRICATION DATA IN THE SAN LUIS MINE (UPPER)

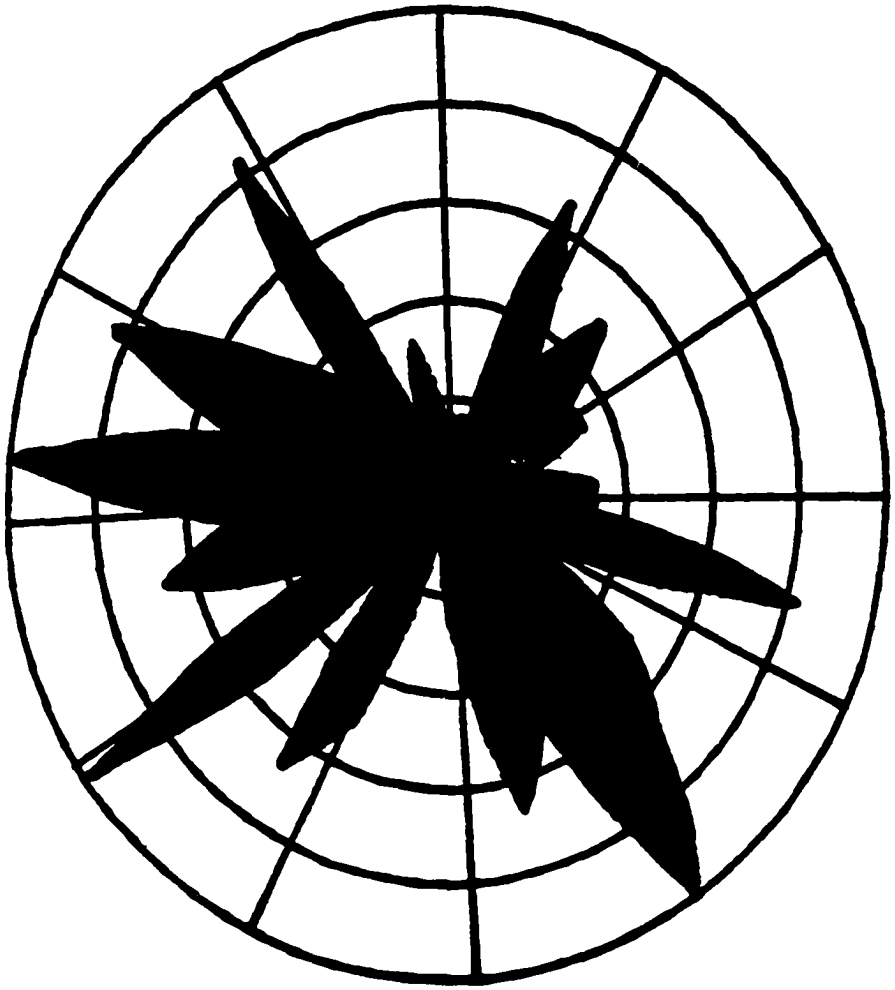

Cobble Orientation Data and Chi-Square Test Results
for the San Luis Mine (upper cobble layer)

Azimuth Interval	Frequency	Azimuth Interval	Frequency
0 - 9	1	180-189	1
10 - 19	1	190-199	0
20 - 29	4	200-209	3
30 - 39	2	210-219	4
40 - 49	3	220-229	1
50 - 59	2	230-239	6
60 - 69	2	240-249	2
70 - 79	1	250-259	4
80 - 89	2	260-269	3
90 - 99	2	270-279	6
100-109	5	280-289	3
110-119	1	290-299	5
120-129	3	300-309	3
130-139	4	310-319	2
140-149	6	320-329	5
150-159	3	330-339	1
160-169	4	340-349	2
170-179	2	350-359	1

Chi-Square Test Results

The expected number of observations per interval = 2.8

The tangent Theta = 1.22

The calculated value of Chi-Square = 2.40

It is less than the value 4.61 at the 90.0 level.

The null hypothesis which states "the distribution of the cobbles is random and has no preferred orientation" cannot be rejected.

The orientation of the cobbles may therefore be random.

GRAPHIC PLOT OF IMBRICATION DATA IN THE LUIS MINE (LOWER)

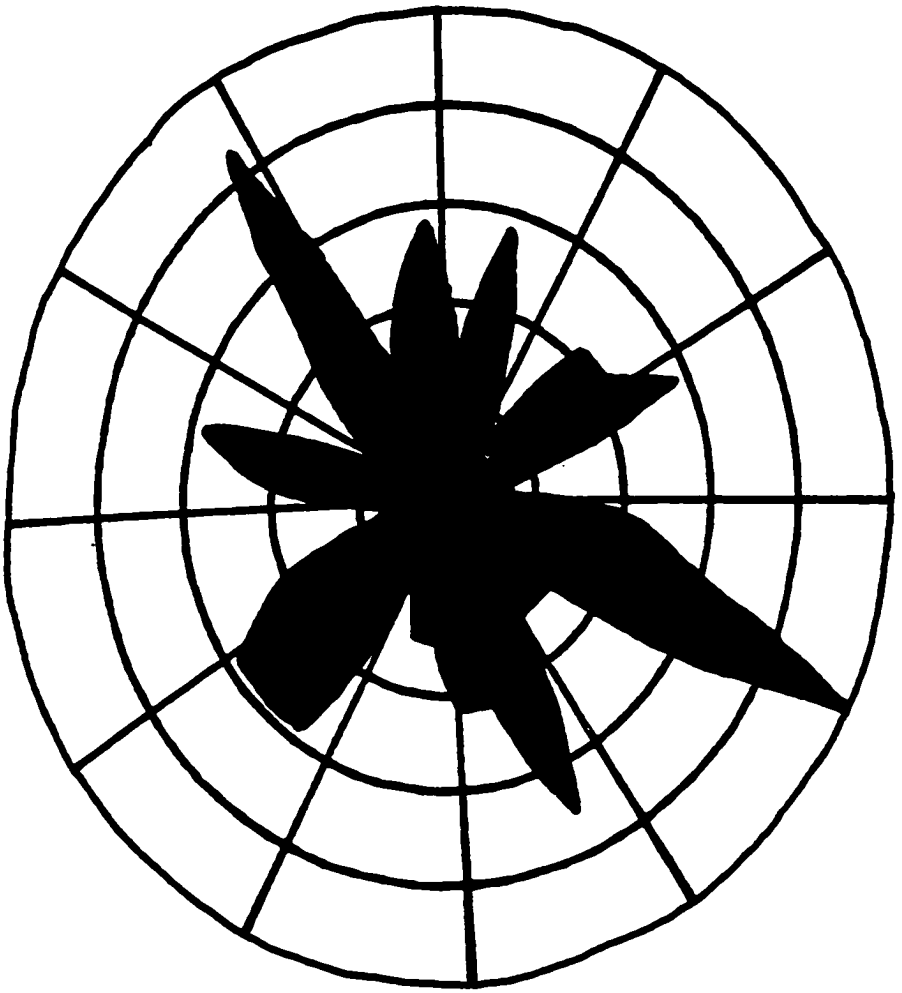

Cobble Orientation Data and Chi-Square Test Results
for the San Luis Mine (lower cobble layer)

Azimuth Interval	Frequency	Azimuth Interval	Frequency	Chi-Square Test Results
0 - 9	2	180-189	2	The expected number of observations
10 - 19	4	190-199	2	per interval = 2.8
20 - 29	2	200-209	1	
30 - 39	1	210-219	4	The tangent Theta = -2.95
40 - 49	3	220-229	4	
50 - 59	3	230-239	4	The calculated value of Chi-Square
60 - 69	4	240-249	3	= 0.11
70 - 79	1	250-259	1	
80 - 89	1	260-269	1	It is less than the value 4.61
90 - 99	3	270-279	3	at the 90.0 level.
100-109	4	280-289	4	
110-119	7	290-299	1	The null hypothesis which states
120-129	2	300-309	2	"the distribution of the cobbles
130-139	2	310-319	3	is random and has no preferred
140-149	2	320-329	6	orientation" cannot be rejected.
150-159	5	330-339	2	
160-169	3	340-349	3	The orientation of the cobbles may
170-179	3	350-359	4	therefore be random.

GRAPHIC PLOT OF IMBRICATION DATA IN THE SANTO DOMINGO 1 MINE

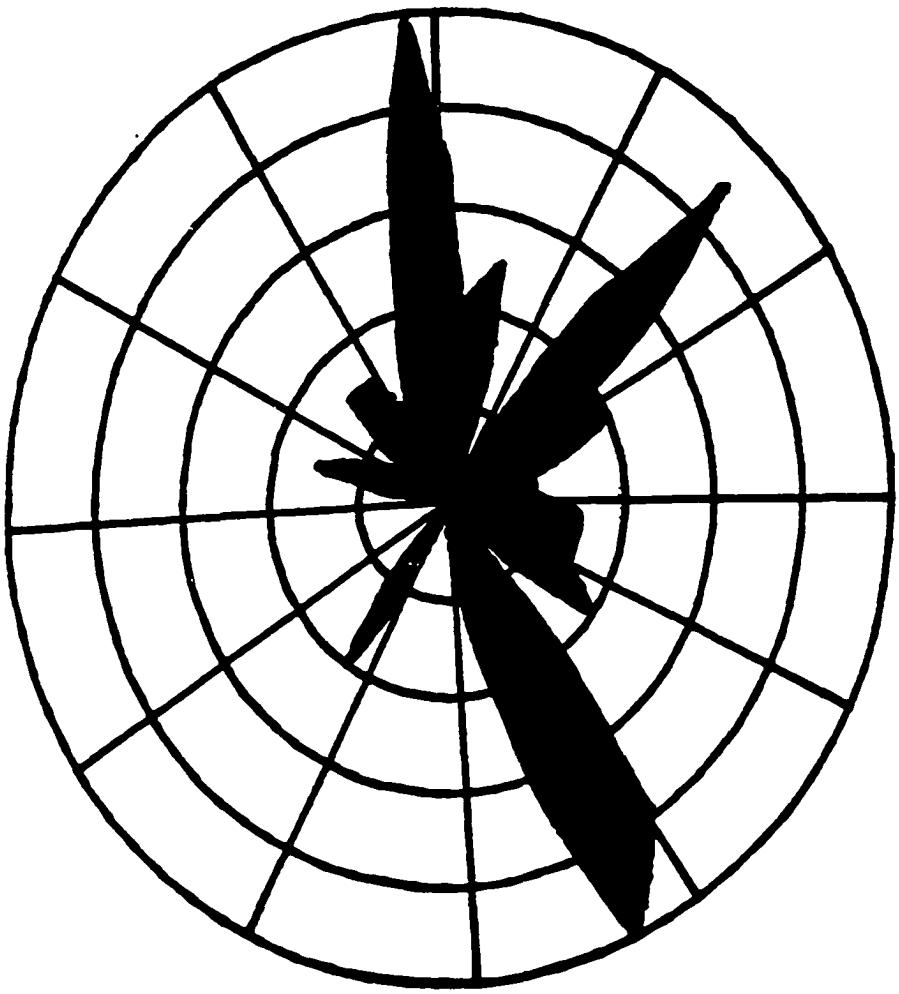

Cobble Orientation Data and Chi-Square Test Results
for the Santo Domingo I Mine

Azimuth Interval	Frequency	Azimuth Interval	Frequency
0 - 9	4	180-189	0
10 - 19	4	190-199	0
20 - 29	0	200-209	1
30 - 39	2	210-219	4
40 - 49	9	220-229	0
50 - 59	4	230-239	0
60 - 69	4	240-249	0
70 - 79	2	250-259	0
80 - 89	2	260-269	0
90 - 99	3	270-279	0
100-109	3	280-289	3
110-119	3	290-299	2
120-129	4	300-309	1
130-139	0	310-319	3
140-149	8	320-329	3
150-159	10	330-339	2
160-169	4	340-349	4
170-179	1	350-359	10

Chi-Square Test Results

The expected number of observations per interval = 2.8

The tangent Theta = 1.84

The calculated value of Chi-Square = 18.64

Exceeds the value 9.21 at the 99.0 level.

The null hypothesis which states "the distribution of the cobbles is random and has no preferred orientation" is rejected.

The preferred orientation is 61.5 degrees.

GRAPHIC PLOT OF IMBRICATION DATA IN THE SANTO DOMINGO 2 MINE

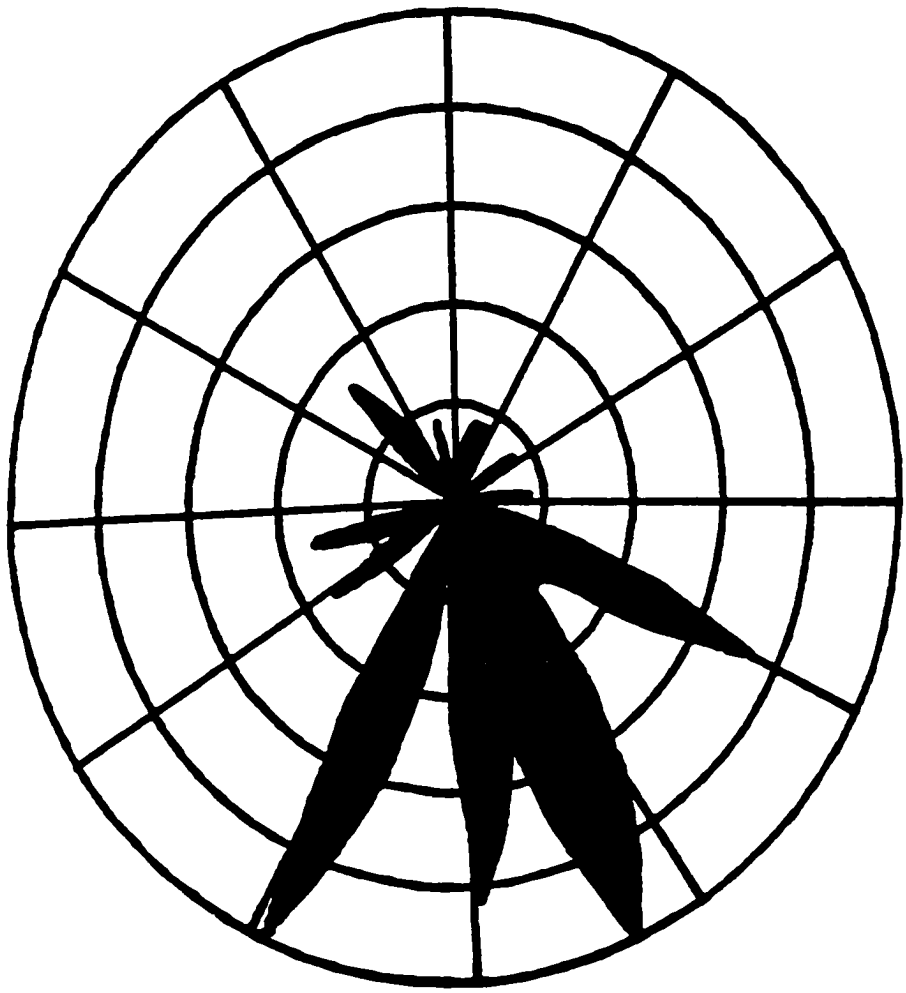

Cobble Orientation Data and Chi-Square Test Results
for the Santo Domingo II Mine

Azimuth Interval	Frequency	Azimuth Interval	Frequency
0 - 9	1	180-189	1
10 - 19	2	190-199	7
20 - 29	2	200-209	12
30 - 39	0	210-219	0
40 - 49	0	220-229	0
50 - 59	2	230-239	4
60 - 69	0	240-249	1
70 - 79	0	250-259	4
80 - 89	2	260-269	0
90 - 99	0	270-279	0
100-109	3	280-289	0
110-119	9	290-299	0
120-129	3	300-309	0
130-139	3	310-319	4
140-149	8	320-329	2
150-159	12	330-339	0
160-169	6	340-349	2
170-179	10	350-359	0

Chi-Square Test Results

The expected number of observations per interval = 2.8

The tangent Theta = -0.26

The calculated value of Chi-Square = 56.65

Exceeds the value 9.21 at the 99.0 level.

The null hypothesis which states "the distribution of the cobbles is random and has no preferred orientation" is rejected.

The preferred orientation is 165.5 degrees.

GRAPHIC PLOT OF IMBRICATION DATA IN THE TRAVESIA MINE

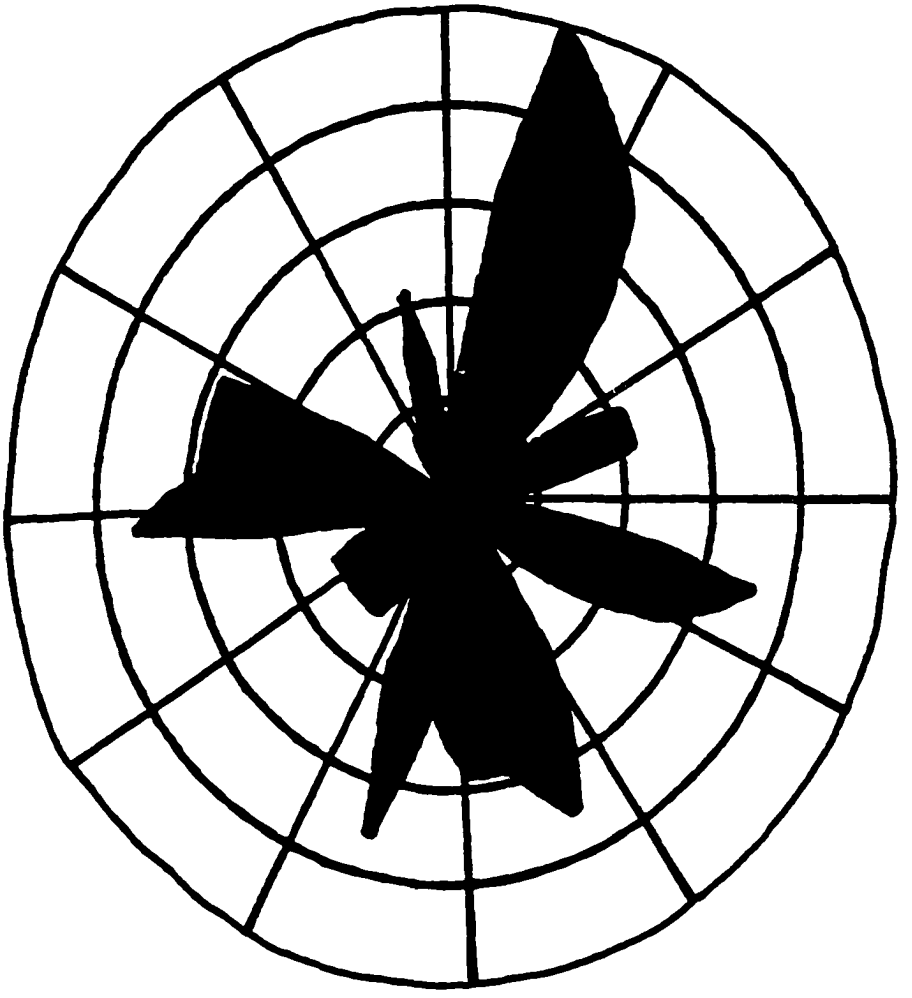

Cobble Orientation Data and Chi-Square Test Results for the Travesia Mine

Azimuth Interval	Frequency	Azimuth Interval	Frequency
0 - 9	2	180-189	3
10 - 19	7	190-199	5
20 - 29	6	200-209	1
30 - 39	5	210-219	2
40 - 49	3	220-229	2
50 - 59	1	230-239	2
60 - 69	3	240-249	2
70 - 79	3	250-259	1
80 - 89	1	260-269	5
90 - 99	1	270-279	4
100-109	5	280-289	4
110-119	4	290-299	4
120-129	2	300-309	0
130-139	0	310-319	0
140-149	3	320-329	1
150-159	5	330-339	1
160-169	4	340-349	3
170-179	4	350-359	1

Chi-Square Test Results

The expected number of observations per interval = 2.8

The tangent Theta = -3.49

The calculated value of Chi-Square = 0.77

It is less than the value 4.61 at the 90.0 level.

The null hypothesis which states "the distribution of the cobbles is random and has no preferred orientation" cannot be rejected.

The orientation of the cobbles may therefore be random.

APPENDIX C

Summary Tables of the Principal Component Analysis of the Cobble Gravel Matrix Heavy Mineral Assemblages

Appendix C

Heavy Mineral Percentages For 28 Cobble Gravel Matrix Samples
(Percentages obtained from point-counts of at least 300 grains per sample)
(From Darby and Whittecar, 1984)

Sample	Hornblende	Zircon	Sphene	Monazite	Epidote	Andalusite	Allunite
SD1-3	45.82	6.57	6.95	7.64	0.00	22.83	0.00
SD2-2	30.97	8.84	19.91	13.27	0.88	24.33	0.00
TRA-3	38.66	11.04	3.31	0.00	0.00	36.83	0.00
EPI-1	32.45	2.64	5.29	15.23	0.00	31.12	0.00
MAG-7	23.47	6.95	13.04	14.78	0.00	26.95	0.00
MAG-5	42.71	3.81	7.63	2.15	0.69	32.63	0.00
SD1-2	61.49	3.37	0.00	7.85	0.00	11.48	0.00
HIP-4	16.14	18.63	27.95	4.96	0.62	24.84	0.00
MAG-2	35.71	26.78	0.00	12.50	0.00	19.64	0.00
SJO-3	57.14	7.14	0.00	2.85	0.00	20.00	0.00
MAR-4	50.29	8.52	9.70	2.35	0.00	20.88	0.00
SJU-3/4	21.72	13.11	0.00	0.00	2.89	45.18	7.94
MAR-3	40.37	13.04	14.59	11.18	0.00	19.87	0.00
SITE 6-1	17.90	8.18	10.21	3.14	0.00	46.10	0.00
SD2-9	52.53	2.01	1.96	1.31	11.31	24.67	2.25
ALC-3	13.52	12.35	12.35	15.88	0.00	35.88	0.00
ANA-1	40.22	0.45	7.95	7.61	0.00	35.22	0.00
MAR-8	6.41	21.79	7.69	17.94	0.00	39.74	0.00
SJO-5	24.69	0.00	0.00	14.81	0.00	37.03	0.00
HIP-3	4.08	32.24	0.00	5.10	0.00	48.36	0.00
PAN-3	3.68	38.58	20.24	9.87	0.00	13.04	0.00
SJO-4	11.84	15.26	15.13	0.00	0.00	44.07	5.10
PAN-2	6.31	46.39	21.73	0.00	0.00	8.24	3.72
ANT-1	7.44	20.00	18.60	26.04	0.00	11.62	0.00
ANG-2	3.87	12.90	33.54	32.25	0.00	14.83	0.00
HIP-6	13.45	13.83	19.72	12.71	0.00	35.97	0.00
ANG-3	5.34	15.80	17.83	9.81	0.31	45.10	0.00
HIP-9	7.37	18.81	15.33	10.99	0.00	42.81	0.00

Appendix C

Heavy Mineral Percentages For 28 Cobble Gravel Matrix Samples
(Percentages obtained from point-counts of at least 300 grains per sample)
(From Darby and Whittecar, 1984)
continued

Sample	Wollastonite	Hematite	Apatite	Biotite	Olivine	Rutile	Garnet
SD1-3	0.00	0.00	0.00	0.00	2.13	0.00	0.00
SD2-2	0.00	1.76	0.00	0.00	0.00	0.00	0.00
TRA-3	0.00	0.00	2.44	0.00	0.00	0.00	3.86
EPI-1	0.00	4.63	0.00	1.98	0.00	0.00	0.00
MAG-7	0.00	0.00	3.47	0.00	4.30	0.00	2.60
MAG-5	0.00	0.00	0.00	2.08	0.00	0.00	4.14
SD1-2	0.00	0.00	0.32	1.29	0.00	5.19	0.00
HIP-4	0.00	0.00	0.00	0.00	1.24	0.00	0.00
MAG-2	0.00	0.00	1.78	3.50	0.00	0.00	0.00
SJO-3	0.00	0.00	0.00	2.85	1.42	0.00	0.00
MAR-4	0.00	0.00	1.76	1.17	0.00	0.58	0.00
SJU-3/4	0.00	0.00	0.00	6.71	0.00	0.00	0.00
MAR-3	0.93	0.00	0.00	0.00	0.00	0.00	0.00
SITE 6-1	0.00	0.00	1.17	5.14	0.00	0.00	0.00
SD2-9	0.00	0.00	0.32	0.64	0.00	0.00	0.00
ALC-3	0.00	0.00	0.00	1.76	0.00	0.00	1.17
ANA-1	2.27	0.00	0.00	0.00	0.00	0.00	0.00
MAR-8	3.84	0.00	0.00	2.56	0.00	0.00	0.00
SJO-5	16.04	0.00	0.00	2.46	0.00	0.00	0.00
HIP-3	0.00	0.00	0.00	4.08	0.00	0.00	0.00
PAN-3	11.65	0.00	0.00	0.00	0.00	0.00	0.00
SJO-4	0.00	0.00	0.00	3.80	0.00	0.00	0.00
PAN-2	0.00	0.00	0.00	0.00	0.00	1.05	10.99
ANT-1	7.90	0.00	0.00	1.39	0.00	0.00	0.00
ANG-2	0.00	0.00	0.00	0.00	0.00	1.93	0.64
HIP-6	2.01	0.00	2.04	0.00	0.00	0.00	0.00
ANG-3	0.00	0.00	0.00	4.72	0.00	0.00	0.00
HIP-9	0.00	0.00	0.00	1.30	0.00	0.00	2.13

Appendix C

Heavy Mineral Percentages For 28 Cobble Gravel Matrix Samples
(Percentages obtained from point-counts of at least 300 grains per sample)
(From Darby and Whittecar, 1984)
continued

Sample	Cassiterite	Topaz	Tourmaline
SD1-3	0.00	0.05	7.48
SD2-2	0.00	0.00	0.00
TRA-3	0.55	0.00	3.31
EPI-1	0.00	6.62	0.00
MAG-7	0.00	0.00	4.30
MAG-5	0.00	0.00	4.16
SD1-2	0.00	0.00	9.09
HIP-4	0.00	0.00	5.59
MAG-2	0.00	0.00	0.00
SJO-3	0.00	0.00	8.57
MAR-4	0.00	0.00	4.70
SJU-3/4	0.00	0.00	0.00
MAR-3	0.00	0.00	0.00
SITE 6-1	0.00	0.00	2.50
SD2-9	0.00	0.00	0.00
ALC-3	0.00	0.00	0.00
ANA-1	0.00	0.00	0.00
MAR-8	0.00	0.00	0.00
SJO-5	0.00	0.00	4.08
HIP-3	0.00	0.00	4.08
PAN-3	0.00	0.00	0.00
SJO-4	0.00	0.00	0.00
PAN-2	0.00	0.00	1.57
ANT-1	0.00	0.00	6.97
ANG-2	0.00	0.00	0.00
HIP-6	0.00	0.00	0.00
ANG-3	0.00	0.00	0.00
HIP-9	0.00	0.00	0.00

Appendix C

Factor Analysis of Heavy Mineral Data from Cobble Gravel Matrix Samples

Factor Loadings for the First Three Eigenvectors

Mineral Type	Factor 1	Factor 2	Factor 3
Hornblende	0.991	- 0.101	- 0.054
Zircon	- 0.706	- 0.343	- 0.602
Sphene	- 0.626	- 0.449	0.358
Monazite	- 0.365	- 0.320	0.736
Epidote	0.295	0.077	- 0.083
Andalusite	- 0.196	0.975	0.004
Allunite	- 0.103	0.210	- 0.385
Wollastonite	- 0.215	- 0.109	0.152
Hematite	0.109	0.033	0.235
Apatite	0.158	0.035	- 0.014
Biotite	- 0.101	0.063	- 0.250
Olivine	0.155	- 0.110	0.127
Rutile	0.248	- 0.383	0.050
Garnet	- 0.188	- 0.264	- 0.416
Cassiterite	- 0.039	0.396	- 0.005
Topaz	0.019	0.328	0.126
Tourmaline	0.440	- 0.240	- 0.069

Appendix C

Factor Analysis of Heavy Mineral Data from Cobble Gravel Matrix Samples

Factor Scores for Each Sample for the First Three Eigenvectors

Sample	Factor 1	Factor 2	Factor 3
SD1-3	1.084	- 0.376	0.061
SD2-2	0.198	- 0.516	0.873
TRA-3	0.716	0.694	- 0.814
EPI-1	0.511	0.373	0.935
MAG-7	0.001	- 0.128	0.910
MAG-5	0.966	0.418	- 0.069
SD1-2	1.943	- 1.050	- 0.119
HIP-4	- 0.625	- 0.630	0.073
MAG-2	0.355	- 0.764	- 1.236
SJO-3	1.678	- 0.447	- 0.659
MAR-4	1.234	- 0.557	- 0.363
SJU-3/4	- 0.029	1.527	- 0.943
MAR-3	0.612	- 0.841	0.156
SITE 6-1	- 0.248	1.420	0.067
SD2-9	1.531	0.032	- 0.268
ALC-3	- 0.566	0.492	0.704
ANA-1	0.858	0.628	0.640
MAR-8	- 1.010	0.662	0.079
SJO-5	0.260	0.944	1.067
HIP-3	- 1.137	1.379	- 1.748
PAN-3	- 1.406	- 1.577	- 1.113
SJO-4	- 0.666	1.147	- 0.426
PAN-2	- 1.353	- 1.990	- 2.490
ANT-1	- 0.966	- 1.517	1.083
ANG-2	- 1.241	- 1.517	2.509
HIP-6	- 0.673	0.308	0.672
ANG-3	- 1.046	1.052	0.337
HIP-9	- 0.981	0.835	0.083

APPENDIX D

Summary Tables of the Discriminant Function Analysis of the Elemental Composition of Volcanic Ash Magnetite

Appendix D

Chemical Composition of Magnetite From Volcanic Ash Samples
(Composition listed in parts per million as determined from AAS analysis)

Sample	Aluminium	Calcium	Magnesium	Copper	Iron	Manganese
ALC-5	2511.10	365.57	9333.30	144.50	411400.0	1680.00
BLA-5	9200.00	117.50	9333.30	59.00	516000.0	2830.00
SD1-1	12544.40	187.20	11999.90	33.90	658000.0	2830.00
SJU-6	9200.00	307.80	13333.30	28.90	640000.0	2830.00
ANA-4	9200.00	295.20	12666.60	28.90	682000.0	3020.00
MAR-1	2511.10	815.40	12666.60	23.90	555800.0	2640.00
PAN-5	0.00*	1075.10	11333.30	23.90	561800.0	2060.00
SD2-3	5855.60	574.20	7999.90	33.90	652000.0	3020.00
HIP-2	2511.10	954.90	13999.90	28.90	537800.0	2640.00
SD1-4	9200.00	219.20	11333.30	13.80	638000.0	2830.00
SJO-6	0.00*	802.40	13333.30	33.90	507800.0	2450.00
SJU-7	2511.10	720.00	12666.60	48.90	531800.0	4950.00
ANA-8	12544.40	466.20	10666.60	23.90	676200.0	3220.00
SD2-5	12544.40	453.60	9333.30	13.80	676200.0	3020.00
ANA-8R	9200.00	401.40	9333.30	23.90	652000.0	2830.00
HIP-10	9200.00	130.10	5333.30	646.00	634000.0	2060.00
SD1-7	12544.40	390.20	11333.30	23.90	688000.0	3220.00
SJU-8	9200.00	415.80	11333.30	33.90	658000.0	3020.00
SD1-7R	12544.40	428.40	9999.90	38.90	670000.0	2830.00
SJU-9	9200.00	300.20	9333.30	23.90	667000.0	2830.00
SJU-9R	9200.00	383.90	9333.30	43.90	652000.0	3020.00
SD1-8	12544.40	231.80	9999.90	18.80	640000.0	2830.00

* These values were measured at or below the values for the standard blank.

Appendix D

Chemical Composition of Magnetite From Volcanic Ash Samples
(Composition listed in parts per million as determined from AAS analysis)
continued

Sample	Nickel	Zinc	Vanadium	Titanium	Chromium	Terrace Elevation Group
ALC-5	123.00	215.00	1515.50	120815.0	500.40	1
BLA-5	208.00	706.00	2522.50	47825.0	627.80	2
SD1-1	171.50	969.00	2522.50	61655.0	508.10	2
SJU-6	110.50	1001.00	2522.50	61655.0	415.80	3
ANA-4	98.50	969.00	2234.00	47825.0	437.40	3
MAR-1	123.00	346.00	1753.00	96235.0	514.80	2
PAN-5	86.50	445.00	1512.50	133120.0	373.50	1
SD2-3	74.00	576.00	2378.00	80950.0	627.80	2
HIP-2	62.00	215.00	1656.50	70875.0	295.70	2
SD1-4	86.50	969.00	2282.00	24770.0	451.40	2
SJO-6	110.50	510.00	1608.50	98540.0	387.90	2
SJU-7	74.00	248.00	1224.00	82400.0	203.90	3
ANA-8	123.0G	739.00	2233.50	24770.0	430.20	3
SD2-5	98.50	772.00	2185.50	31685.0	437.40	2
ANA-8R	135.00	838.00	2089.50	31685.0	409.10	3
HIP-10	2210.00	805.00	3051.50	31685.0	932.00	2
SD1-7	123.00	936.00	2041.50	27075.0	475.50	2
SJU-8	110.50	903.00	2330.00	40905.0	437.90	3
SD1-7R	196.00	838.00	2185.50	45520.0	444.20	2
SJU-9	110.50	1132.00	2474.50	57045.0	458.60	3
SJU-9R	135.00	1067.00	2666.50	88570.0	550.40	3
SD1-8	110.50	1001.00	2522.50	52435.0	507.90	2

Appendix D

Canonical Discriminant Function Analysis of Volcanic Magnetite Chemistry

Canonical Discriminant Functions

Function	Eigenvalue	Percent of Variance	Cummulative Percent	Canonical Correlation
1	5.343	90.02	90.02	0.918
2	0.592	9.98	100.00	0.601

Pooled Within-Groups Correlations Between Discriminating Variables And Canonical Discriminant Functions

Element	Function 1	Function 2
Titanium	- 0.411*	- 0.291
Manganese	0.339*	- 0.289
Iron	0.319*	0.084
Zinc	0.262*	0.083
Aluminium	0.243*	0.180
Chromium	- 0.012	0.490*
Copper	0.041	0.430*
Nickel	0.074	0.425*
Calcium	- 0.241	- 0.328*
Vanadium	0.216	0.221*
Magnesium	0.030	- 0.063*

Appendix D

Canonical Discriminant Function Analysis of Volcanic Magnetite Chemistry

Summary Table

Sample	Actual Group	Highest Probability Group	P(D/G)	P(G/D)	Second Highest Group	P(G/D)	Discriminant Scores Funct. 1	Funct. 2
ALC-5	1	1	0.480	1.000	2	0.000	- 7.561	0.026
BLA-5	2	2	0.626	0.863	3	0.137	1.057	1.055
SD1-1	2	2	0.856	0.971	3	0.029	0.500	1.070
SJU-6	3	3	0.723	0.963	2	0.037	1.689	- 1.468
ANA-4	3	3	0.246	0.505	2	0.495	1.831	0.842
MAR-1	2	2	0.101	0.989	1	0.013	- 1.730	1.968
PAN-5	1	1	0.480	1.000	2	0.000	- 5.340	- 1.443
SD2-3	2	2	0.570	0.962	3	0.038	- 0.248	- 0.387
HIP-2	2	2	0.657	0.867	3	0.133	0.194	- 0.257
SD1-4	2**	3	0.321	0.744	2	0.256	2.280	0.409
SJO-6	2	2	0.344	0.998	1	0.002	- 1.501	0.273
SJU-7	3	3	0.117	0.978	2	0.023	2.380	- 1.793
ANA-8	3	3	0.562	0.635	2	0.365	1.532	0.231
SD2-5	2	2	0.549	0.907	3	0.093	- 0.034	- 0.450
ANA-8R	3	3	0.218	0.558	2	0.442	0.327	- 1.136
HIP-10	2	2	0.240	0.998	3	0.002	0.439	2.334
SD1-7	2	2	0.374	0.994	3	0.006	0.585	2.003
SJU-8	3	3	0.591	0.865	2	0.135	2.157	- 0.221
SD1-7R	2	2	0.523	0.999	3	0.001	- 0.935	- 0.073
SJU-9	3	3	0.417	0.931	2	0.069	0.811	- 1.833
SJU-9R	3	3	0.956	0.905	2	0.095	1.352	- 1.034
SD1-8	2	2	0.738	0.889	3	0.111	0.215	- 0.115

Classification Results

Actual Group	Number of Cases	Predicted Group Membership 1	2	3
Group 1	2	2	0	0
		100%	0%	0%
Group 2	12	0	11	1
		0%	91.7%	8.3%
Group 3	8	0	0	8
		0%	0%	100%

Percent of "Grouped" Cases Correctly Classified: 95.45%